AWARD NUMBER: W81XWH-17-1-0346

TITLE: Receptor for AGE (RAGE) Signal Transduction in Amyotrophic Lateral Sclerosis: In Vivo Imaging and Novel Therapeutic Approaches

PRINCIPAL INVESTIGATOR: Ann Marie Schmidt, MD

CONTRACTING ORGANIZATION: New York University, New York, NY

REPORT DATE: October 2021

TYPE OF REPORT: FINAL

PREPARED FOR: U.S. Army Medical Research and Development Command
Fort Detrick, Maryland 21702-5012

DISTRIBUTION STATEMENT: Approved for Public Release;
Distribution Unlimited

The views, opinions and/or findings contained in this report are those of the author(s) and should not be construed as an official Department of the Army position, policy or decision unless so designated by other documentation.

REPORT DOCUMENTATION PAGE

Form Approved
OMB No. 0704-0188

Public reporting burden for this collection of information is estimated to average 1 hour per response, including the time for reviewing instructions, searching existing data sources, gathering and maintaining the data needed, and completing and reviewing this collection of information. Send comments regarding this burden estimate or any other aspect of this collection of information, including suggestions for reducing this burden to Department of Defense, Washington Headquarters Services, Directorate for Information Operations and Reports (0704-0188), 1215 Jefferson Davis Highway, Suite 1204, Arlington, VA 22202-4302. Respondents should be aware that notwithstanding any other provision of law, no person shall be subject to any penalty for failing to comply with a collection of information if it does not display a currently valid OMB control number. **PLEASE DO NOT RETURN YOUR FORM TO THE ABOVE ADDRESS.**

1. REPORT DATE	**2. REPORT TYPE**	**3. DATES COVERED**
October 2021	FINAL	01Jul2017 – 30Jun2021

4. TITLE AND SUBTITLE
Receptor for AGE (RAGE) Signal Transduction in Amyotrophic Lateral Sclerosis: In Vivo Imaging and Novel Therapeutic Approaches

5a. CONTRACT NUMBER
W81XWH-17-1-0346

5b. GRANT NUMBER

5c. PROGRAM ELEMENT NUMBER

6. AUTHOR(S)
Ann Marie Schmidt, MD

E-Mail: AnnMarie.Schmidt@nyulangone.org

5d. PROJECT NUMBER

5e. TASK NUMBER

5f. WORK UNIT NUMBER

7. PERFORMING ORGANIZATION NAME(S) AND ADDRESS(ES)
550 First Avenue
New York, NY 10016

8. PERFORMING ORGANIZATION REPORT NUMBER

9. SPONSORING / MONITORING AGENCY NAME(S) AND ADDRESS(ES)

U.S. Army Medical Research and Development Command
Fort Detrick, Maryland 21702-5012

10. SPONSOR/MONITOR'S ACRONYM(S)

11. SPONSOR/MONITOR'S REPORT NUMBER(S)

12. DISTRIBUTION / AVAILABILITY STATEMENT

Approved for Public Release; Distribution Unlimited

13. SUPPLEMENTARY NOTES

14. ABSTRACT
ALS is a fatal neurodegenerative disorder resulting in paralysis of skeletal muscle and respiratory failure, with higher incidence in persons with military service. Pathological levels of receptor for advanced glycation end products (RAGE) ligands and RAGE accumulate in ALS in the CNS in humans and mice. We previously treated male *SOD1*^{G93A} mice with sRAGE, the extracellular ligand-binding domains of RAGE; sRAGE prolonged life span and improved motor function vs. vehicle. sRAGE is not a viable therapeutic agent. During this grant, we showed: (1) RAGE expression in microglia in the ALS spinal cord exerts maladaptive effects on survival and motor function in male *SOD1*^{G93A} mice. (2) We showed that a key chemical probe, RAGE229 small molecule antagonist of RAGE, shows promise to affect survival and motor function in *SOD1*^{G93A} mice and to reduce pathological neuroinflammation in the spinal cord. (3) We tracked mitochondrial metabolism in *SOD1*^{G93A} mice; compared to non-*SOD1*^{G93A} mice or *SOD1*^{G93A} mice treated with RAGE229, vehicle-treated *SOD1*^{G93A} mice showed the lowest mitochondrial tracer uptake in the spinal cord. CD11B+ microglia content in the ventral horn was reduced in the RAGE229 vs. vehicle mice. This work indicates that is logical to target RAGE-DIAPH1 in ALS.

15. SUBJECT TERMS
Amyotrophic lateral sclerosis, DIAPH1, Microglia, Neurodegeneration, Receptor for advanced glycation end products, Small molecule antagonists

16. SECURITY CLASSIFICATION OF:			**17. LIMITATION OF ABSTRACT**	**18. NUMBER OF PAGES**	**19a. NAME OF RESPONSIBLE PERSON**
a. REPORT	**b. ABSTRACT**	**c. THIS PAGE**			USAMRMC
Unclassified	Unclassified	Unclassified	Unclassified	79	**19b. TELEPHONE NUMBER** *(include area code)*

TABLE OF CONTENTS

1. INTRODUCTION:

Amyotrophic lateral sclerosis (ALS) is a fatal neurodegenerative disorder that results in paralysis and death within a few years of diagnosis. Evidence indicates that in both male and female U.S. Veterans, the incidence of ALS is increased compared to age-matched non-Veteran persons. Because of the devastation of this disorder, urgent efforts are required to identify the causes of and new therapies for ALS. Published work from our laboratory and others has shown that the receptor for advanced glycation end products (RAGE) is highly expressed in human ALS spinal cord, particularly in microglia, and to increased degrees vs. age-matched control subject spinal cord. We previously published that RAGE and its pro-inflammatory and pro-oxidative ligands, S100/calgranulins, amphoterin (high mobility group box 1 (HMGB1)), and advanced glycation end products (AGEs), are highly expressed in human ALS spinal cord. Our published work tested administration of a soluble form of RAGE in the mutant *SOD1*^{G93A} mouse model of ALS. We treated male mutant *SOD1*^{G93A} mice with either soluble RAGE (sRAGE), a recombinant protein that sequesters RAGE ligands and suppresses their engagement of the cell surface receptor RAGE, or vehicle, murine serum albumin (MSA), beginning at age 56 days (pre-symptomatic) and continued once daily until sacrifice (20% weight loss *or* the inability of the animal to right itself within 20 seconds when placed on its side). Probability of survival and life span, motor function (grip strength and performance in hanging cage test) and spinal cord neuronal counts at sacrifice were significantly higher in sRAGE- vs. MSA-treated mice. These findings formed the basis of two specific goals for our successfully completed grant: (1) Identification of the specific mechanisms by which RAGE contributes to ALS; and (2) To begin to develop a more feasible strategy to target RAGE, rather than a recombinant protein, our laboratory developed and recently reported on the generation of novel small molecule inhibitors of the interaction of the RAGE cytoplasmic domain with its intracellular signaling effector, DIAPH1. These small molecules block RAGE signaling and suppress RAGE-mediated inflammation in animals and are CNS-permeable. Therefore, we hypothesize that administration of these small molecules to *SOD1*^{G93A} mice might exert beneficial effects in murine model of ALS. Collectively, these questions form the basis of our studies.

2. KEYWORDS:

1). Amyotrophic lateral sclerosis
2). DIAPH1
3). Microglia
4). Neurodegeneration
5). Receptor for advanced glycation end products
6). Small molecule antagonists

3. ACCOMPLISHMENTS:

A. What were the major goals of the project?

Aim 1: We will test the hypothesis that microglia RAGE, through ligand-driven upregulation of inflammatory and pro-oxidative stress and suppression of reparative processes in the ALS spinal cord, mediates neuronal death and loss of motor function.
Task 1: Generate ALS mice (SOD1^{G93A}) with microglia deletion of *Ager*
Task 2: PET Imaging

Aim 2: We will test the hypothesis that small molecule inhibitors of RAGE signal transduction will significantly prolong survival and delay neurodegeneration in mutant *SOD1*^{G93A} mice in proof-of-concept studies.

B. What was accomplished under these goals?

B.i. Major Activities
TASK 1: *Generate ALS mice (SOD1*^{G93A}) with microglia deletion of *Ager*
The breeding scheme as outlined in the proposal is generating the male and female mice needed for study. We used the *SOD1*^{G93A} mouse model into which we bred the *Cx3cr1*^{ERT2} cre recombinase mice and the *Ager* flox/flox. We carefully managed this breeding such that at breeding intervals we reintroduced new *SOD1*^{G93A} breeders and, therefore, the copy number in all offspring tested has been acceptable. Tamoxifen has been administered to all mice in the study on day 90 in order to ensure deletion of microglia *Ager* and not in the periphery by approximately day 100 (disease onset). The following endpoints are completed, including: analysis of survival, establishing the humane endpoint, and functional tests as outlined (motor function tests including hanging wire test, grip strength and righting reflex), isolation of microglia, and pathological analyses). Based on the efficiency of breeding, all of the mice have now been generated to test Aim 1 hypothesis.

Aim 1: We will test the hypothesis that microglia RAGE, through ligand-driven upregulation of inflammatory and pro-oxidative stress and suppression of reparative processes in the ALS spinal cord, mediates neuronal death and loss of motor function.

Our major activities include the completion of the breeding *SOD1*^{G93A} mice into the *Ager* flox/flox background and then intercrossing these mice into the *Cx3cr1* ERT2 cre recombinase background and we successfully generated the following lines of mice (both males and females).
SOD1^{G93A} / *Ager*$^{flox/flox}$ / *Cx3cr1*$^{CreERT2\ +/wt}$ (ALS+, Microglia specific *Ager* deletion)
SOD1^{G93A} / *Ager*$^{flox/flox}$ / *Cx3cr1*$^{CreERT2\ wt/wt}$ (ALS + *Ager* expressed in all cells)
SOD1^{G93A} / *Cx3cr1*$^{CreERT2\ +/wt}$ (ALS + *Ager* expressed in all cells; controls for CRE mice)

TASK 2: PET Imaging
In collaboration with Dr. Ding, we performed PET imaging of the ALS and control mice.

AIM 2: We will test the hypothesis that small molecule inhibitors of RAGE signal transduction will significantly prolong survival and delay neurodegeneration in mutant *SOD1*^{G93A} mice in proof-of-concept studies. Our lab made significant progress to identify the optimal small molecule that met multiple criteria to go forward for in vivo testing.

B.ii. Specific Objectives
Objective in Aim 1: We will test the hypothesis that microglia RAGE, through ligand-driven upregulation of inflammatory and pro-oxidative stress and suppression of reparative processes in the ALS spinal cord, mediates neuronal death and loss of motor function.
There were two major tasks: generation of ALS mice with microglia deletion of *Ager* and PET imaging of ALS vs. control mice to discern if there were differences in neuroinflammation
Objective in Aim 2: We will test the hypothesis that small molecule inhibitors of RAGE signal transduction will significantly prolong survival and delay neurodegeneration in mutant *SOD1*^{G93A} mice in proof-of-concept studies.

B.iii. Significant Results or Key Outcomes
Aim 1:
TASK 1: ALS, RAGE and Microglia

Results
We sought to examine if microglia expressed RAGE in a prototypic murine model of ALS, the *SOD1*^{G93A} model. We began by performing immunohistochemistry (IHC) in *SOD1*^{G93A} and wild-type (WT) mice (C57BL/6J background) lumbar spinal cord tissue at age 120 days. The overlap area of RAGE with the myeloid marker, integrin subunit alpha m (CD11B), was higher in *SOD1*^{G93A} mice vs. littermate WT control mice (Figure 1 A-B). While RAGE is expressed in multiple cell-types in spinal cord, the findings that RAGE overlap with microglia is increased in *SOD1*^{G93A} mice implicating the AGE-RAGE pathway alteration in glia, suggested it was logical to probe potential roles for microglia RAGE in ALS-like pathology in the *SOD1*^{G93A} mouse model.

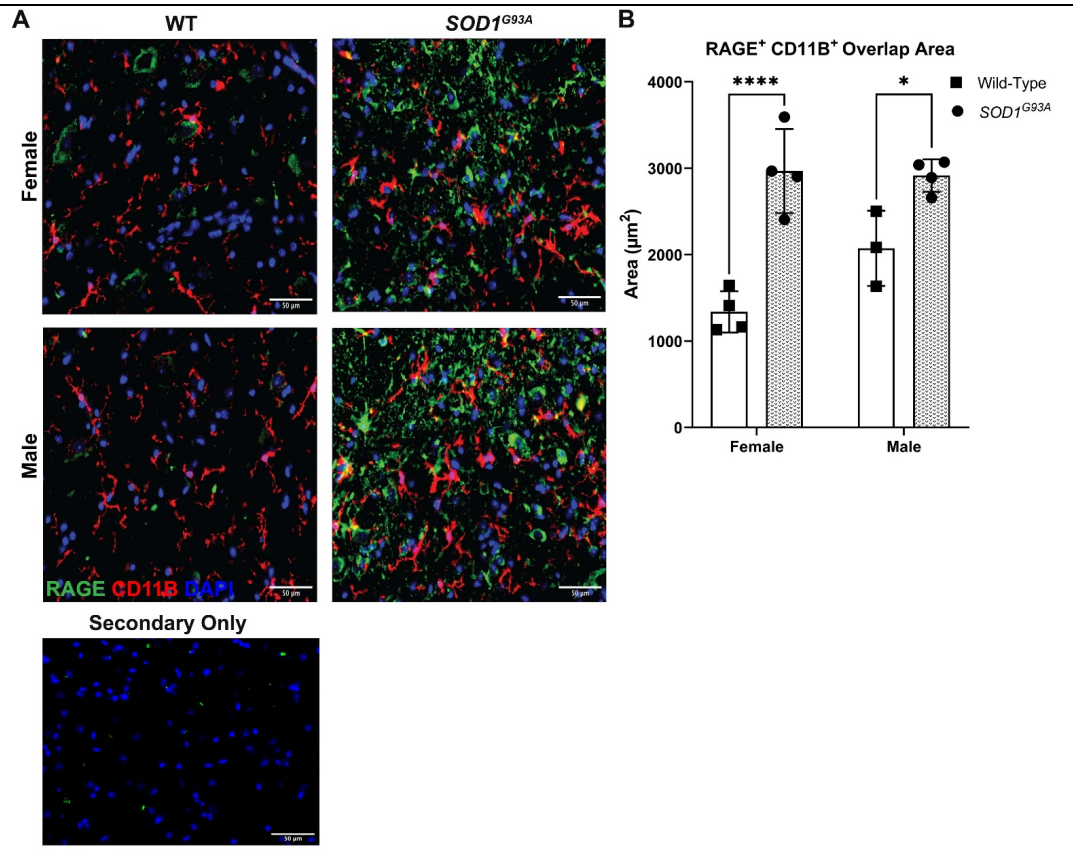

Figure 1: $SOD1^{G93A}$ mice exhibit increased $RAGE^{+}$ microglia at the age of 120 days. **A.** Representative images of CD11B and RAGE staining in the ventral horn of $SOD1^{G93A}$ mouse lumbar spinal cord. Scale bar: 50 µm. **B.** Quantification of overlap of $CD11B^{+}$ $RAGE^{+}$ area. *N*=3 male WT mice, *N*=4 male $SOD1^{G93A}$ mice, *N*=4 female WT mice, and *N*=4 female $SOD1^{G93A}$ mice. Mean ± SD. Two-way ANOVA with post-hoc Tukey's test. * p=0.0192, **** p<0.0001.

Based on these findings, we sought to assess whether microglia RAGE affects the pathological progression of $SOD1^{G93A}$ mice. We employed a tamoxifen (TAM)-inducible model in which microglia expressed *Ager* during development and early life and administered TAM to all mice at the age of 90 days to induce *Ager* deletion in $SOD1^{G93A}$ $Ager^{fl/fl}$ $Cx3cr1^{Cre/+}$, and $SOD1^{G93A}$ $Ager^{+/+}$ $Cx3cr1^{Cre/+}$ mice to evaluate potential roles for RAGE in the progression of pathology (Figure 2 A). We confirmed knock-down of *Ager* expression in primary CD11B cell isolates from CNS tissues (Figure 2 B). RAGE overlap with IBA1, but not GFAP, was decreased in $SOD1^{G93A}$ $Ager^{fl/fl}$ $Cx3cr1^{Cre/+}$ lumbar spinal cord tissue relative to Cre-expressing controls at the end of the study, suggesting *Ager* knock-down in microglia was maintained (Figure 2 C-D). RAGE overlap with the pan neuronal marker microtubule-associated protein 2 (MAP2) at the age of 120 days did not differ between the two genotypes, suggesting that neuronal *Ager* was not modulated by this approach in this study.

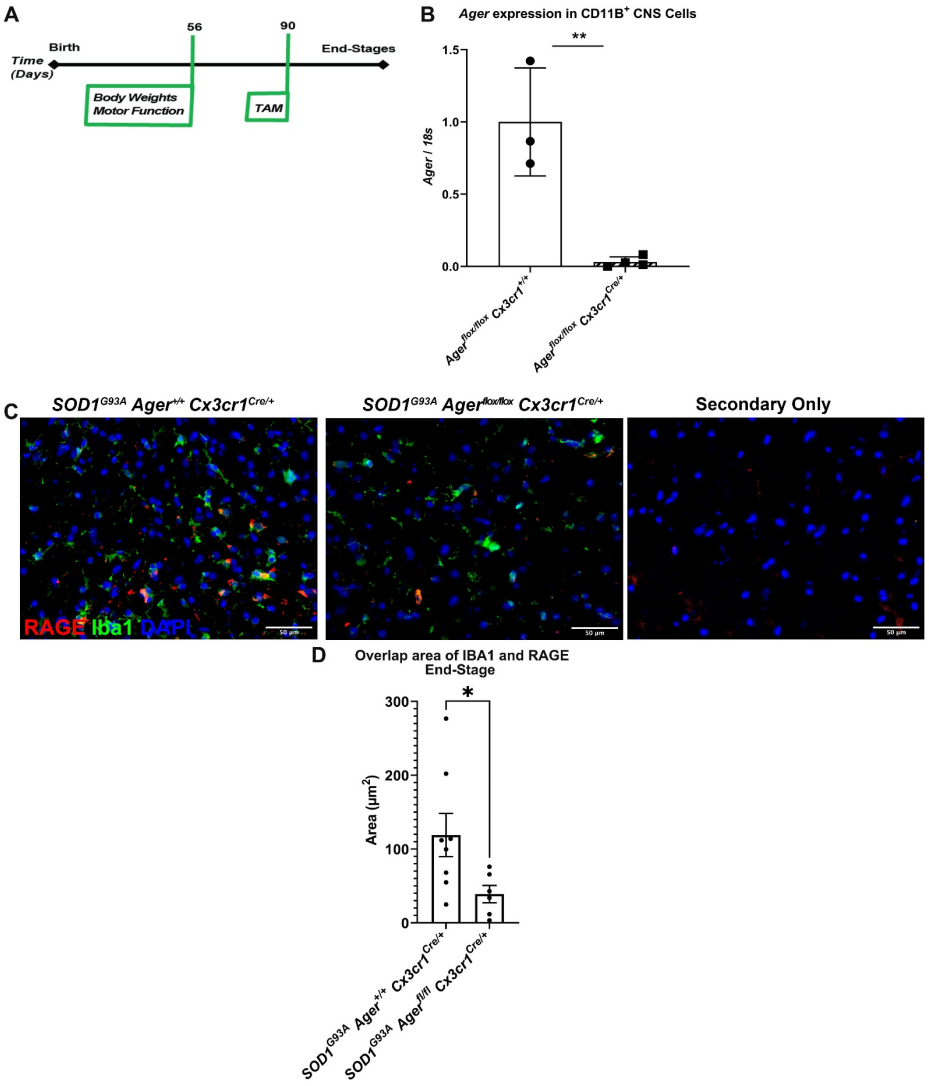

Figure 2. Study design and validation of microglia Ager deletion.
A. Timing of Tamoxifen (TAM) administration and behavioral assessments of animals. **B.** Quantification of *Ager* transcripts in primary CD11B^{+} isolates by RT-qPCR thirty days after TAM administration. **C.** Representative images of IBA1 and RAGE staining in the ventral horn of *SOD1^{G93A}* mouse lumbar spinal cord at end-stage. Scale bar: 50 µm. **D.** Quantification of IBA1 and RAGE overlap area. Mean±SD. In **B**, *N*=3 *Ager*$^{fl/fl}$ *Cx3cr1*$^{+/+}$ mice and *N*=4 *Ager*$^{fl/fl}$ *Cx3cr1*$^{Cre/+}$ mice. In **C-D**, *N*=6 *SOD1^{G93A} Ager*$^{fl/fl}$ *Cx3cr1*$^{Cre/+}$ mice, *N*=8 *SOD1^{G93A} Ager*$^{+/+}$ *Cx3cr1*$^{Cre/+}$ mice. Independent two sample two-sided *t*-test. ** p=0.0031, *p=0.0437.

As *Cx3cr1* Cre-expressing mice, regardless of the administration of TAM, or not, are heterozygous for the *Cx3cr1* locus, we evaluated *SOD1^{G93A} Ager*$^{+/+}$ *Cx3cr1*$^{Cre/+}$ (microglia *Ager*-expressing, *Cx3cr1* Cre-expressing) and *SOD1^{G93A} Ager*$^{fl/fl}$ *Cx3cr1*$^{Cre/+}$ (microglia *Ager* deficient, *Cx3cr1*-Cre expressing) mice. We found that male *SOD1^{G93A} Ager*$^{fl/fl}$ *Cx3cr1*$^{Cre/+}$ mice displayed significantly longer survival relative to *SOD1^{G93A} Ager*$^{+/+}$ *Cx3cr1*$^{Cre/+}$ mice, median lifespan of 159 (range: 149d-175d) days vs. 152 days (range: 136d-171d) days, respectively; p<0.05 (Figure 3 A). We did not observe differences in lifespan between the

female mice groups (Figure 3 B). These data suggested that microglia RAGE may contribute to pathology progression in male *SOD1*^{G93A} mice.

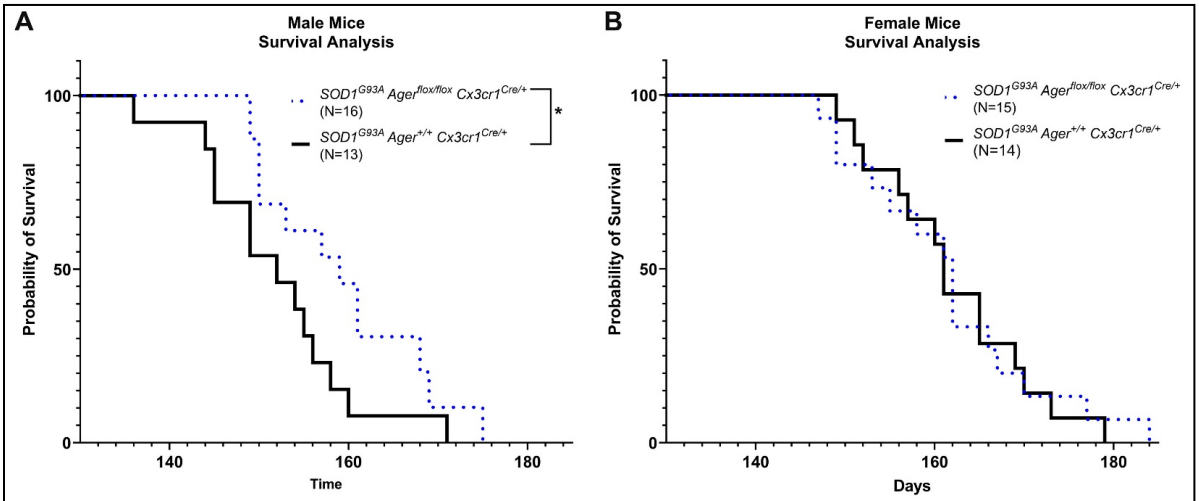

Figure 3: Microglia Ager deletion exerts sex-dependent effects on survival in SOD1^{G93A} *mice.* ***A****. Kaplan–Meier estimates of percent of male mice surviving plotted vs. age (days). N=16 SOD1*^{G93A} *Ager*$^{fl/fl}$ *Cx3cr1*$^{Cre/+}$ *mice, and N=13 SOD1*^{G93A} *Ager*$^{+/+}$ *Cx3cr1*$^{Cre/+}$ *mice.* ***B****. Kaplan–Meier estimates of percent of female mice surviving plotted vs. age (days). N=15 SOD1*^{G93A} *Ager*$^{fl/fl}$ *Cx3cr1*$^{Cre/+}$ *mice, and N=14 SOD1*^{G93A} *Ager*$^{+/+}$ *Cx3cr1*$^{Cre/+}$ *mice. The Logrank test was performed to compare the survival distributions between groups.* * *p=0.0496.*

We next investigated if microglia *Ager* contributed to the progressive motor function decline experienced by *SOD1*^{G93A}. Mixed effects analysis of motor function data indicated a significant interaction between time and genotype in male but not female mice (*p=0.038)* suggesting that male but not female *SOD1*^{G93A} *Ager*$^{fl/fl}$ *Cx3cr1*$^{Cre/+}$ mice had time-dependent protection in motor function (Figure 4 A-B). However, there were no significant differences in motor function at any one time point after multiple corrections in either male or female mice (Figure 4 A-B).

As *SOD1*^{G93A} mice experience pronounced weight loss with disease progression, we next examined if microglia *Ager* expression modulated this weight loss. Mixed effects analysis of body weight data normalized to weight at tamoxifen administration indicated significant interactions between time and genotype in male and female mice (*p=0.0067, p=0.0134* respectively*)* suggesting that in *SOD1*^{G93A} *Ager*$^{fl/fl}$ *Cx3cr1*$^{Cre/+}$ mice there are time dependent alterations in body weight (Figure 4 C-D). However, there were no significant differences in normalized body-weight measures at any single time point after multiple corrections in male or female mice (Figure 4 C-D). As female mice did not display any significant differences in survival, or motor function, we focused our in-depth mechanistic analyses on male mice.
While no significant differences in motor function or body weight were noted at any single time point, there were time-dependent reductions in the rate of motor function decline and weight in male *SOD1*^{G93A} *Ager*$^{fl/fl}$ *Cx3cr1*$^{Cre/+}$ mice suggesting a slower rate of disease

progression. This led us to consider the possibility that microglia *Ager* deletion may have affected the numbers of surviving motor neurons within the lumbar ventral horn. We examined the number of surviving motor neurons by IHC at the age of 120 days in male mice and found significantly higher numbers of motor neurons, as labeled by NeuN, DAPI and choline acetyltransferase (ChAT), in the lumbar ventral horn in the *SOD1*^{G93A} *Ager*$^{fl/fl}$ *Cx3cr1*$^{Cre/+}$ mice relative to the Cre-recombinase expressing controls (Figure 4 E-F). Altogether, these data suggest that deletion of microglia *Ager* may reduce/delay neuron death in male *SOD1*^{G93A} mice. These findings led us to perform additional experiments to provide insight into the mechanisms by which this protection may occur.

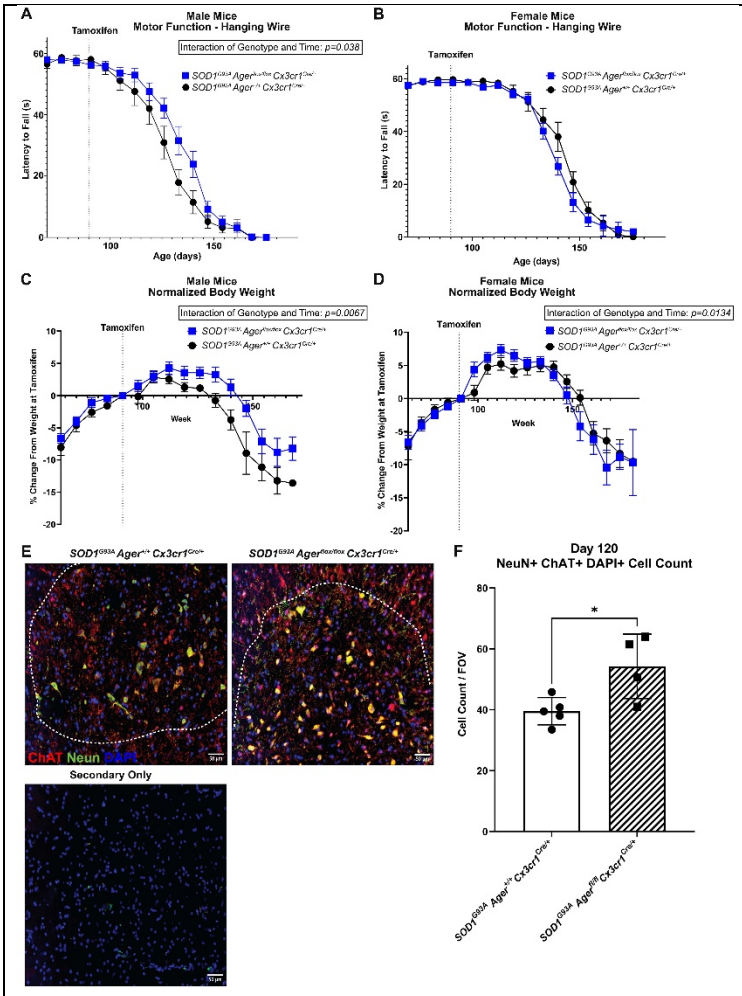

Figure 4: SOD1^{G93A}*mice with microglia Ager deletion exhibit sex-dependent effects on pathology.*
A. Latency to fall as measured by hanging wire test in male mice. **B.** Latency to fall as measured by hanging wire test in female mice. **C.** Normalized body weight to weight at tamoxifen administration of male mice. **D.** Normalized body weight to weight at tamoxifen administration of female mice. Dashed lines indicates age at tamoxifen administration. Mean±SEM. **E.** Representative images of NeuN and DAPI staining in the lumbar spinal cord ventral horn. Scale bar: 50µm. **F.** Quantification of NeuN^{+} DAPI^{+} cell number. Mean±SD. In A and C (male mice): *N*=16 *SOD1*^{G93A} *Ager*$^{fl/fl}$ *Cx3cr1*$^{Cre/+}$ mice, and *N*=13 *SOD1*^{G93A} *Ager*$^{+/+}$ *Cx3cr1*$^{Cre/+}$ mice. In B and D (female mice): *N*=15 *SOD1*^{G93A} *Ager*$^{fl/fl}$ *Cx3cr1*$^{Cre/+}$ mice, and *N*=14 *SOD1*^{G93A} *Ager*$^{+/+}$ *Cx3cr1*$^{Cre/+}$ mice. In E-F (male mice): *N*=4 *SOD1*^{G93A} *Ager*$^{fl/fl}$ *Cx3cr1*$^{Cre/+}$ mice, and *N*=5 *SOD1*^{G93A} *Ager*$^{+/+}$ *Cx3cr1*$^{Cre/+}$ mice. In A-D: Independent two-sample two-sided *t*-test was used to assess the group difference at each time point. Mixed effects analysis was utilized to evaluate effects of genotype, time and the interaction between genotype and time. In A: Genotype*Time interaction effect: *p*=0.0378. In C: Genotype effect: *p*=0.0157, Genotype*Time interaction effect: *p*=0.0067. In D: Genotype*Time interaction effect= *p*=0.0134. In F: Independent two sample two-sided *t*-test. In F: * *p*=0.0224.

To uncover cell intrinsic and cell-cell communication pathway mechanisms underlying the benefits of microglia *Ager* deletion in male *SOD1*^{G93A} mice, we performed RNA-seq on isolated lumbar spinal cord tissue from male *SOD1*^{G93A} *Ager*$^{fl/fl}$ *Cx3cr1*$^{Cre/+}$ mice and *SOD1*^{G93A}

Ager$^{+/+}$ *Cx3cr1*$^{Cre/+}$ mice at humane endpoint (end-stage). We identified 78 differentially-expressed genes between the two genotypes (Figure 5). Overrepresentation analysis of the differential gene list indicated enrichment for several KEGG Pathways, which included: "Cardiac muscle contraction", "Calcium signaling pathway", "PPAR signaling pathway", "Regulation of actin cytoskeleton", and "Cholesterol metabolism". Furthermore, canonical pathway analysis using Ingenuity Pathway Analysis (IPA) indicated enrichment of several pathways within the differential gene list including "Calcium signaling", "Actin cytoskeleton signaling" and "Integrin signaling." These data suggest genotype-dependent effects on cell-cell crosstalk mechanisms, as exemplified by alterations of lipid, metabolic, and integrin signaling gene sets.

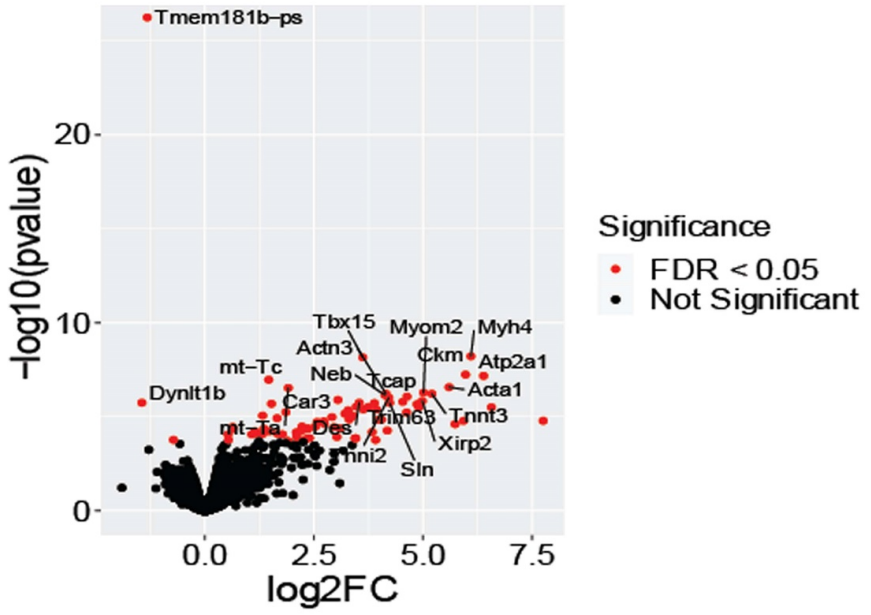

Figure 5: Differential expression analysis between male SOD1^{G93A} *mice with microglia devoid of Ager and Cre-expressing controls.* Volcano plot displaying differentially expressed genes between *SOD1*^{G93A} *Ager*$^{fl/fl}$ *Cx3cr1*$^{Cre/+}$ and *SOD1*^{G93A} *Ager*$^{+/+}$ *Cx3cr1*$^{Cre/+}$ mice. The y-axis is $-\log_{10}$(p-value) and x-axis is the Log_2 fold change of each gene analyzed. Red colored genes are significantly differentially expressed with an FDR <0.05. The top twenty significant genes are labeled. *N*=4 independent mice/group.

To further address this concept, we analyzed potential causal networks that may be modulated in our dataset, which could explain the observed transcriptomic changes. As *Ager* was deleted solely in *Cx3cr1*-expressing cells, we limited our analysis to potential cytokines that could originate from microglia and cause transcriptomic alterations across multiple cell types which would be present in the bulk RNA-sequencing data. We identified several significant putative causal networks belonging to numerous cytokine families, including interleukin-1 (IL1), interleukin-3, interferon-α (IFN-α), and interferon-β (IFN-β).

To evaluate potential roles of microglia RAGE in mediating cytokine expression changes we turned to an *in vitro* system. We first conducted a commercially-available cytokine screen to

evaluate RAGE-dependent effects of RAGE ligand carboxymethyllysine (CML)-AGE, a ligand increased in *SOD1*^{G93A} spinal cords and in human patient tissues, on BV2 microglia-like cells. An interesting candidate discovered by this approach was *Il1a*, as this was also predicted by the RNA-seq causal network analysis. In fact, in validation experiments, CML-AGE significantly induced *Il1a* expression, which was significantly reduced by pre-treatment with a RAGE inhibitor in BV2 cells. Furthermore, lentiviral transduction of BV2 cells with short hairpin RNA to significantly reduce *Ager* expression in BV2 cells prevented the CML-AGE associated increase in *Il1a* expression. Expression of *Malat1*, a differentially expressed inflammation-associated lncRNA in the microglia *Ager*-deficient spinal cord, exhibited a RAGE-dependent increase in BV2 cells in response to CML-AGE. Collectively, these results pointed to significant modulation of intrinsic microglia inflammation. In one or more cell types, prompted by microglia *Ager* deletion, fundamental changes in general cellular health are observed, as exemplified by alterations in actin cytoskeleton and calcium related pathways, both of which would be predicted to fundamentally alter cell intrinsic and intercellular communication properties in the spinal cord. To verify the implications of these transcriptomic alterations, we examined these points specifically in end-stage tissues.

The RNA-seq data analysis suggested that microglia *Ager* deletion resulted in reduction in IL1 and IFN signaling, both of which were previously suggested to be dysfunctional in ALS models and in patients. In fact, *in vitro* experiments supported microglia RAGE affecting *Il1a* and *Malat1* expression. Beyond the number and density of microglia, their specific gene expression patterns aid in designation of these cells as pro-damage vs. homeostatic phenotype. Specifically, the c-type lectin domain containing 7a protein (CLEC7A) is an established marker of pro-damage/disease-associated microglia, which has been shown to be highly upregulated in *SOD1*^{G93A} microglia. By IHC, at end-stage, we found that there was a significant reduction in CLEC7A^{+} area, and CLEC7A^{+} cell number in *SOD1*^{G93A} *Ager*$^{fl/fl}$ *Cx3cr1*$^{Cre/+}$ vs. *SOD1*^{G93A} *Ager*$^{+/+}$ *Cx3cr1*$^{Cre/+}$ mice (Figure 6 A-C), suggesting that an attenuated or altered DAM phenotype was induced by deletion of microglia *Ager*. These key findings raise the possibility that RAGE contributes to a cell-intrinsic transition of microglia from a homeostatic to a dysfunctional phenotype.

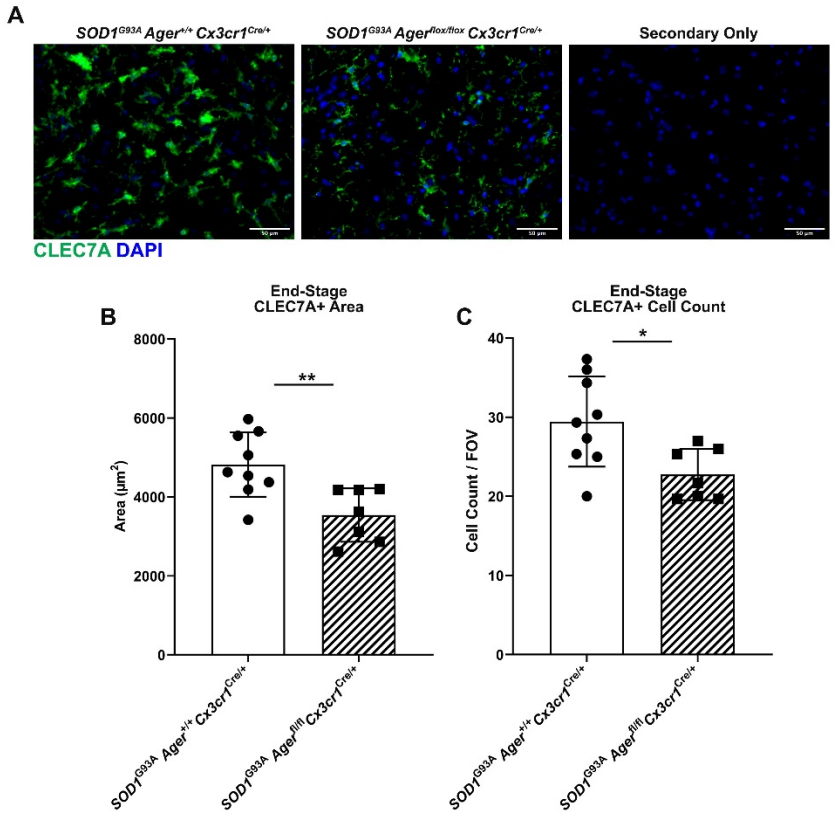

Figure 6: Microglia Ager deletion in male SOD1^{G93A} mice reduces the accumulation of disease-associated microglia at end-stage. **A.** Representative images of CLEC7A staining in the lumbar spinal cord ventral horn of the indicated mouse groups. Scale bar: 50µm. **B.** Quantification of CLEC7A^{+} area. **C.** Quantification of CLEC7A^{+} DAPI^{+} cell number. Mean±SD. *N*=7 *SOD1*^{G93A} *Ager*$^{fl/fl}$ *Cx3cr1*$^{Cre/+}$ mice and *N*=9 *SOD1*^{G93A} *Ager*$^{+/+}$ *Cx3cr1*$^{Cre/+}$ mice. Independent two sample two-sided *t*-test. In B: ** $p<0.0048$. In C: * $p=0.0154$.

The RNA-seq results indicated reduction of a putative causal network involving IL1. In this context, accumulating evidence suggests that microglia-secreted molecules complement component 1q (C1q), IL1α, and TNF can induce astrocyte reactivity and promote neurotoxicity. Prompted by this consideration, we thus investigated if the *SOD1*^{G93A} *Ager*$^{fl/fl}$ *Cx3cr1*$^{Cre/+}$ mice displayed alterations in astrocytes. At end-stage, we found that GFAP^{+} area was significantly lower in *SOD1*^{G93A} *Ager*$^{fl/fl}$ *Cx3cr1*$^{Cre/+}$ mice relative to Cre-expressing controls (Figure 7 A-B). Recent work has suggested distinct reactive astrocyte phenotypes and identified markers of those states. AMIGO2, adhesion molecule with Ig-like domain 2, was proposed as a marker of "A1" reactive inflammatory astrocytes induced specifically by C1q, IL1α and TNF. Although it is acknowledged that this classification likely does not illuminate the breadth of astrocyte properties and contributions to ALS operative *in vivo*, we nevertheless examined if the GFAP alterations were concomitant alongside alterations in "A1" astrocytes to begin to define if microglia RAGE might impact astrocyte gene expression. Indeed, we found that GFAP^{+} AMIGO2^{+} overlap area was significantly reduced in *SOD1*^{G93A} *Ager*$^{fl/fl}$ *Cx3cr1*$^{Cre/+}$ mice vs. the Cre-expressing controls (Figure 7 A,C). Altogether, these data suggest

that microglia *Ager* deletion may reduce astrocytic dysfunction likely through altered cytokine expression.

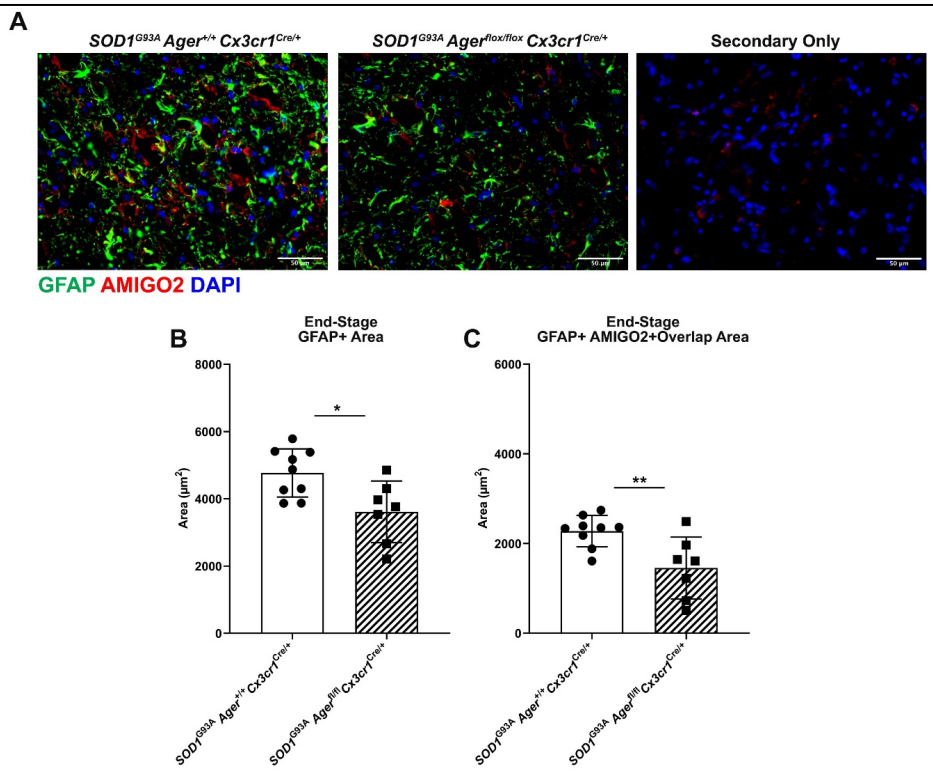

Figure 7: Reactive A1 astrocytes are reduced in male SOD1^{G93A} mice by microglia Ager deletion. ***A.*** *Representative images of GFAP and AMIGO2 staining in the lumbar spinal cord ventral horn of the indicated mouse groups.* ***B.*** *Quantification of GFAP$^+$ area.* ***C.*** *Quantification of GFAP$^+$ and AMIGO2$^+$ overlap area. Mean±SD. N=7 SOD1^{G93A} Ager$^{fl/fl}$ Cx3cr1$^{Cre/+}$ mice, and N=9 SOD1^{G93A} Ager$^{+/+}$ Cx3cr1$^{Cre/+}$ mice. Independent two sample two-sided t-test. In B: * p=0.0132. In C: ** p=0.0076.*

We next considered that it was important to also examine microglia and expression of CLEC7A at a time point within the progression phase, but short of end-stage analysis. It is important to note that microglial CLEC7A expression increases over time in this model, and not all microglia may have notable expression of CLEC7A at 120 days of age. Thus, we addressed this point by examining the expression of both CD11B and CLEC7A at day 120. The results indicated significant reductions in the amount of CD11B$^+$ cells and CD11B$^+$ area in *SOD1^{G93A}* mice devoid of microglia *Ager* (Figure 8 A-C). Similar to the end-stage tissue analysis, we observed reduced CLEC7A$^+$ area at day 120 (Figure 8 D-E). Altogether, these data suggested that RAGE expression on microglia may contribute to the promotion of microgliosis (Figure 8 A-C), and may affect CLEC7A expression at a stage within the microglia phenotypic transition but prior to frank end-stage tissue pathologies (Figure 8 D-E). As such, we surmised that the overall RAGE-dependent mechanisms in microglia in *SOD1^{G93A}* mice were likely through alterations in microglia cell intrinsic and cell-cell communication pathways between microglia and other cell-types.

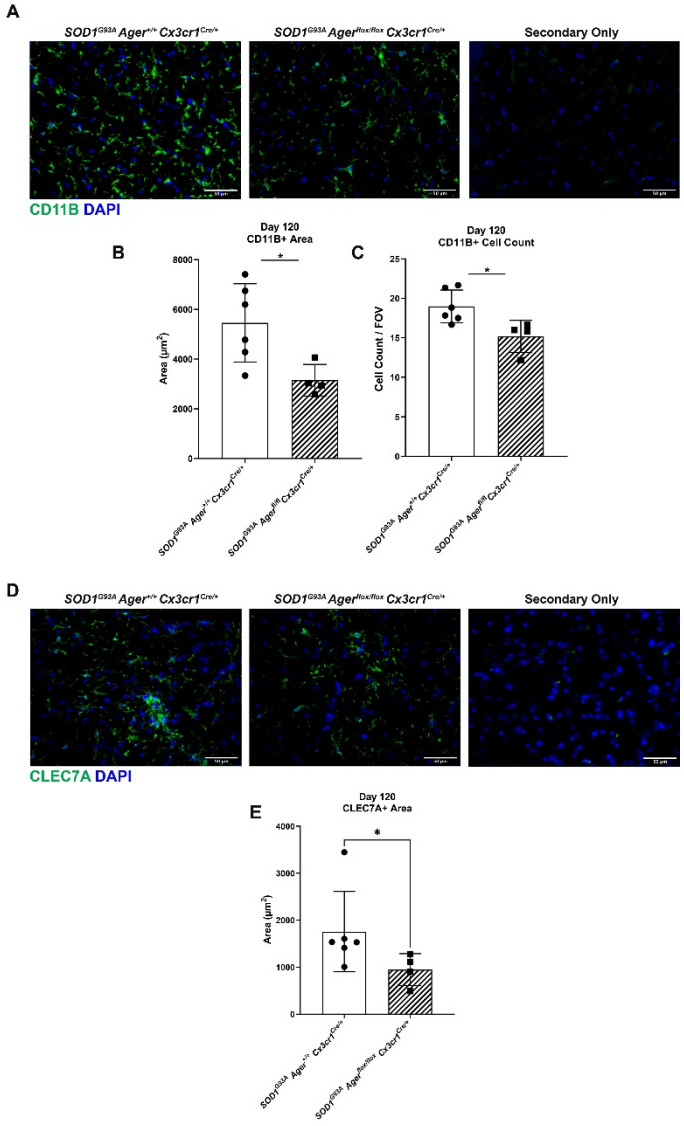

Figure 8: Microglia Ager deletion in male SOD1^{G93A} mice reduces microgliosis at 120 days of age.
A. *Representative images of CD11B staining in the lumbar spinal cord ventral horn of the indicated mouse groups.* ***B.*** *Quantification of CD11B^{+} area.* ***C.*** *Quantification of CD11B^{+} DAPI^{+} cell number.* ***D.*** *Representative images of CLEC7A staining in the lumbar spinal cord ventral horn of the indicated mouse groups.* ***E.*** *Quantification of CLEC7A^{+} area. Mean±SD. N=4 SOD1^{G93A} Ager$^{fl/fl}$ Cx3cr1$^{Cre/+}$ mice, N=6 SOD1^{G93A} Ager$^{+/+}$ Cx3cr1$^{Cre/+}$ mice. In B-C: Independent two sample two-sided t-test. In E: Mann-Whitney U-test. In B: * p=0.0253. In C: * p=0.0212. In E: *p=0.0381.*

TASK 2: PET Imaging

These studies were based on the premise that evidence suggests that Translocator Protein (TSPO) target of the tracer [^{11}C]PBR28) is involved in cellular and mitochondrial functions, as knockout of TSPO in human C20 microglia significantly decreased membrane potential and cytosolic calcium levels and reduced respiratory function. When "rescued" by overexpression of TSPO, increased oxygen consumption was restored along with respiratory function. It is conceivable that [^{11}C]PBR28 is measuring the state of mitochondrial function/metabolism rather than "inflammation". We performed studies to test the effects of RAGE229 in murine ALS. Remarkably, compared to WT (non-*SOD1^{G93A}*) mice (BLUE) or *SOD1^{G93A}* mice treated with small molecule and CNS-permeable small molecule antagonist of RAGE-DIAPH1 interaction, called RAGE229 (GREEN) (intraperitoneal, d 90-120), the vehicle-treated *SOD1^{G93A}* mice (RED) showed the lowest PBR uptake in the T13, L1, L2 and L3 spinal cord (Figure 9). At sacrifice (d 120), CD11B+ microglia content in the ventral horn of the lumbar

spinal cord was reduced in the RAGE229 vs. vehicle-treated mice (Figure 9).

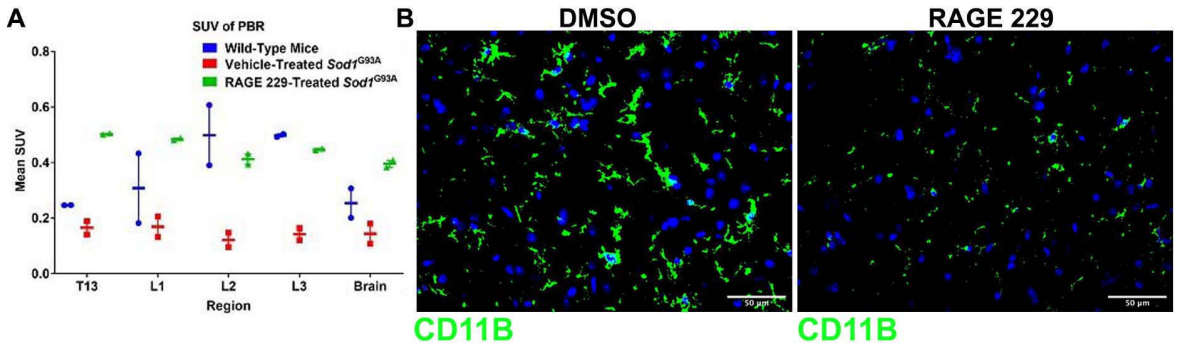

Figure 9. Administration of RAGE229 to SOD1^{G93A} mice restores uptake of TSPO-ligand [11]PBR28 to WT levels and reduces microgliosis. A). *CNS permeable RAGE229 or vehicle was administered by IP 2x daily from age 90 d to 120-125 d old male mice injected with [^{11}]PBR28 and subjected to PET and CT scans. The uptake within the whole brain and spinal cord T13, and L1-L3 regions was monitored and quantified as standardized uptake values (SUV). The last four time points of the scan are used to generate the mean SUV for each animal.* ***B).*** *In the mice described in A, treatment with RAGE229 vs. DMSO resulted in reduced CD11B+ staining (microglia) (green) (blue=DAPI), consistent with reduced microglia/myeloid cells. Representative image of N=3 mice/group is shown. Scale bar: 50 µm*

AIM 2:

In order to identify small molecule antagonists of the cytoplasmic tail (ct) RAGE-DIAPH1 interaction, we previously screened 59,000 ChemBridge CT488 library compounds at a single concentration, 10 µM. Thirteen compounds which specifically bound to ctRAGE, not DIAPH1, were identified with nM dissociation constants. In vascular cells, they blocked RAGE ligand-inflammation and migration, suppressed ischemic injury in the diabetic heart and blocked upregulation of inflammation after infusion of RAGE ligands into mice. From the 13 compounds, we identified two lead series (LS); LSII from "Compound 11" and LSI from "Compounds 3 and 4".

RAGE229*:* The 2-phenylquinoline scaffold is the high priority series (LSII) based on highly favorable *in vitro/in vivo* potency, *in vitro* ADME (Absorption, Distribution, Metabolism and Excretion), physical-chemical properties and *in vivo* PK in two species. After screening >250 analogues, RAGE229 has emerged as a strong candidate chemical probe for further testing. Extensive candidate selection profiling was performed by us and Contract Research Organizations (CROs) using several scale-ups of RAGE229 (>97.5% or >99.5% purity, with no impurity >0.3% or >0.1%, respectively). K_D=3 nM was established in *in vitro* binding to ctRAGE and there was selective activity in inhibition of RAGE ligand-stimulated vascular cell migration assay (IC_{50}=3 nM). ADME-PK properties were favorable and after PO dosing, high Cmax was observed (µM range) after 10 mg/kg was administered in rat and 5 mg/kg in dog, respectively. RAGE229 demonstrated high oral bioavailability (%F=54-100%). RAGE229 had a brain:plasma ratio >0.7 in mice. Experiments *in vivo* testing the effects of RAGE229 on delayed type hypersensitivity driven inflammation illustrated dose-dependent reduction in foot

pad inflammation by RAGE229.

We analyzed the effects of RAGE229 vs. vehicle on body weight and motor function after the age of 17 weeks when the most pronounced effects are noted. Early data suggest protective effects of RAGE229 vs. vehicle on weight loss and on decline of motor function by hanging wire test. At the humane endpoint, lumbar spinal cord was retrieved from RAGE229 vs. vehicle-treated mice for immunofluorescence microscopy (Figure 10).

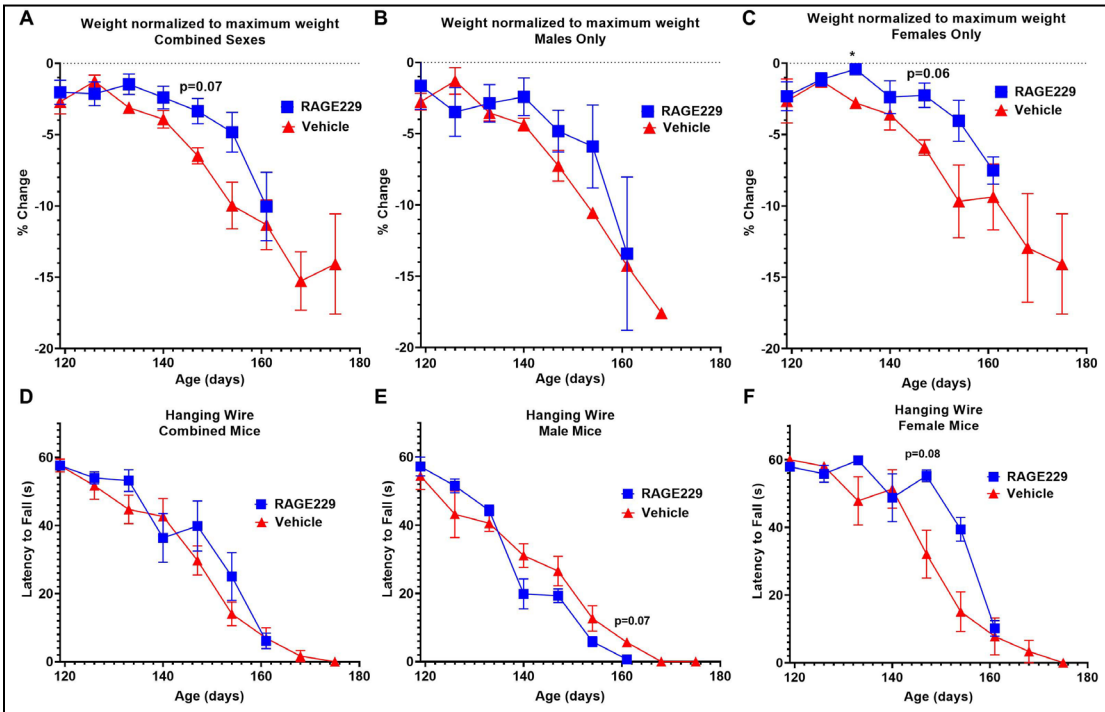

Figure 10. SOD1^{G93A} mice treated with RAGE229 may exhibit decreased weight loss and motor function decline after the age of 17 weeks. Percent change in body weight from maximum weight in RAGE229 or vehicle-treated SOD1^{G93A} mice of both sexes (A), male mice (B), and female (C) mice after the age of 119 d. B. Latency to fall as measured by the hanging wire test in RAGE229 or vehicle-treated SOD1^{G93A} mice of both sexes (D), male mice (E), and female (F) mice after the after the age of 119 d. In A and D, N=7 mice/group. In B and E, N=3 mice/group. In C and F, N=4 mice/group. Independent two-sample two-sided t-tests with post-hoc Holm-Sidak test was used to assess the group difference at each time point. Mean±SEM is shown.

We combined male/female mice in the analysis and found that there were no differences in CD11B+ area (Figure 11). In addition to general markers of microglia, we assessed levels of CLEC7A, an established marker of the pro-damage DAM phenotype in microglia and found that there were trends to reduced CLEC7A (pro-damage DAM marker) (area and intensity) in RAGE229- vs. vehicle-treated mice (Figure 11). Furthermore, there were trends to increased NeuN/ChAT (motor neuron) area in RAGE229- vs. vehicle (Figure 11).

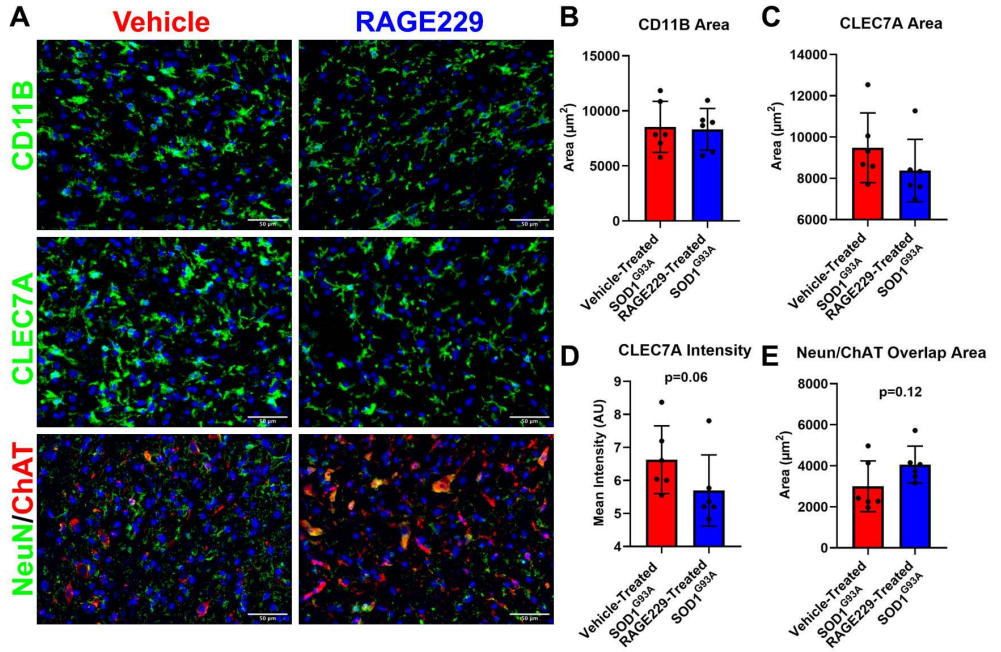

Figure 11. RAGE229 treatment initiated at 8 weeks of age of SOD1^{G93A} mice may reduce microglia transition to a DAM phenotype and reduce motor neuron death at sacrifice. **A.** Representative images of CD11B, CLEC7A, and NeuN and ChAT immunohistochemistry in lumbar spinal cord of indicated mouse groups. **B, C.** Quantification of CD11B and CLEC7A area after automated thresholding respectively. **D.** Quantification of CLEC7A intensity. E. Quantification of NeuN and ChAT overlap suggestive of motor neurons. N=6 mice/group. Mean±SD. Unpaired Student's t test used in B,C, and E. Mann-Whitney test used in D.

We found that there were no differences in GFAP- or the pro-damage reactive astrocyte marker, AMIGO2 between the two groups (combined male and female mice) (Figure 12). Collectively, these data suggest that RAGE229 may reduce weight loss and delay loss of motor function in *SOD1^{G93A}* mice, in parallel with reducing pro-damage DAM microglia markers and sparing motor neurons (at humane sacrifice), without effects on astrocyte content (GFAP) or

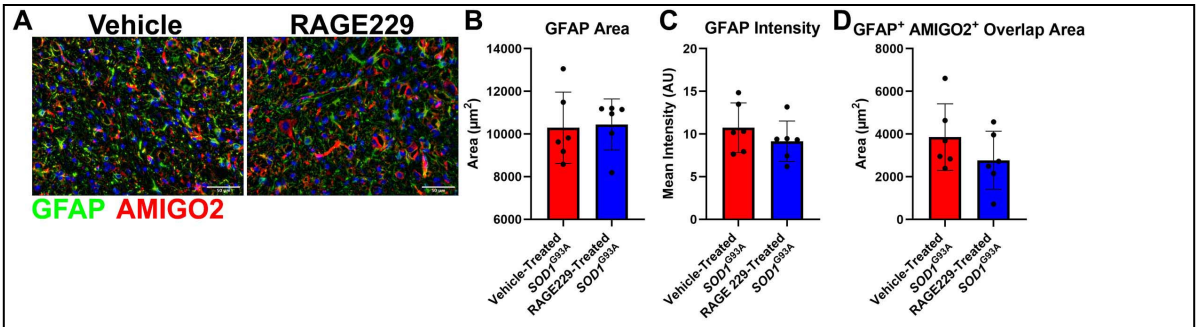

Figure 12. RAGE229 treatment initiated at 8 weeks of age of SOD1^{G93A} mice may not alter astrocytes at sacrifice. A. Representative images of GFAP, and AMIGO2 immunohistochemistry in lumbar spinal cord of indicated mouse groups. DAPI (blue) was used to counterstain nuclei. B. Quantification of GFAP area after automated thresholding. C. Quantification of GFAP intensity. D. Quantification of GFAP and AMIGO2 overlap suggestive of "A1" reactive astrocytes. N=6 mice/group. Mean±SD. Mann-Whitney test used in B. Unpaired Student's t test used in C, and D.

reactivity, at least on account of no differences in AMIGO2. As above, multiple mice remain on study through to humane endpoint.

Finally, it has been shown that in murine models, RAGE expression is attenuated in animals treated with RAGE antagonists. As RAGE ligands directly upregulate RAGE expression, blocking the pathological effects of RAGE ligands reduces RAGE expression. Critically, at humane sacrifice, RAGE229-treated *SOD1*^{G93A} mice displayed significantly reduced RAGE+ area and trends to lower RAGE intensity in the lumbar spinal cord vs. vehicle (Figure 13).

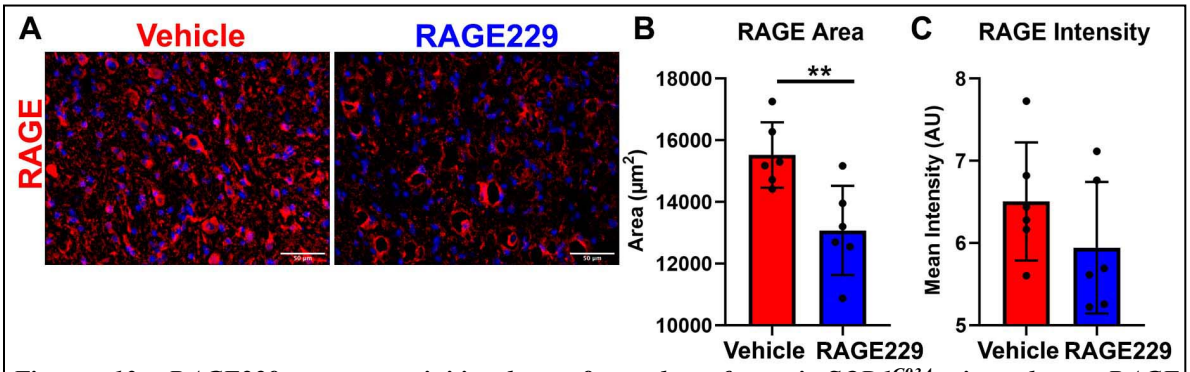

Figure 13. RAGE229 treatment initiated at 8 weeks of age in SOD1^{G93A} mice reduces RAGE immunoreactivity at sacrifice. A. Representative images of RAGE immunohistochemistry in lumbar spinal cord. B. Quantification of RAGE area after automated thresholding. C. Quantification of RAGE mean intensity. N=6 mice/group (male/female combined). Mean±SD. Unpaired Student's t test. ** p<0.01

Although RAGE229 is not the final clinical candidate as more refinement is needed to achieve all the ideal parameters, these key data provide critical support and proof of concept for this chemical probe to block RAGE-DIAPH1 and exert therapeutic effects in murine model of ALS.

C. **What opportunities for training and professional development has the project provided?**

The project was not intended to provide training and professional development opportunities, hence, based on this type of grant mechanism, there is "nothing to report."

However, there were extensive opportunities for training and professional development:

One of the PI's graduate students, Michael MacLean, has been exposed to extensive opportunities for training in the following areas:

- ALS: understanding of epidemiology, pathogenesis and history of therapeutic appraoches
- ALS: understanding of epidemiology with respect to veterans
- Breeding of *SOD1*^{G93A} mice and serial assessment of copy number
- Functional testing of SOD^{G93A} mice (hanging cage wire, grip strength)
- Monitoring of *SOD1*^{G93A} mice
- Establishing the humane endpoint (serial body weights and righting reflex)

- Using Automacs to isolate microglia
- Immunofluroesence microscopy to detect RAGE and cell types
- Performing RNA sequencing and data analysis
- Preparation of abstracts and presentations

Abstracts:
Maclean M, Schmidt AM. Transformative Research in Neurodegenerative Disease and Neuropsychiatric Disorders: 2017 Innovators in Science Award Symposium" on Wednesday, November 29, 2017

MacLean M, Juranek J, Cuddapah S, Hu J, Gugger P, Li H, Schmidt AM. Microglia RAGE exacerbates the procession of amyotrophic lateral sclerosis in male but not female SOD1G93A mice. Glia in Health & Disease; 2020 July 16; Cold Spring Harbor, NY, United States.

MacLean M, Juranek J, Cuddapah S, Derk J, Schmidt AM. RAGE Signaling in Microglia: a potential contributor to neuroinflammation in Amyotrophic Lateral Sclerosis. Keystone Symposia: Neural Environment in Disease: Glial Responses and Neuroinflammation; 2019 June 16; Keystone, CO, United States.

MacLean M, Juranek J, Derk J, Schmidt AM. Microglial RAGE: A Possible Contributor to Neuroinflammation in ALS. New York Academy of Sciences: Neuro-Immunology: The Impact of Immune Function on Alzheimer's Disease; 2018 September 25; New York, New York.

MacLean M, Juranek J, Derk J, Schmidt AM. RAGE Signaling in Microglia: a potential contributor to neuroinflammation in ALS. Glia in Health & Disease; 2017 July 19; Cold Spring Harbor, NY, United States.

Peer Reviewed Manuscripts

Derk J, MacLean M, Juranek J, and Schmidt AM. *The Receptor for Advanced Glycation End products (RAGE) and Mediation of Inflammatory Neurodegeneration.* Journal of Alzheimer's Disease and Parkinsonism 2018;8(1). pii: 421. doi: 10.4172/2161-0460.1000421. Epub 2018 Jan 24.

MacLean M, Derk J, Ruiz HH, Juranek JK, Ramasamy R, Schmidt AM. The Receptor for Advanced Glycation End Products (RAGE) and DIAPH1: Implications for vascular and neuroinflammatory dysfunction in disorders of the central nervous system. Neurochem Intl 2019 Jun;126:154-164. doi: 10.1016/j.neuint.2019.03.012. Epub 2019 Mar 20.

MacLean M, Juranek J, Cuddapah S, Lopez-Diez R, Ruiz HH, Hu J, Frye L, Li H, Gugger PF, Schmidt AM. Microglia RAGE exacerbates the progression of neurodegeneration within the *SOD1*^{G93A} murine model of amyotrophic lateral sclerosis in a sex-dependent manner. J Neuroinflammation 18(1):139, 2021.

MacLean M, Lopez Diez R, Vasquez C, Gugger PF, Schmidt AM. Neuron-glia communication perturbations in murine *SOD1*^{G93A} spinal cord. In Revision, 2021.

D. **How were the results disseminated to communities of interest?**

Nothing to report.

For the scientific community, we disseminated findings through scientific meetings (and abstracts/presentations) and publications.

E. **What do you plan to do during the next reporting period to accomplish the goals?**
Final Progress Report: N/A

4. **IMPACT:**

A. **What was the impact on the development of the principal discipline(s) of the project?**
1). We have identified that in the ALS mouse (called *SOD1*^{G93A}) spinal cord, that the molecule called receptor for AGE or RAGE is highly expressed and particularly it is expressed in activated microglia, and not the unstimulated microglia in the spinal cord. This finding, based on the known biology of RAGE, strongly implicates this molecule in the pathogenesis of ALS and loss of neurons in the spinal cord, which causes, ultimately, paralysis and death.

2). We have found that a lead molecule that blocks RAGE actions, which is a small molecule compound, is able to enter the central nervous system, of which the spinal cord, is a part. We have now found the optimal means to deliver this molecule in the food of the mice. This key finding means that we will be able to treat the mouse model of ALS, the *SOD1*^{G93A} mouse, with this agent to test if it improves survival and motor function.

3). We have found that by using noninvasive imaging of the ALS mouse spinal cord we can discern activated microglia (in the *SOD1*^{G93A} mice) from no glial activation in a normal mouse that does not have ALS.

4). Our data reveal that deletion of microglia RAGE is protective in male *SOD1*^{G93A} mice when compared to the cre control (ALS). These key data suggest that RAGE in microglia may exert negative effects and further strenthens the relevance of this target for ALS. It is essential to now test distinct models of ALS and particularly in male and female mice.

Taken together these findings hold great promise to:

1) Identify an important pathway in the pathogenesis of ALS
2) Identify a non invasive way to track glial inflammation in ALS (as a part of future therapeutic programs using the imaging as a way to indicate if agents might be effective, or not)
3) Identify a new treatment for ALS

B. **What was the impact on other disciplines?**

Nothing to report

C. **What was the impact on technology transfer?**

At this time, we are working aggressively toward the development of an analogue of RAGE229 that is enabled for Phase I clinical trials. At this time, we do not have this agent but are confident that the data obtained in murine models with RAGE229 will exert positive impact for the ultimate testing of RAGE-DIAPH1 small molecule antagonists in ALS in clinical trials.

D. **What was the impact on society beyond science and technology?**

Nothing to report

5. **CHANGES/PROBLEMS:**
   A. **Changes in approach and reasons for change:** Nothing to report
   B. **Actual or anticipated problems or delays and actions or plans to resolve them.**
      Nothing to report
   C. **Changes that had a significant impact on expenditures.**
      Nothing to report
   D. **Significant changes in use or care of human subjects, vertebrate animals, biohazards, and/or select agents.**
      Nothing to report
   E. **Significant changes in use or care of human subjects**
      Nothing to report
   F. **Significant changes in use or care of vertebrate animals.**
      Nothing to report
   G. **Significant changes in use of biohazards and/or select agents.**
      Nothing to report

6. **PRODUCTS:**

A. **Publications, conference papers, and presentations**

Abstracts:

Maclean M, Schmidt AM. Transformative Research in Neurodegenerative Disease and Neuropsychiatric Disorders: 2017 Innovators in Science Award Symposium" on Wednesday, November 29, 2017

MacLean M, Juranek J, Cuddapah S, Hu J, Gugger P, Li H, Schmidt AM. Microglia RAGE exacerbates the procession of amyotrophic lateral sclerosis in male but not female SOD1G93A mice. Glia in Health & Disease; 2020 July 16; Cold Spring Harbor, NY, United States.

MacLean M, Juranek J, Cuddapah S, Derk J, Schmidt AM. RAGE Signaling in Microglia: a potential contributor to neuroinflammation in Amyotrophic Lateral Sclerosis. Keystone Symposia: Neural Environment in Disease: Glial Responses and Neuroinflammation; 2019 June 16; Keystone, CO, United States.

MacLean M, Juranek J, Derk J, Schmidt AM. Microglial RAGE: A Possible Contributor to Neuroinflammation in ALS. New York Academy of Sciences: Neuro-Immunology: The Impact of Immune Function on Alzheimer's Disease; 2018 September 25; New York, New York.

MacLean M, Juranek J, Derk J, Schmidt AM. RAGE Signaling in Microglia: a potential contributor to neuroinflammation in ALS. Glia in Health & Disease; 2017 July 19; Cold Spring Harbor, NY, United States.

B. **Journal publications.**

Derk J, MacLean M, Juranek J, and Schmidt AM. *The Receptor for Advanced Glycation End products (RAGE) and Mediation of Inflammatory Neurodegeneration.* Journal of Alzheimer's Disease and Parkinsonism 2018;8(1). pii: 421. doi: 10.4172/2161-0460.1000421. Epub 2018 Jan 24.

MacLean M, Derk J, Ruiz HH, Juranek JK, Ramasamy R, Schmidt AM. The Receptor for Advanced Glycation End Products (RAGE) and DIAPH1: Implications for vascular and neuroinflammatory dysfunction in disorders of the central nervous system. Neurochem Intl 2019 Jun;126:154-164. doi: 10.1016/j.neuint.2019.03.012. Epub 2019 Mar 20.

MacLean M, Juranek J, Cuddapah S, Lopez-Diez R, Ruiz HH, Hu J, Frye L, Li H, Gugger PF, Schmidt AM. Microglia RAGE exacerbates the progression of neurodegeneration within the

SOD1^{G93A} murine model of amyotrophic lateral sclerosis in a sex-dependent manner. J Neuroinflammation 18(1):139, 2021.

MacLean M, Lopez Diez R, Vasquez C, Gugger PF, Schmidt AM. Neuron-glia communication perturbations in murine *SOD1*^{G93A} spinal cord. In Revision, 2021.

C. **Books or other non-periodical, one-time publications.**
Nothing to report

D. **Other publications, conference papers, and presentations.**
Nothing to report

E. **Website(s) or other Internet site(s).**
Nothing to report

F. **Technologies or techniques**
Nothing to report

G. **Inventions, patent applications, and/or licenses**
Nothing to report

H. **Other Products**
Nothing to report

7. PARTICIPANTS & OTHER COLLABORATING ORGANIZATIONS

A. **What individuals have worked on the project?**

Ann Marie Schmidt

Project Role: Principal Investigator

Researcher Identifier: SCHMIDTAM (eRA Commons ID)

Nearest Person Month Worked: 1.0 Person Month (Years 1, 2, NCE #1 and #2)

Contribution to Project: Dr. Schmidt oversees all aspect of the project, project team, mouse care and use, data analyses and all interactions with co-investigators.

Funding Support: N/A

Yu-Shin Ding

Project Role: Co-investigator

Researcher Identifier: YU_SHIN_DING (eRA Commons ID)

Nearest Person Month Worked: 2 Person Months (Years 1 and 2)

Contribution to Project: Dr. Ding has overseen the implementation and performance of the imaging studies on the mice using [^{11}C]PBR28 as outlined in the protocol.

Funding Support: N/A

Judyta Juranek

Project Role: Associate Research Scientist

Researcher Identifier: JKJ2110CU (eRA Commons ID)

Nearest Person Month Worked: 10 Person Months (Year 1); 12 Person Months (Year 2)

Contribution to Project: Dr. Juranek's role has been to monitor the mouse behavioral endpoints, humane endpoint determinations and she has overseen and organized the mice allocated to imaging studies. She performs the biochemical and molecular analyses on the mouse tissues.

Funding Support: N/A

Huilin Li

Project Role: Co-investigator

Research Identifier: LIHUILIN09 (eRA Commons ID)

Nearest Person Month Worked: 1 Person Month (Years 1 and 2)

Contribution to Project: Dr. Li oversees all aspects of power calculations and statistical analysis of the data.

Funding Support: N/A

Jiyuan Hu

Project Role: Post-doctoral research scientist

Researcher Identifier: HUJI010 (eRA Commons ID)

Nearest Person Month Worked: 1 Person Month (Years 1 and 2)

Contribution to Project: Dr. Hu works with Dr. Li; she is a biostatistician who has performed all aspects of power calculations and statistical analysis.

Funding Support: N/A

Michael MacLean

Project Role: Graduate Student

Researcher Identifier: mm8848 (eRA Commons ID)

Nearest Person Month Worked: 6 Person Months (Year 1); 8 Person Months (Year 2)

Contribution to Project: Mr. MacLean breeds and genotypes the mice and works together with Dr. Juranek to perform the behavioral analyses, humane endpoint determinations and the indicated biochemical and molecular analyses.

Funding Support: Mr. MacLean is funded by the Sackler graduate school at NYU School of Medicine.

B. **Has there been a change in the active other support of the PD/PI(s) or senior/key personnel since the last reporting period?**

NCE #2: 07/01/2020 – 06/30/2021

Schmidt, Ann Marie
ACTIVE
1R01DK109675 04/01/16-03/31/22 0.06 calendar
NIH No Cost Extension
RAGE/mDia1, Macrophage Trafficking and Inflammation in High Fat Feeding
Major goal of this application is to understand macrophage-adipocyte interactions in high fat feeding and obesity.
Role: PI

1R01HL132516 12/09/16-11/30/21 0.06 calendar
NIH No Cost Extension
RAGE/mDia1, Macrophage Trafficking and Inflammation in Regression of Diabetic Atherosclerosis
The major goal of this grant is to probe the mechanisms by which macrophage (Mø) RAGE impairs regression of atherosclerosis in diabetic or IR mice.
Role: Multi-PIs (Schmidt & Ramasamy-Contact-PI)

P01HL131481 05/01/17-04/30/22 3.0 calendar
NIH (Fisher: PI) P01
Macrophage Dysfunction in Obesity, Diabetes and Atherosclerosis
Major goal of this application is to determine mechanisms of macrophage trafficking, metabolism and inflammation in the context of RAGE/DIAPH1 in obesity
Role: Project 3 and Core C Leader

(THIS AWARD)
USAMRAA Dept. of the Army 07/01/17-06/30/21 0.04 calendar
No Cost Extension
Receptor for AGE (RAGE) Signal Transduction in Amyotrophic Lateral Sclerosis: In Vivo Imaging and Novel Therapeutic Approaches
Major goals of this grant includes testing the hypothesis that microglia RAGE, through ligand-driven upregulation of inflammatory and pro-oxidative stress and suppression of reparative processes in the ALS spinal cord, mediates neuronal death and loss of motor function and probing the hypothesis that PBMM-specific deletion of Ager attenuates neuronal stress, accumulation of Aβ and amyloid plaques, synaptic dysfunction and cognitive impairment in APPswe/PS1 mice.
Role: PI

USAMRAA Dept. of the Army 09/30/17-04/29/22 1.08 calendar
No Cost Extension
RAGE/Diaph1, Diabetes, and Kidney Disease: Mechanisms and Novel Therapeutic Strategies
Major goals for this grant involves (a) testing the hypothesis that RAGE and DIAPH1 mediate podocyte dysfunction in DN through disengagement of homeostatic actin cytoskeleton dynamics and upregulation of pro-inflammatory and pro-fibrotic molecules (b) testing the hypothesis that RAGE and DIAPH1-expressing macrophages contribute to structural and functional derangements in DN through upregulation of tissue-destructive and profibrotic mediators and (c) determining if administration of novel small molecule antagonists of RAGE-DIAPH1 interaction in diabetic mice protects against DN.
Role: PI (Ramasamy-Partnering PI)

American Heart Association 04/01/17-03/31/22 2.4 calendar
No Cost Extension
Braking Inflammation in Obesity & Metabolic Dysfunction: Translational and Therapeutic Opportunities
The major goal of this grant is to investigate the novel hypothesis that impaired adipocyte, macrophage and other inflammatory cell signal transduction thwarts weight loss and its anti-inflammatory and metabolic benefits, at least in part through the activation of the receptor for advanced glycation endproducts, or RAGE pathway, which has been shown to regulate a unique repertoire of inflammatory and metabolic processes.
Role: Center Director, Project 1 Leader

1P01HL146367-01 08/01/19-06/30/24 3.0 calendar
NHLBI
Macrophages, Cell-Cell Communication, Ischemic Injury in Diabetes and the RAGE/DIAPH1 Signaling Axis
The major goal of this grant is to probe the mechanisms and identify new therapies for untoward monocyte and macrophage responses in ischemia, which, together with cellular perturbation in the microenvironment, amplify damage in myocardial infarction and peripheral arterial disease, especially in diabetes.
Role: PI

1R01DK122456-01A1 07/01/20-03/31/25 1.2 calendar
NIDDK
Targeting RAGE/DIAPH1: Novel Therapeutic Strategy for Diabetic Complications
The major goal of this grant is to develop small molecule antagonists to treat diabetic complications.
Role: MPI (Schmidt (contact PI)/Ramasamy)

<u>INACTIVE</u>
(ENDED)
P01HL60901 07/15/11-11/30/18 0.12 calendar
NIH No Cost Extension
RAGE and Mechanisms of Vascular Dysfunction
This grant focuses on the mechanisms by which diabetes accelerates atherosclerosis via RAGE.
Role: Project 1 and Core A Leader, Core C Co-Leader

1R24DK103032 08/01/14-07/31/19 0.06 calendar
NIH No Cost Extension

Targeting RAGE-mDia1 in Diabetic Complications: Mechanisms & Therapeutics
Major goal of this application is to develop small molecule inhibitors of the interaction of the RAGE cytoplasmic domain with DIAPH1.
Role: PI

Alzheimer's Association 03/01/17-02/29/20 0.24 calendar

RAGE, Diaph1, Microglia and Alzheimer's disease
Major goal of this grant is to probe the hypothesis that microglial-specific Ager deletion modulates neuronal stress, accumulation of Aβ and amyloid plaques, synaptic and cognitive dysfunction in APPswe/PS1 mice.
Role: PI

OVERLAP: None

C. **What other organizations were involved as partners?**
N/A

8. **SPECIAL REPORTING REQUIREMENTS**
N/A

9. **APPENDICES:**

Original journal publications:

1. Derk J, MacLean M, Juranek J, and Schmidt AM. *The Receptor for Advanced Glycation End products (RAGE) and Mediation of Inflammatory Neurodegeneration.* Journal of Alzheimer's Disease and Parkinsonism 2018; 8(1). pii: 421. doi: 10.4172/2161-0460.1000421. Epub 2018 Jan 24.

2. MacLean M, Derk J, Ruiz HH, Juranek JK, Ramasamy R, Schmidt AM. The Receptor for Advanced Glycation End Products (RAGE) and DIAPH1: Implications for vascular and neuroinflammatory dysfunction in disorders of the central nervous system. Neurochem Intl 2019 Jun;126:154-164. doi: 10.1016/j.neuint.2019.03.012. Epub 2019 Mar 20.

3. MacLean M, Juranek J, Cuddapah S, Lopez-Diez R, Ruiz HH, Hu J, Frye L, Li H, Gugger PF, Schmidt AM. Microglia RAGE exacerbates the progression of neurodegeneration within the *SOD1*^{G93A} murine model of amyotrophic lateral sclerosis in a sex-dependent manner. J Neuroinflammation 18(1):139, 2021.

Author Manuscript

Author Manuscript

Author Manuscript

Author Manuscript

HHS Public Access

Author manuscript

J Alzheimers Dis Parkinsonism. Author manuscript; available in PMC 2019 January 24.

Published in final edited form as:

J Alzheimers Dis Parkinsonism. 2018 ; 8(1): . doi:10.4172/2161-0460.1000421.

The Receptor for Advanced Glycation Endproducts (RAGE) and Mediation of Inflammatory Neurodegeneration

Julia Derk[1], **Michael MacLean**[1], **Judyta Juranek**[1], and **Ann Marie Schmidt**[1,*]

[1]Diabetes Research Program, Division of Endocrinology, Diabetes and Metabolism, NYU School of Medicine, 550 First Avenue, Smilow 906, New York, NY, 10016, USA

Introduction

The Receptor for Advanced Glycation Endproducts (RAGE) is an immunoglobulin-type, transmembrane receptor that is expressed on numerous cell types in the Central Nervous System (CNS) and periphery, such as neurons, astrocytes, microglia, mononuclear phagocytes, epithelial, and endothelial cells (ECs). RAGE binds a discrete repertoire of ligands, including nonenzymatically glycated proteins and lipids also known as advanced glycation endproducts (AGEs), for which the receptor is named, in addition to multiple members of the S100/calgranulin family, oligomeric forms of Aβ, high mobility group box 1 (HMGB1), phosphatidylserine (PS), and lysophosphatidic acid [1–8]. Extensive evidence has implicated RAGE as a critical player in regulating inflammation, as well as oxidative and cellular stress in a variety of organ niches and disease settings, including the CNS during neurodegeneration [5, 6, 9–14].

This review will focus on the current state of knowledge regarding RAGE and neurodegeneration. Specifically, we will detail the effect of RAGE signal transduction on cellular stress, pinpoint clues into RAGE pathophysiology in the context(s) of increased RAGE ligand burden, discuss the systemic consequences of RAGE-driven inflammation in the CNS as a whole, and report on the increasing number of published genome wide association study (GWAS) findings that evoke strong indications for RAGE as a putative driver of cellular and systemic dysfunction during key neurodegenerative pathologies, most specifically Alzheimer's disease (AD), Parkinson's disease (PD), Amyotrophic Lateral Sclerosis (ALS), and Multiple Sclerosis (MS).

RAGE Signal Transduction

Our laboratory recently discovered that upon ligand engagement of the extracellular domains of RAGE, the RAGE cytoplasmic domain binds to its intracellular effector molecule, Diaphanous 1 (DIAPH1) [15, 16]. DIAPH1 has subsequently been shown to be required for signal transduction induced by RAGE ligand binding, including the activation of mitogen activated protein kinases (MAPK), Rho GTPases, and phosphatidylinositol 3-kinase (PI3K)/Akt signaling. RAGE-DIAPH1 signaling effects are dependent on many factors,

*Author to whom correspondence may be addressed: Dr. Ann Marie Schmidt (AnnMarie.Schmidt@nyumc.org).

Author Manuscript Author Manuscript Author Manuscript Author Manuscript

including, but not limited to: cell-type, ligand form and ligand concentration, and the duration of signal induction (acute vs. chronic) [17–22]. The implications of activation of these signaling cascades are substantial, and predominantly pathological. The RAGE-DIAPH1 interaction drives the generation of reactive oxygen species (ROS), the induction of cellular migration, the upregulation of inflammatory cytokines, and subsequent downregulation of ATP binding cassette (ABC) cholesterol transporters, such as ABCA1 and ABCG1, thereby mediating intracellular lipid accumulation and consequent cellular dysfunction [9, 23–25].

Besides its role in RAGE-DIAPH1-mediated inflammation, DIAPH1 is a dynamic mediator of actin cytoskeleton stability and rearrangement, as well as regulation of transcription factors [15, 26–28]. It was recently reported that DIAPH1 was highly expressed in human gliomas; however, the specifics of DIAPH1 expression, including the cellular localization and the potential DIAPH1-mediated mechanisms of *in vivo* dysfunction in the rodent or human CNS have not been elucidated [29]. Beyond this report, very little is known about DIAPH1 expression pattern and functions in the CNS of normal or degenerating models of humans; there are no known SNPs in *DIAPH1* that increase or decrease neurodegenerative disease risk. However, the impact of RAGE-DIAPH1 signal transduction in peripheral cells exhibits prominent overlap with the patterns of cellular dysfunction observed in neurodegeneration, including the increased production of ROS and pro-inflammatory cytokines and the downregulation of homeostatic molecules such as neurotrophins and cholesterol/lipid handlers. This signaling culminates in significant alterations in critical cellular functions, such as migration, phagocytosis, replication, and cell death, particularly in cells of myeloid and endothelial origin, but also in neurons [4, 12, 30–32].

Connecting the dots: potential RAGE mechanisms in Alzheimer's disease

Alzheimer's disease (AD) is a neurodegenerative disorder that impacts millions of people worldwide and is not curable. While the primary risk factor for AD is advanced age, recent insights from genomic technology implicate inflammatory lipid and cytokine signaling in microglia, the myeloid cells of the CNS, as a prominent correlate of disease. Specifically, human GWAS suggest a powerful link between inflammatory pathways, including complement, chemokines, and influential lipid and cholesterol molecules, such as Triggering Receptor Expressed on Myeloid Cells 2 (TREM2), ABCA7, Apolipoprotein E variant 4 (APOE4), and others with AD susceptibility [14, 20, 33–41]. Additional analyses within animal models have illuminated various molecules critical to the innate immune system as major contributors to increased or decreased rate of AD progression, such as Chemokine Receptor Type 2 (CCR2), Chemokine Receptor 1 (CX3CR1 or GPR1), complement components (C1q and C3), and Chemokine Ligand 8 (CXCL8) [35, 42–55].

The most prominent risk alleles and impairments were observed in humans and mice with loss-of-function mutations or deletions of the aforementioned chief lipid handling molecules. However, burgeoning data in humans and rodent models also indicate that systemic inflammation and transient infections in the periphery are sufficient to increase production of RAGE ligands, particularly AGEs and oligomeric Aβ. In contexts in which these ligands accumulate in the CNS, RAGE signaling is causally implicated in exacerbating

Author Manuscript Author Manuscript Author Manuscript Author Manuscript

ongoing neurodegenerative disease. Atop these multiple mechanisms of augmented RAGE ligand production in AD, there is also prominent downregulation of specific detoxification mechanisms, which inhibit production of pre-AGEs such as methylglyoxal (MG) [56]. Glyoxalase 1 (GLO1), the principal enzyme that detoxifies MG, mitigates AGE production and is upregulated in the early and mid-stages of AD in human subjects. However, in the late and progressive stages of AD dysfunction, depletion of the enzyme's chief and essential cofactor, glutathione, reduces overall activity of the GLO1-AGE detoxifying system, thus facilitating increased AGE production and accumulation [56, 57]. Altogether, these findings underscore a potentially profound link between inflammation, both peripheral and central, which prompts the question: To what extent might anti-AGE/RAGE therapies provide protective measures for neurodegeneration and AD, given the prominence of cellular stress driven by increased RAGE ligand burden [58–60]?

Population-based studies have emerged suggesting links between RAGE, dementia, and AD. Genetic sequence variations in 20 genes associated with inflammatory signaling were recently probed for possible associations with dementia risk. From 1,462 Swedish dementia cases and 1,929 controls that were composed of twin and unrelated case-control samples, investigators identified a potential association of sequence variations near the gene encoding RAGE (*AGER*), to increased risk for dementia and AD, in two independent samples. Further, a recent structural analysis utilizing MRI technology revealed that atrophy of the right hippocampus substructure CA1 during AD progression was significantly correlated to the single nucleotide polymorphism (SNP) variant rs2070600 within *AGER* [61]. Notably, this variant has been previously associated with increased affinity to ligands and increased ligand-stimulated inflammation in cultured cells, in conjunction with decreased levels of circulating soluble RAGE (sRAGE) [62]. sRAGE is a short, soluble isoform of RAGE, and putative "decoy" receptor. Because it lacks the intracellular and cytoplasmic domains required for signaling, sRAGE is predicted to protect against inflammation and RAGE-dependent cellular stress by sequestering RAGE ligands and preventing their engagement of the full-length, transmembrane RAGE [63, 64]. Thus, in humans bearing this SNP, lower sRAGE concentrations may directly amplify ligand burden and availability for signal transduction through full-length RAGE. This increases cellular stress, impairs lipid and cholesterol handling for the cells, in addition to promoting increased ROS production, thereby forging a feed-forward, self-perpetuating loop of inflammatory cellular stress in ECs, myeloid cells, and others within the CNS niche, including astrocytes, neurons, and oligodendrocytes.

Many of the mechanistic studies of RAGE in AD-like mouse models have been conducted in animals that are globally devoid of *Ager* and animals with dominant negative-RAGE (DN-RAGE) targeted to myeloid cells, using the macrophage scavenger receptor. DN-RAGE is composed of the extracellular RAGE domains and the transmembrane domain; hence, although ligand binding to this construct is intact and it is tethered to the cell membrane, signaling is abrogated on account of deletion of the cytoplasmic domain. These DN-RAGE studies have indicated that RAGE signal abrogation confers a benefit for AD progression and suggest a role for RAGE in myeloid cells during AD [10, 12, 39, 65]. However, there are possible caveats to these studies, particularly since it is plausible that DN-RAGE may also act as a decoy receptor and "ligand sink", much like sRAGE, and mice devoid of *Ager* or

Author Manuscript Author Manuscript Author Manuscript Author Manuscript

expressing DN-RAGE constitutively from birth may develop differently than a wild-type animal. Therefore, further investigation utilizing greater cell type- and temporal specificity would be key for definitively determining a role for RAGE in AD.

RAGE molecules expressed on ECs are also known to facilitate the transport of Aβ into and across the blood brain barrier (BBB) during AD, implicating RAGE in mediating the increased pools of ligand concentrations found during disease progression [9, 66]. Since AGE production is increased in oxidized environments and RAGE engagement drives ROS production, there are additional entry points into the aforementioned feed-forward loop in which RAGE ligand binding drives increased RAGE ligand abundance, increased RAGE-DIAPH1 signaling, and therefore increased ROS and AGEs. Together, this AGE-generating loop and the reduced expression of Low Density Lipoprotein Receptor-related Protein 1 (LRP1), the chief molecule responsible for transporting Aβ out of the brain, in AD, collectively dysregulate the flux and trapping of AGEs and Aβ within the CNS as degeneration progresses [67]. Collectively, these data provide strong evidence for the RAGE-DIAPH1 signaling axis as a prominent mediator of inflammation and cellular dysfunction in a variety of cell types during AD, particularly by igniting an unconstrained iterative loop of signal propagation driving cell-intrinsic and cell-to-cell stress signals that mediate prominent impairments during AD.

Of note, the extracellular RAGE inhibitor, Azeliragon, is currently in Stage 3 clinical trials to investigate the therapeutic potential of RAGE inhibition in AD patients. Initially, in an 18-month Stage 2 clinical trial of 399 patients, the trial was preemptively halted when Azeliragon (then by the name of TPP488) was shown to be deleterious to patients at high doses (60 mg for 6 days followed by 20 mg), but protective at low doses (15 mg for 6 days followed by 5 mg) [68, 69]. Currently, a Stage 3 study granted Fast Track designation by the United States Food and Drug Administration, is being conducted that utilizes the low dose (5 mg for 18 months) vs. placebo. This trial, entitled the STEADFAST Study, was recently extended for an optional 2 year continuation in multiple countries across the world [70].

RAGE and Parkinson’s Disease, a second manifestation of the cellular dysfunction

Parkinson’s disease (PD) is another common neurodegenerative disorder that impacts millions of people worldwide and is characterized by the specific loss of nigrostriatal dopaminergic neurons and locomotor deficits [71]. While the cerebral location and neuronal subsets that degenerate in PD are distinct from AD, there are prominent cellular activation mechanisms driving inflammation and perturbation of neurons at the nexus of the two disorders. Akin to AD, the initiation of PD pathogenesis is still not clearly elucidated. However, there are many disease processes correlated to PD and AD pathogeneses, which could potentially be related to RAGE-DIAPH1 signaling, such as enhanced oxidative stress, innate immune activation, protein aggregation, and neuronal death.

Multiple lines of evidence suggest a potential role for RAGE and its ligands in the pathogenesis of PD. First, the same *AGER* rs2070600 SNP that was implicated in CA1 atrophy during AD, was also correlated to the highest risk for PD development of all known

Author Manuscript Author Manuscript Author Manuscript Author Manuscript

AGER SNPs in a Turkish cohort GWAS (N=174 PD patients and N=150 healthy controls) [72]. In addition, when compared to healthy controls, PD patients have recently been shown to possess higher concentrations of S100B and HMGB1, two known RAGE ligands, in the substantia nigra and cerebral spinal fluid (CSF) [73–75]. In rodent models, numerous studies have indicated that animals derive prominent protection from PD-like impairments when RAGE signaling was blocked through genetic ablation of S100B/RAGE or by the administration of a RAGE inhibitor, FPS-ZM1, a blood-brain barrier (BBB) permeable, high affinity, multimodal blocker of RAGE [73]. Either strategy was sufficient to abrogate a variety of impairments observed in the PD-like rodent models, such as apoptosis of dopaminergic cells; locomotor defects; neuroinflammatory microgliosis and astrogliosis, as measured by increased ionized calcium binding adaptor molecule 1 (IBA1) and glial fibrillary acidic protein (GFAP) staining, respectively; tyrosine hydroxylase (and therefore dopamine) deficits; NF-$_K$B activation; and tumor necrosis factor alpha (TNFα) upregulation in the presence of PD-like syndromes induced by toxins. While many of these benefits only partially rescued cellular deficits or delayed the onset of disease, it is possible that RAGE-based interventions in AD and PD may provide meaningful avenues for therapeutic intervention in either condition of neurodegeneration.

Amyotrophic Lateral Sclerosis, another inflammatory syndrome of the CNS?

Amyotrophic Lateral Sclerosis (ALS) is a fatal neurodegenerative disorder characterized by progressive motor function loss and muscle atrophy. Much like AD and PD, many of the gene mutations linked to ALS have also been shown to drive inflammatory glial activation, oxidative stress, and neuronal loss. There is prominent overlap of disease phenotypes in ALS to other disorders with regard to the cellular consequences of RAGE-DIAPH1 signaling, although further investigation is required to elucidate these mechanisms. [76]. Several studies have reported increased concentrations of RAGE ligands in the spinal cord [77–79] and CSF of ALS patients [80]. Conversely, serum sRAGE was decreased in human ALS patients, thereby putatively increasing ligand burden available for binding to and inducing signaling through full-length RAGE [81]. While little mechanistic evidence is available linking RAGE and ALS, our laboratory recently showed that RAGE and its ligands are increased in the spinal cord of ALS patients [78].

Furthermore, this increase of RAGE and its ligands was recapitulated in one of the most commonly employed ALS rodent models, murine lines containing the familial G93A mutation in superoxide dismutase 1 (*SOD1*), as discovered in human ALS populations [3, 82, 83]. In these models, nerve growth factor (NGF) is post-translationally modified by oxidation and contributes to RAGE signaling-induced motor neuron death when normal motor neurons are co-cultured with SOD1 G93A astrocytes [84]. In addition, C6 rat astrocytoma cells overexpressing mutant SOD1 G93A protein displayed significantly increased RAGE ligand S100B expression and, intriguingly, inhibition of this process by siRNA targeting *S100b* ameliorated the inflammatory profile of these cells [3].

Author Manuscript Author Manuscript Author Manuscript Author Manuscript

In the SOD1 G93A mice, daily administration of recombinant sRAGE extended lifespan and duration of healthy body weight, while slowing the onset of motor function loss [82]. Importantly, sRAGE treatment not only reduced motor neuron death but also decreased astrogliosis, indicating a more homeostatic profile in multiple cell types [82]. Altogether, a burgeoning body of literature suggests that RAGE activation, driven by an increased availability of ligands, is likely a contributing factor to ALS pathology. However, further work utilizing established BBB-permeable inhibitors of RAGE-DIAPH1 would be paramount in elucidating the value of targeting this signaling axis as a potential therapeutic target for slowing the progression inflammatory and neuron-perturbing signaling in ALS.

Multiple Sclerosis and experimental autoimmune encephalopathy (EAE)

Multiple Sclerosis (MS) is a debilitating neurodegenerative disease in which autoimmune tissue-destructive processes are implicated. In human subjects, the *AGER* rs2070600 SNP was associated with MS in several studies [63, 85]. However, in a different study of a Hungarian community, this SNP was not present. Although, another SNP within the *AGER* promoter suggested altered transcription, rather than differences in ligand binding and sRAGE production, may be contributing to the risk of MS within this population [86].

With respect to sRAGE, akin to other inflammatory neurodegenerative syndromes discussed above, MS patients display lower serum levels of sRAGE relative to control patients and this decreased sRAGE inversely correlates with disease progression [87]. In addition, RAGE ligands are also increased in active MS lesions, as observed by immunohistochemistry. Further, *AGER* mRNA and RAGE ligand protein concentrations were increased in serum, CSF, and mononuclear cells in both niches during MS [87–91]. Interestingly, patients treated with disease-modifying drugs display a prominent reduction of serum HMGB1 when compared to untreated MS patients, which correlated to a better disease prognosis [90]. Fingolimod, a sphingosine-1P (S1P) analogue, has also been utilized to treat relapse-remitting MS in human patients, and induces a significant reduction in serum HMGB1 after 6 months of treatment while increasing sRAGE, albeit this study was conducted in a small patient cohort (n=17) [91].

Induction of experimental autoimmune encephalomyelitis (EAE), in which mice are immunized with myelin basic protein (MBP), has been utilized to study the molecular mechanisms underlying MS. Studies have reported increased RAGE in the spinal cords of mice with EAE [88, 92], whereas blockade of RAGE signaling by recombinant sRAGE administered concomitantly with EAE induction in mice, significantly reduced immune cell infiltration into the brain and the severity of the disease [92]. However, controversy arose after a report that *Ager* deficient mice with EAE displayed no differences in disease severity [58].

Three distinct, but not exclusive possibilities may explain these seemingly conflicting results. First, recombinant sRAGE may exert some of its effects independent of RAGE signaling. It is possible that sRAGE is functioning as a pathological ligand sink in this instance that not only reduces RAGE signaling but other inflammatory signals as well through different receptors to which RAGE ligands may also bind. Second, the deletion of

Author Manuscript Author Manuscript Author Manuscript Author Manuscript

Ager from every cell may imbue detrimental effects due to unknown roles of RAGE in homeostatic functions and thus, a complete blockade of this signaling, as opposed to dampening, may reduce the benefits of RAGE inhibition. Third, it is well established that MS and EAE models in mice are characterized by periods of exacerbation vs. remittance of disease; hence, the timing of RAGE inhibition or *Ager* deletion *in vivo* may critically impact phenotypic outcomes.

Collectively, these considerations suggest that RAGE signaling is likely contributing to inflammatory perturbation in MS. Potential therapeutic interventions should investigate the possibilities of abrogating disease pathology by quenching RAGE ligands and/or preventing RAGE inflammatory signaling as well, although a much more detailed analysis of when and how to do so would still need to be conducted.

Conclusions

As summarized in the Figure, the manifestations of AD, PD, ALS and MS are distinct in nature, impacting differential subsets of neurons and regional variability within the CNS. However, there are common underlying threads that strongly suggest similarities among these neurodegeneration syndromes, including increased accumulation of RAGE ligands and expression of RAGE, processes that trigger oxidative and cellular stress, and myeloid, neuronal, astrocytic, and endothelial dysfunction. The last decade of research has generated a strong body of evidence to suggest that RAGE signaling plays a prominent role in the pathophysiology of these inflammatory neurodegenerative syndromes, although many of the specific details remain to be fully elucidated. Although these findings are illuminative, multiple questions remain to be addressed, such as, does RAGE signaling participate in disease induction and/or as a potentiation/progression mechanism in these disorders? Why do we sometimes discern differential outcomes upon the use of sRAGE, RAGE inhibitors, or, in animal models, DN-RAGE expression or genetic ablation of *Ager*? To what extent does RAGE play time-dependent roles during discrete periods of disease and in distinct cell types, in models vs. humans, and are the effects of RAGE specific to aging or prominent across the lifespan? Are there specific patient populations for which RAGE-based therapies would be most or least beneficial? To this end, the future application of recent insights from human GWAS data for the use of genetic testing in conjunction with measuring circulating sRAGE levels might be the first steps to determine the subpopulations in which the administration of RAGE inhibitors may increase healthspan. RAGE presents itself as an attractive target for inhibition, when aiming for therapies that assuage cognitive decline during neurodegeneration through interfering with feed-forward loops of inflammation and oxidative and cellular stress.

A new age in science is upon us where we are poised to integrate these varied questions. Excitingly, the novel discoveries that have revealed the genetics of disease susceptibility have occurred while many laboratories are concurrently flourishing in their revelations on the cellular and molecular mechanisms of RAGE signal transduction, and novel fields have developed to optimize cell targeting and isolation technology, RAGE inhibitors, and more nuanced approaches for clinical trials. Does this mounting evidence suggest a prominent role for RAGE signal transduction in accelerating the pathogenesis of inflammatory

Author Manuscript Author Manuscript Author Manuscript Author Manuscript

neurodegeneration, irrespective of the disease subtype? Further work will undoubtedly be required to determine to what extent and in which specific contexts inhibiting RAGE signaling will protect the CNS from neurodegeneration. However, these developing studies have shown clear benefits of RAGE abrogation, and the future shows promise, particularly as we begin to take a more integrative approach to understanding the complex mechanisms of these devastating diseases and the possibilities of relief through meaningful interventions.

Acknowledgments

We thank Ms. Latoya Woods for the expert assistance in preparation of this review. In addition, we are appreciative of our funding organizations: The National Institute of Health (National Institute on Aging), U.S. Department of Defense, and the Alzheimer's Association.

References

1. Xu Y, et al. Advanced glycation end product (AGE)-receptor for AGE (RAGE) signaling and up-regulation of Egr-1 in hypoxic macrophages. J Biol Chem. 2010; 285(30):23233–40. [PubMed: 20507991]
2. Walker D, et al. Receptor for advanced glycation endproduct modulators: a new therapeutic target in Alzheimer's disease. Expert Opin Investig Drugs. 2015:1–7.
3. Serrano A, et al. The Astrocytic S100B Protein with Its Receptor RAGE Is Aberrantly Expressed in SOD1(G93A) Models, and Its Inhibition Decreases the Expression of Proinflammatory Genes. Mediators Inflamm. 2017; 2017:1626204. [PubMed: 28713206]
4. Schmidt AM, et al. Regulation of human mononuclear phagocyte migration by cell surface-binding proteins for advanced glycation end products. J Clin Invest. 1993; 91(5):2155–68. [PubMed: 8387541]
5. Yan SD, et al. Glycated tau protein in Alzheimer disease: a mechanism for induction of oxidant stress. Proc Natl Acad Sci U S A. 1994; 91(16):7787–91. [PubMed: 8052661]
6. Yan SD, et al. RAGE and amyloid-beta peptide neurotoxicity in Alzheimer's disease. Nature. 1996; 382(6593):685–91. [PubMed: 8751438]
7. Kislinger T, et al. N(epsilon)-(carboxymethyl)lysine adducts of proteins are ligands for receptor for advanced glycation end products that activate cell signaling pathways and modulate gene expression. J Biol Chem. 1999; 274(44):31740–9. [PubMed: 10531386]
8. Rai V, et al. Lysophosphatidic acid targets vascular and oncogenic pathways via RAGE signaling. The Journal of Experimental Medicine. 2012; 209(13):2339. [PubMed: 23209312]
9. Giri R, et al. beta-amyloid-induced migration of monocytes across human brain endothelial cells involves RAGE and PECAM-1. Am J Physiol Cell Physiol. 2000; 279(6):C1772–81. [PubMed: 11078691]
10. Lue LF, et al. Involvement of microglial receptor for advanced glycation endproducts (RAGE) in Alzheimer's disease: identification of a cellular activation mechanism. Exp Neurol. 2001; 171(1): 29–45. [PubMed: 11520119]
11. Mi W, et al. Cystatin C inhibits amyloid-beta deposition in Alzheimer's disease mouse models. Nat Genet. 2007; 39(12):1440–2. [PubMed: 18026100]
12. Fang F, et al. RAGE-dependent signaling in microglia contributes to neuroinflammation, Abeta accumulation, and impaired learning/memory in a mouse model of Alzheimer's disease. FASEB J. 2010; 24(4):1043–55. [PubMed: 19906677]
13. Morales-Corraliza J, et al. Immunization targeting a minor plaque constituent clears beta-amyloid and rescues behavioral deficits in an Alzheimer's disease mouse model. Neurobiol Aging. 2013; 34(1):137–45. [PubMed: 22608241]
14. Chauhan G, et al. Association of Alzheimer's disease GWAS loci with MRI markers of brain aging. Neurobiol Aging. 2015; 36(4):1765 e7–16.
15. Tominaga T, et al. Diaphanous-related formins bridge Rho GTPase and Src tyrosine kinase signaling. Mol Cell. 2000; 5(1):13–25. [PubMed: 10678165]

Author Manuscript Author Manuscript Author Manuscript Author Manuscript

16. Hudson BI, et al. Interaction of the RAGE cytoplasmic domain with diaphanous-1 is required for ligand-stimulated cellular migration through activation of Rac1 and Cdc42. J Biol Chem. 2008; 283(49):34457–68. [PubMed: 18922799]
17. Manigrasso MB, et al. Small Molecule Inhibition of Ligand-Stimulated RAGE-DIAPH1 Signal Transduction. Scientific Reports. 2016; 6:22450. [PubMed: 26936329]
18. Koch M, et al. Structural Basis for Ligand Recognition and Activation of RAGE. Structure. 18(10): 1342–1352.
19. Park H, Boyington JC. The 1.5 Å Crystal Structure of Human Receptor for Advanced Glycation Endproducts (RAGE) Ectodomains Reveals Unique Features Determining Ligand Binding. Journal of Biological Chemistry. 2010; 285(52):40762–40770. [PubMed: 20943659]
20. Lander HM, et al. Activation of the Receptor for Advanced Glycation End Products Triggers a p21 ras -dependent Mitogen-activated Protein Kinase Pathway Regulated by Oxidant Stress. Journal of Biological Chemistry. 1997; 272(28):17810–17814. [PubMed: 9211935]
21. McDonald DR, et al. β-Amyloid Fibrils Activate Parallel Mitogen-Activated Protein Kinase Pathways in Microglia and THP1 Monocytes. The Journal of Neuroscience. 1998; 18(12):4451–4460. [PubMed: 9614222]
22. He M, et al. Receptor for advanced glycation end products binds to phosphatidylserine and assists in the clearance of apoptotic cells. EMBO reports. 2011; 12(4):358–364. [PubMed: 21399623]
23. Westerterp M, et al. Deficiency of ABCA1 and ABCG1 in Macrophages Increases Inflammation and Accelerates Atherosclerosis in Mice. Circulation research. 2013; 112(11)
24. Daffu G, et al. RAGE Suppresses ABCG1-Mediated Macrophage Cholesterol Efflux in Diabetes. Diabetes. 2015; 64(12):4046–60. [PubMed: 26253613]
25. Arancio O, et al. RAGE potentiates Abeta-induced perturbation of neuronal function in transgenic mice. EMBO J. 2004; 23(20):4096–105. [PubMed: 15457210]
26. Posey SC, Bierer BE. Actin stabilization by jasplakinolide enhances apoptosis induced by cytokine deprivation. J Biol Chem. 1999; 274(7):4259–65. [PubMed: 9933626]
27. Fukata M, Nakagawa M, Kaibuchi K. Roles of Rho-family GTPases in cell polarisation and directional migration. Curr Opin Cell Biol. 2003; 15(5):590–7. [PubMed: 14519394]
28. Toure F, et al. Formin mDia1 mediates vascular remodeling via integration of oxidative and signal transduction pathways. Circ Res. 2012; 110(10):1279–93. [PubMed: 22511750]
29. Zhang C, et al. Knockdown of Diaph1 expression inhibits migration and decreases the expression of MMP2 and MMP9 in human glioma cells. Biomedicine & Pharmacotherapy. 2017; 96(Supplement C):596–602. [PubMed: 29035824]
30. Saleh A, et al. Receptor for advanced glycation end-products (RAGE) activates divergent signaling pathways to augment neurite outgrowth of adult sensory neurons. Experimental Neurology. 2013; 249(Supplement C):149–159. [PubMed: 24029001]
31. Bucciarelli LG, et al. RAGE and modulation of ischemic injury in the diabetic myocardium. Diabetes. 2008; 57(7):1941–51. [PubMed: 18420491]
32. Rouhiainen A, et al. Regulation of monocyte migration by amphoterin (HMGB1). Blood. 2004; 104(4):1174–82. [PubMed: 15130941]
33. Guerreiro R, et al. TREM2 variants in Alzheimer's disease. N Engl J Med. 2013; 368(2):117–27. [PubMed: 23150934]
34. Jonsson T, et al. Variant of TREM2 associated with the risk of Alzheimer's disease. N Engl J Med. 2013; 368(2):107–16. [PubMed: 23150908]
35. Hickman SE, El Khoury J. TREM2 and the neuroimmunology of Alzheimer's disease. Biochem Pharmacol. 2014; 88(4):495–8. [PubMed: 24355566]
36. Abuznait AH, Kaddoumi A. Role of ABC transporters in the pathogenesis of Alzheimer's disease. ACS Chem Neurosci. 2012; 3(11):820–31. [PubMed: 23181169]
37. Villegas-Llerena C, et al. Microglial genes regulating neuroinflammation in the progression of Alzheimer's disease. Curr Opin Neurobiol. 2015; 36:74–81. [PubMed: 26517285]
38. Cramer PE, et al. ApoE-directed therapeutics rapidly clear beta-amyloid and reverse deficits in AD mouse models. Science. 2012; 335(6075):1503–6. [PubMed: 22323736]

Author Manuscript Author Manuscript Author Manuscript Author Manuscript

39. Zhang ZG, et al. Inflammation in Alzheimer's Disease and Molecular Genetics: Recent Update. Arch Immunol Ther Exp (Warsz). 2015; 63(5):333–44. [PubMed: 26232392]

40. Tannahill GM, et al. Succinate is an inflammatory signal that induces IL-1beta through HIF-1alpha. Nature. 2013; 496(7444):238–42. [PubMed: 23535595]

41. Barzilay JI, et al. The impact of salsalate treatment on serum levels of advanced glycation end products in type 2 diabetes. Diabetes Care. 2014; 37(4):1083–91. [PubMed: 24255104]

42. Ransohoff RM, Perry VH. Microglial physiology: unique stimuli, specialized responses. Annu Rev Immunol. 2009; 27:119–45. [PubMed: 19302036]

43. Lee S, et al. CX3CR1 deficiency alters microglial activation and reduces beta-amyloid deposition in two Alzheimer's disease mouse models. Am J Pathol. 2010; 177(5):2549–62. [PubMed: 20864679]

44. Saederup N, et al. Selective chemokine receptor usage by central nervous system myeloid cells in CCR2-red fluorescent protein knock-in mice. PLoS One. 2010; 5(10):e13693. [PubMed: 21060874]

45. Prinz M, et al. Heterogeneity of CNS myeloid cells and their roles in neurodegeneration. Nat Neurosci. 2011; 14(10):1227–35. [PubMed: 21952260]

46. Butovsky O, et al. Identification of a unique TGF-beta-dependent molecular and functional signature in microglia. Nat Neurosci. 2014; 17(1):131–43. [PubMed: 24316888]

47. Katsumoto A, et al. Ontogeny and functions of central nervous system macrophages. J Immunol. 2014; 193(6):2615–21. [PubMed: 25193935]

48. Heneka MT, et al. Neuroinflammation in Alzheimer's disease. Lancet Neurol. 2015; 14(4):388–405. [PubMed: 25792098]

49. Ransohoff RM, El Khoury J. Microglia in Health and Disease. Cold Spring Harb Perspect Biol. 2015

50. El Khoury J, et al. Microglia, scavenger receptors, and the pathogenesis of Alzheimer's disease. Neurobiol Aging. 1998; 19(1 Suppl):S81–4. [PubMed: 9562474]

51. Hickman SE, et al. The microglial sensome revealed by direct RNA sequencing. Nat Neurosci. 2013; 16(12):1896–905. [PubMed: 24162652]

52. Schafer Dorothy P, et al. Microglia Sculpt Postnatal Neural Circuits in an Activity and Complement-Dependent Manner. Neuron. 74(4):691–705.

53. Bilimoria PM, Stevens B. Microglia function during brain development: New insights from animal models. Brain Res. 2015; 1617:7–17. [PubMed: 25463024]

54. Schafer DP, Stevens B. Microglia Function in Central Nervous System Development and Plasticity. Cold Spring Harb Perspect Biol. 2015; 7(10)

55. Wu Y, et al. Microglia: Dynamic Mediators of Synapse Development and Plasticity. Trends Immunol. 2015; 36(10):605–13. [PubMed: 26431938]

56. Kuhla B, et al. Age- and stage-dependent glyoxalase I expression and its activity in normal and Alzheimer's disease brains. Neurobiology of Aging. 2007; 28(1):29–41. [PubMed: 16427160]

57. More SS, Vartak AP, Vince R. Restoration of Glyoxalase Enzyme Activity Precludes Cognitive Dysfunction in a Mouse Model of Alzheimer's Disease. ACS Chemical Neuroscience. 2013; 4(2): 330–338. [PubMed: 23421684]

58. Liliensiek B, et al. Receptor for advanced glycation end products (RAGE) regulates sepsis but not the adaptive immune response. J Clin Invest. 2004; 113(11):1641–50. [PubMed: 15173891]

59. Gasparotto J, et al. Receptor for advanced glycation endproducts mediates sepsis-triggered amyloid-β accumulation, tau phosphorylation, and cognitive impairment. Journal of Biological Chemistry. 2017

60. Holmes C, et al. Systemic inflammation and disease progression in Alzheimer disease. Neurology. 2009; 73(10):768–774. [PubMed: 19738171]

61. Wang ZX, et al. Genetic Association of HLA Gene Variants with MRI Brain Structure in Alzheimer's Disease. Molecular Neurobiology. 2017; 54(5):3195–3204. [PubMed: 27056077]

62. Hofmann MA, et al. RAGE and arthritis: the G82S polymorphism amplifies the inflammatory response. Genes And Immunity. 2002; 3:123. [PubMed: 12070776]

Author Manuscript Author Manuscript Author Manuscript Author Manuscript

63. Li K, et al. A functional p.82G>S polymorphism in the RAGE gene is associated with multiple sclerosis in the Chinese population. Mult Scler. 2011; 17(8):914–21. [PubMed: 21511691]

64. Miller S, et al. The Ser82 RAGE Variant Affects Lung Function and Serum RAGE in Smokers and sRAGE Production In Vitro. PLOS ONE. 2016; 11(10):e0164041. [PubMed: 27755550]

65. Wang Y, et al. Synergistic exacerbation of mitochondrial and synaptic dysfunction and resultant learning and memory deficit in a mouse model of diabetic Alzheimer's disease. J Alzheimers Dis. 2015; 43(2):451–63. [PubMed: 25096625]

66. Deane R, et al. RAGE mediates amyloid-β peptide transport across the blood-brain barrier and accumulation in brain. 2003; 9:907.

67. Qosa H, et al. Mixed oligomers and monomeric amyloid-β disrupts endothelial cells integrity and reduces monomeric amyloid-β transport across hCMEC/D3 cell line as an in vitro blood–brain barrier model. Biochimica et Biophysica Acta (BBA) - Molecular Basis of Disease. 2014; 1842(9): 1806–1815.

68. Burstein A, et al. Effect of TTP488 in patients with mild to moderate Alzheimer's disease. BMC Neurology. 2014; 14(1):12. [PubMed: 24423155]

69. Galasko D, et al. Clinical trial of an inhibitor of RAGE-Abeta interactions in Alzheimer disease. Neurology. 2014; 82(17):1536–42. [PubMed: 24696507]

70. Ongoing Azelirgon Clinical Trial

71. Goetz CG. The History of Parkinson's Disease: Early Clinical Descriptions and Neurological Therapies. Cold Spring Harbor Perspectives in Medicine. 2011; 1(1):a008862. [PubMed: 22229124]

72. Oliveira SA, et al. Association study of parkin gene polymorphisms with idiopathic parkinson disease. Archives of Neurology. 2003; 60(7):975–980. [PubMed: 12873854]

73. Gasparotto J, et al. Targeted inhibition of RAGE in substantia nigra of rats blocks 6-OHDA–induced dopaminergic denervation. Scientific Reports. 2017; 7(1):8795. [PubMed: 28821831]

74. Sathe K, et al. S100B is increased in Parkinson's disease and ablation protects against MPTP-induced toxicity through the RAGE and TNF-α pathway. Brain. 2012; 135(11):3336–3347. [PubMed: 23169921]

75. Teismann P, et al. Receptor for advanced glycation endproducts (RAGE) deficiency protects against MPTP toxicity. Neurobiology of Aging. 2012; 33(10):2478–2490. [PubMed: 22227007]

76. Hardiman O, et al. Amyotrophic lateral sclerosis. Nat Rev Dis Primers. 2017; 3:17085.

77. Kikuchi S, et al. Detection of N epsilon-(carboxymethyl)lysine (CML) and non-CML advanced glycation end-products in the anterior horn of amyotrophic lateral sclerosis spinal cord. Amyotroph Lateral Scler Other Motor Neuron Disord. 2002; 3(2):63–8. [PubMed: 12215227]

78. Juranek JK, et al. Receptor for Advanced Glycation End Products and its Inflammatory Ligands are Upregulated in Amyotrophic Lateral Sclerosis. Front Cell Neurosci. 2015; 9:485. [PubMed: 26733811]

79. Casula M, et al. Toll-like receptor signaling in amyotrophic lateral sclerosis spinal cord tissue. Neuroscience. 2011; 179:233–43. [PubMed: 21303685]

80. Kaufmann E, et al. The advanced glycation end-product N epsilon-(carboxymethyl)lysine level is elevated in cerebrospinal fluid of patients with amyotrophic lateral sclerosis. Neurosci Lett. 2004; 371(2-3):226–9. [PubMed: 15519762]

81. Ilzecka J. Serum-soluble receptor for advanced glycation end product levels in patients with amyotrophic lateral sclerosis. Acta Neurol Scand. 2009; 120(2):119–22. [PubMed: 19053950]

82. Juranek JK, et al. Soluble RAGE Treatment Delays Progression of Amyotrophic Lateral Sclerosis in SOD1 Mice. Front Cell Neurosci. 2016; 10:117. [PubMed: 27242430]

83. Lo Coco D, et al. Distribution and cellular localization of high mobility group box protein 1 (HMGB1) in the spinal cord of a transgenic mouse model of ALS. Neurosci Lett. 2007; 412(1): 73–7. [PubMed: 17196331]

84. Kim MJ, et al. Nitration and Glycation Turn Mature NGF into a Toxic Factor for Motor Neurons: A Role for p75(NTR) and RAGE Signaling in ALS. Antioxid Redox Signal. 2017

85. Caillier SJ, et al. Uncoupling the roles of HLA-DRB1 and HLA-DRB5 genes in multiple sclerosis. J Immunol. 2008; 181(8):5473–80. [PubMed: 18832704]

Author Manuscript Author Manuscript Author Manuscript Author Manuscript

86. Tiszlavicz Z, et al. RAGE gene polymorphisms in patients with multiple sclerosis. J Mol Neurosci. 2009; 39(3):360–5. [PubMed: 19757202]

87. Sternberg Z, et al. Soluble receptor for advanced glycation end products in multiple sclerosis: a potential marker of disease severity. Mult Scler. 2008; 14(6):759–63. [PubMed: 18505774]

88. Andersson A, et al. Pivotal advance: HMGB1 expression in active lesions of human and experimental multiple sclerosis. J Leukoc Biol. 2008; 84(5):1248–55. [PubMed: 18644848]

89. Barateiro A, et al. S100B as a Potential Biomarker and Therapeutic Target in Multiple Sclerosis. Mol Neurobiol. 2016; 53(6):3976–3991. [PubMed: 26184632]

90. Sternberg Z, et al. High-mobility group box 1 in multiple sclerosis. Immunol Res. 2016; 64(2): 385–91. [PubMed: 26100980]

91. Sternberg Z, et al. Fingolimod anti-inflammatory and neuroprotective effects modulation of RAGE axis in multiple sclerosis patients. Neuropharmacology. 2017; 130:71–76. [PubMed: 29197515]

92. Yan SS, et al. Suppression of experimental autoimmune encephalomyelitis by selective blockade of encephalitogenic T-cell infiltration of the central nervous system. Nat Med. 2003; 9(3):287–93. [PubMed: 12598893]

Author Manuscript Author Manuscript Author Manuscript Author Manuscript

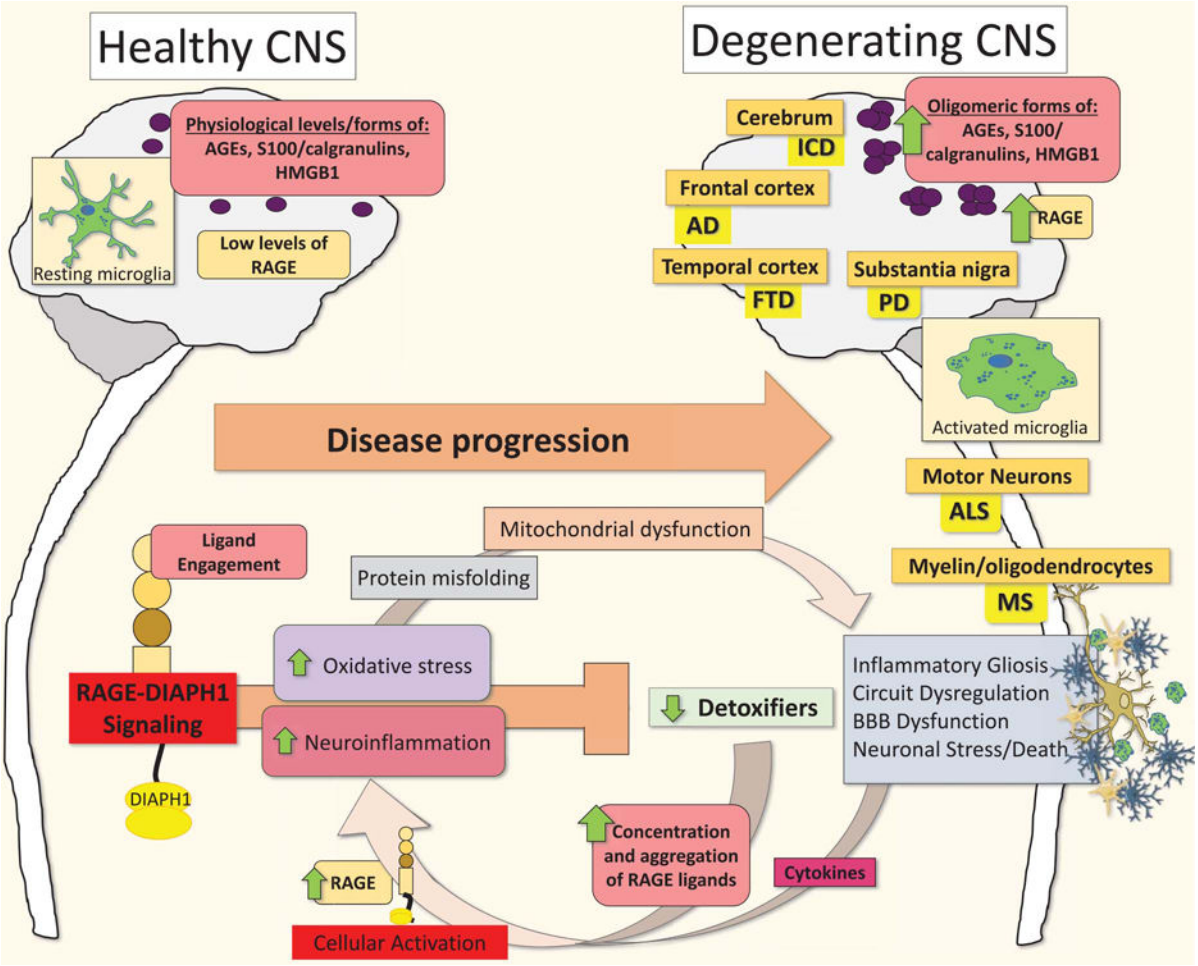

Figure. Working model of RAGE signaling in microglia and the pathogenesis of neurodegenerative disease

Increases in pathological levels and oligomeric forms of RAGE ligands characterize the transition from health and homeostasis to disease- mediating activities in microglia during the progression of AD, PD, ALS and MS. These pathological RAGE ligands promote RAGE-DIAPH1 signaling-induced oxidative stress, cytokine production, gliosis, and inflammation. Inflammatory cell activation further induces increased RAGE and RAGE ligand expression, while decreasing innate detoxifiers, thereby promoting an inflammatory feed-forward loop resulting in strikingly higher degrees of inflammatory gliosis, neuronal stress, BBB dysfunction and, eventually, neuronal death. We posit that activation of the AGE-RAGE-DIAPH1 axis in microglia is an amplifying event and critical final common pathway driving increased cellular stress and inflammation leading to neurodegeneration and the progression of AD, PD, ALS and MS. Abbreviations: AD, Alzheimer's disease; AGEs, advanced glycation end products; ALS, Amyotrophic lateral sclerosis; BBB, blood-brain barrier; HMGB1, high mobility group box protein 1; MS, Multiple Sclerosis; and PD, Parkinson's disease.

Author Manuscript Author Manuscript Author Manuscript Author Manuscript

	RAGE SNPs	Animal Findings		Human Findings	
Alzheimer's disease	rs2070600	**1**	Increased RAGE and ligands	**1**	Increased RAGE and ligands
		2	Mitochondrial Dysfunction	**2**	Hippocampal atrophy associated with SNP
		3	Decreased detoxification molecules	**3**	Decreased sRAGE
		4	Decreased sRAGE		
		5	Oxidative Stress		
		6	Microglia and ECs implicated		
Ischemic Cerebrovascular disease	rs2070600	**1**	Increased RAGE and ligands	**1**	Increased RAGE and ligands
		2	Exacerbated by hyperglycemia in RAGE-dependent manner	**2**	cRAGE (sRAGE) increased acutely after stroke
		3	Strong connections to peripheral monocytes, microglia, and ECs	**3**	RAGE+ Monocyte infiltration
Parkinson's disease	rs2070600	**1**	Increased RAGE and ligands	**1**	Increased RAGE and ligands
		2	RAGE exacerbates all known symptoms of disease in models		
Amyotrophic Lateral Sclerosis and FTD	No known SNPs associated	**1**	Increased RAGE and ligands	**1**	Increased RAGE and ligands
		2	RAGE-induced motor neuron death	**2**	Decreased sRAGE
		3	Stronger implication for astrocytes		
		4	sRAGE treatment beneficial		
Multiple Sclerosis	rs2070600 RAGE promoter	**1**	Increased RAGE and ligands	**1**	Lower sRAGE
		2	sRAGE is protective for lifespan and peripheral infiltration	**2**	RAGE and ligands increased in disease and MS lesions
		3	Most controversial due to lack of protection in global *AGER* KO	**3**	Ligands go down with disease modifying drugs

Neurochemistry International 126 (2019) 154–164

Contents lists available at ScienceDirect

Neurochemistry International

journal homepage: www.elsevier.com/locate/neuint

The Receptor for Advanced Glycation End Products (RAGE) and DIAPH1: Implications for vascular and neuroinflammatory dysfunction in disorders of the central nervous system

Michael MacLean, Julia Derk, Henry H. Ruiz, Judyta K. Juranek, Ravichandran Ramasamy, Ann Marie Schmidt*

Diabetes Research Program, Division of Endocrinology, Diabetes and Metabolism, Department of Medicine, New York University School of Medicine, New York, NY, 10016, USA

A B S T R A C T

The Receptor for Advanced Glycation End Products (RAGE) is expressed by multiple cell types in the brain and spinal cord that are linked to the pathogenesis of neurovascular and neurodegenerative disorders, including neurons, glia (microglia and astrocytes) and vascular cells (endothelial cells, smooth muscle cells and pericytes). Mounting structural and functional evidence implicates the interaction of the RAGE cytoplasmic domain with the formin, Diaphanous1 (DIAPH1), as the key cytoplasmic hub for RAGE ligand-mediated activation of cellular signaling. In aging and diabetes, the ligands of the receptor abound, both in the central nervous system (CNS) and in the periphery. Such accumulation of RAGE ligands triggers multiple downstream events, including upregulation of RAGE itself. Once set in motion, cell intrinsic and cell-cell communication mechanisms, at least in part via RAGE, trigger dysfunction in the CNS. A key outcome of endothelial dysfunction is reduction in cerebral blood flow and increased permeability of the blood brain barrier, conditions that facilitate entry of activated leukocytes into the CNS, thereby amplifying primary nodes of CNS cellular stress. This contribution details a review of the ligands of RAGE, the mechanisms and consequences of RAGE signal transduction, and cites multiple examples of published work in which RAGE contributes to the pathogenesis of neurovascular perturbation. Insights into potential therapeutic modalities targeting the RAGE signal transduction axis for disorders of CNS vascular dysfunction and neurodegeneration are also discussed.

1. Introduction

The Receptor for Advanced Glycation End Products (RAGE) was discovered on account of its ability to bind the products of non-enzymatic glycation and oxidation of proteins/lipids, termed advanced glycation end products (AGEs). In addition to AGEs, RAGE binds a number of distinct ligands, such as those involved in immune/inflammatory responses, such as S100/calgranulins and high mobility group box 1 (HMGB1), and oligomeric forms of amyloid-β peptide (Aβ) (Lopez-Diez et al., 2016; Ramasamy et al., 2016). The consequent discovery that RAGE was a multi-ligand receptor set the stage for a fuller understanding of the biology of RAGE in homeostasis and in disease.

Although the highest expression of RAGE in homeostatic states is in the lung, a plethora of evidence suggests that in both human subjects and in experimental model systems, the expression of the receptor is enhanced in settings in which its ligands become more abundant. For example, in tissues affected by diabetes, aging, neurodegeneration, ischemia/reperfusion injury (Aleshin et al., 2008; Bucciarelli et al., 2006, 2008), chronic inflammation and cancer, higher expression of RAGE has been observed compared to non-affected control tissues (Cipollone et al., 2003; Juranek et al., 2015; Palanissami and Paul, 2018; Yan et al., 1996). RAGE is expressed on multiples different cell types, including vascular cells, such as endothelial cells (ECs) and smooth muscle cells (SMCs); and immune/inflammatory cells, such as neutrophils, monocytes/macrophages, T and B lymphocytes and dendritic cells (Avalos et al., 2010; Daffu et al., 2015; Dumitriu et al., 2005; Moser et al., 2007; Wautier et al., 1996). Vascular and immune cell dysfunction exacerbates cellular homeostasis in RAGE-expressing target cells in chronic diseases, such as neurons, cardiomyocytes, glomerular epithelial cells (podocytes) and skeletal muscle (Shang et al., 2010; Sorci et al., 2003; Tanji et al., 2000; Yan et al., 1996).

The fact that RAGE is differentially expressed in various organs and cell types suggested RAGE-dependent and -independent cell intrinsic and/or cell-cell communication networks in homeostasis and disease. This review highlights the role of RAGE in the central nervous system (CNS) and details how vascular, immune cell, and neuronal interactions might play important roles in disease pathogenesis and progression, and how the temporal cues of such cell intrinsic and cell-cell networking vis-à-vis RAGE may mediate pro-repair and survival vs. pro-inflammatory and anti-repair signals, leading to cell death. Finally, this review will provide insight into novel therapeutic approaches targeting RAGE signaling.

* Corresponding author. New York University School of Medicine, Science Building, 435 East 30th Street, Room 615, New York, NY, 10016, USA.
E-mail address: Annmarie.schmidt@nyumc.org (A.M. Schmidt).

https://doi.org/10.1016/j.neuint.2019.03.012
Received 19 February 2019; Received in revised form 13 March 2019; Accepted 16 March 2019
Available online 20 March 2019
0197-0186/ © 2019 Elsevier Ltd. All rights reserved.

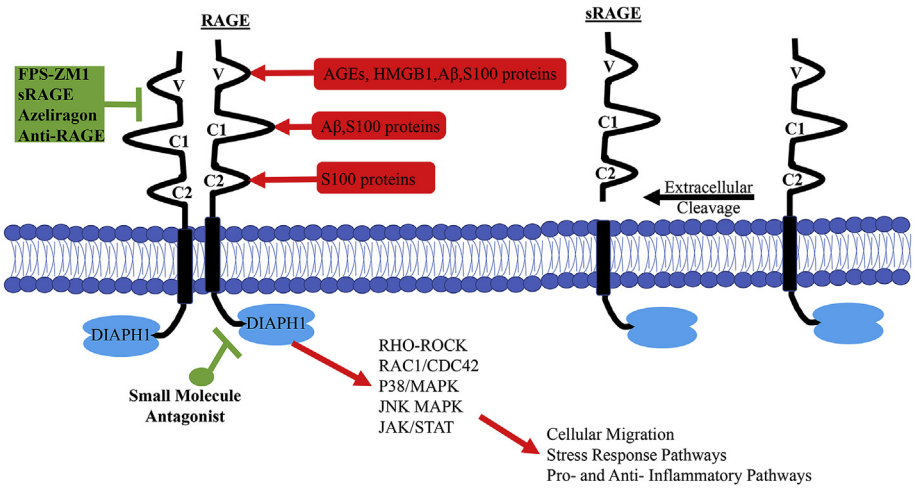

Fig. 1. Schematic of RAGE signal transduction and examples of inhibition by antagonists. The extracellular immunoglobin-like (Ig) domains of RAGE (V, C1, C2) all have been shown to bind RAGE ligands. Many widely-used receptor antagonists (Anti-RAGE antibodies, Azeliragon, and FPS-ZM1) interact with the extracellular domains to prevent ligand engagement. Soluble RAGE (sRAGE) is postulated to sequester RAGE ligands and prevent their engagement with the dimerized full-length receptor. There are two forms of sRAGE: the first is produced by extracellular proteolytic cleavage of the full-length receptor, which liberates the extracellular domains from the transmembrane domain and intracellular domain, and the second is a product of an mRNA splice variant. The formin, Diaphanous-1 (DIAPH1), interacts with the cytoplasmic tail of RAGE and mediates signal transduction. Several candidate small molecule antagonists have been generated to prevent the RAGE-DIAPH1 interaction. RAGE signal transduction is cell-type dependent but can include RHO/ROCK, RAC1/CDC42, P38/MAPK, JNK MAPK and JAK/STAT. These events result in changes to cellular migration, stress responses, and regulation of pro- and anti- inflammatory pathways (NFκB activation) as well as other changes in cellular properties.

2. RAGE structure and soluble forms

RAGE is a member of the immunoglobulin (Ig) superfamily of cell surface molecules. It is composed of three extracellular domains (one V-type and two C-type Ig-like domains). These extracellular domains are followed by a single, hydrophobic transmembrane domain and by a short, less than 45 amino acid cytoplasmic domain, which is essential for RAGE ligand-mediated signaling (Fig. 1). The extracellular domains of RAGE are the sites of known extracellular ligand binding. Although the V-type domain is the preferential binding site for most of the ligand families, other reports have indicated that the C-type domains may also mediate binding of some of the RAGE ligands. The V-type Ig domain itself is heterogeneous, as distinct binding pockets, characterized by their charge or hydrophobicity states, exist on this domain for ligand engagement (Xie et al., 2007, 2008).

The extracellular domains of RAGE, known as soluble RAGE, may exist in soluble form and in *in vitro* and *in vivo* experimentation, appear to sequester RAGE ligands and block their binding to and activation of cell surface receptors, including membrane bound RAGE (Schmidt et al., 1994). There are two forms of soluble RAGEs that have been identified in human subjects (Schmidt, 2015). The first is cell surface-cleaved soluble or sRAGE, which is produced via the actions of metalloproteases or other molecules, such as ADAM-10 (a disintegrin and metalloproteinase domain-containing protein 10) (Raucci et al., 2008), and the second form, called endogenous secretory or esRAGE, is the result of an RNA splice variant (Yonekura et al., 2003). Research tools have been employed to measure total sRAGEs (including cell surface cleaved sRAGE and esRAGE) or esRAGE alone on human subject serum/plasma or other tissue fluids (such as cerebrospinal fluid (CSF)) to assess possible relationships to the state and/or the extent of disease. For example, in diabetes, aging, stroke, subarachnoid hemorrhage (SAH), and in neurodegenerative disorders, such as Alzheimer's Disease (AD) or amyotrophic lateral sclerosis (ALS), measurements of sRAGEs have been reported to distinguish affected vs. unaffected subjects (Emanuele et al., 2005; Ilzecka, 2009; Loomis et al., 2017; Lue et al., 2009; Saito et al., 2017; Sokol et al., 2017; Tang et al., 2017). The extent to which measurements of sRAGEs may serve as reliable and reproducible biomarkers of RAGE-related chronic diseases, however, is uncertain. Given the multiple settings in which RAGE appears to be related to pathobiology, the specificity/sensitivity of soluble RAGEs as a biomarker for disease onset, progression and/or the response to therapeutic intervention, is uncertain and remains to be tested.

3. RAGE and mechanisms of signal transduction

The cytoplasmic domain of RAGE lacks endogenous kinase activity and through a yeast two-hybrid assay, it was discovered that this domain of RAGE bound the FH1 (formin homology 1) domain of Diaphanous1 (DIAPH1) (Hudson et al., 2008). Formins such as DIAPH1 play key roles in actin cytoskeleton rearrangements and regulation of Rho GTPases and serum response factor (SRF)-dependent genes, factors and pathways that regulate cellular migration, signal transduction and stress-responsive gene programs (Chesarone et al., 2010; Kühn and Geyer, 2014). Collectively, these properties have been shown to be key consequences of ligand-RAGE signaling. Multiple studies in SMCs, ECs, macrophages, and cardiomyocytes, for example, indicate that DIAPH1 is required for the effects of RAGE ligands to modulate signal transduction and functional outcomes in these cells (Hudson et al., 2008; Touré et al., 2012; Xu et al., 2010; Zhou et al., 2018). *In vivo*, deletion of *Diaph1* protects from cardiac ischemia-reperfusion injury and hypoxia-related upregulation of *Egr1,* which encodes a transcriptional regulator protein highly expressed in the CNS, such as in microglia, (Landis et al., 1993); diabetes-associated pathologies in the kidney; macrophage inflammation; and restenosis after endothelial denudation of the femoral artery (Manigrasso et al., 2018; O'Shea et al., 2017; Touré et al., 2012; Xu et al., 2010), all phenotypes that parallel the observations in *Ager* (the gene encoding RAGE) null mice in these stress conditions.

Recent work has solved the structure of the RAGE cytoplasmic domain and the nature of its interaction with DIAPH1 and has revealed that mutation of RAGE cytoplasmic domain R5/Q6 amino acid residues to alanine residues resulted in failure to bind DIAPH1 by NMR spectroscopy and failure of RAGE ligand-mediated signal transduction in cultured SMCs (Rai et al., 2012; Xue et al., 2016).

In the section to follow, this review will consider how systemic conditions may modulate the levels of RAGE ligands and RAGE, and, thereby, affect the functions of multiple cell types in the CNS, including those associated with the blood-brain barrier (BBB).

4. Systemic disorders & modulation of the BBB: A spark that ignites CNS dysfunction

The BBB is composed of a continuous monolayer of ECs with closely apposed astrocytic foot processes and pericytes embedded into the nonfenestrated basement membrane of the border. These ECs are connected by tight junctions, which function to regulate entry of large macromolecules, cells and pathogens. Although oxygen and carbon dioxide flow freely, the BBB is responsible for the exclusion of the entry

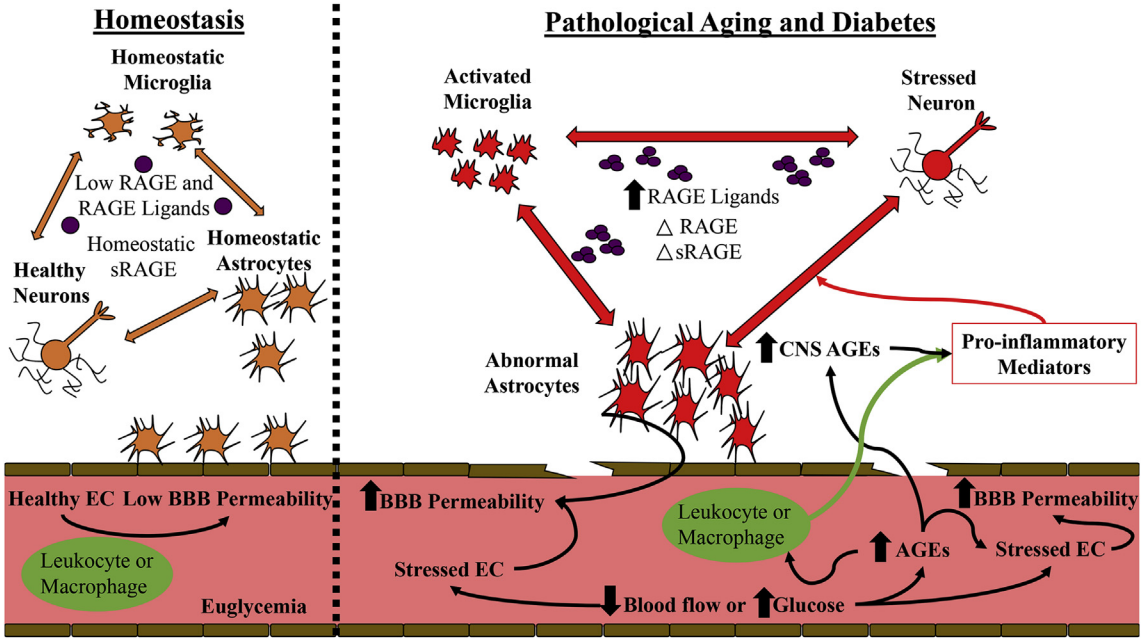

Fig. 2. Working model of RAGE-dependent contributions to blood-brain barrier (BBB) dysfunction. Increases in RAGE ligands, blood glucose and/or decreased blood flow promote the transition from homeostasis to disease by promoting BBB dysfunction, AGE generation, and overall cellular stress within neurons, microglia, astrocytes and endothelial cells (EC). Depending on the disease and aging condition, RAGE and sRAGE levels may be altered. We posit that age-, diabetes-, or neurodegenerative disease- induced AGE accumulation within the CNS and the periphery initiates and perpetuates endothelial permeability and BBB dysfunction, thereby promoting BBB breakdown, at least in part via RAGE signaling.

of species that might cause harm to the vulnerable brain and spinal cord (Iadecola, 2017; Kisler et al., 2017; Presta et al., 2018) and for modulating blood flow appropriately in various locations during activities in which metabolic and oxygenation requirements are altered. Two conditions in which the BBB becomes gradually more compromised include diabetes and natural aging, both known risk factors for neurodegenerative disorders such as AD and other neurodegenerative disorders (Sweeney et al., 2018) and for ischemic stroke; all settings in which RAGE ligands accumulate and are plentiful (Fig. 2).

4.1. Diabetes

Glucose is essential for brain metabolism and is normally transported into the brain by specialized transporters (GLUT). However, in excess, glucose may *directly* activate pathways such as Protein Kinase C and the polyol pathway, thereby activating mechanisms that promote oxidative stress and inflammation, such as in resident microglia. Further, if the BBB is compromised, the influx of periphery-derived immune/inflammatory cells may ensue, thereby augmenting inflammation. In addition, high glucose may upregulate levels of hypoxia-inducible factor-1α (HIF-1α), thereby leading to increased expression of Vascular Endothelial Growth Factor (VEGF) and, consequently, increased vascular permeability (Van Dyken and Lacoste, 2018).

In addition to such potential direct effects of high levels of glucose, increased glucose levels may result in the generation of AGEs. AGEs, via their interactions with their central cell surface receptor, RAGE, may result in amplification of inflammatory and oxidative stress, at least in part through the activation of NF-κB. In streptozotocin-induced type 1 diabetic mice, expression of RAGE was shown to be increased at the BBB (Liu et al., 2009). In non-CNS vascular beds, in diabetic rats, AGEs mediated vascular permeability in a RAGE-dependent manner and in coronary arterioles of type 2 diabetic mice, endothelial dysfunction was reversed by treatment with sRAGE (Gao et al., 2008; Wautier et al., 1996), thus suggesting that sequestration of RAGE ligands and suppression of RAGE/DIAPH1 signaling is beneficial for overall homeostasis and BBB integrity.

4.2. Aging

It is well-established that aging is the chief risk factor for vascular disorders of the brain and for neurodegenerative processes. Reduced blood flow, disruption of microvascular integrity and BBB dysfunction accompany aging (Farkas and Luiten, 2001; Montagne et al., 2015; Park et al., 2018). Recent work, using CSF biomarkers and dynamic contrast-enhanced magnetic resonance imaging in human subjects, has shown that breakdown of the BBB around the hippocampus is a very early marker of cognitive impairment and that these pathologies are independent of Aβ deposition or tau aggregation (Nation et al., 2019). In this context, AGEs increase even in euglycemic aging, based on the nonenzymatic glycation/oxidation of long-lived proteins whose exposure to even normal levels of glucose may, ultimately, result in formation of AGE adducts. In the aortas of aged Fischer 344 rats, the concentration of the key AGE precursor, methylglyoxal (MG), was significantly increased compared with aortas from young Fischer rats. Impaired aging-associated endothelial-dependent relaxation in aortic rings from aged animals was reversed by treatment with sRAGE (Hallam et al., 2010).

Collectively, these considerations suggest that one of the components of BBB dysfunction in key settings linked to neurodegeneration and vascular damage to the CNS is the ligand-RAGE pathway. The extent to which DIAPH1 may, or may not, contribute to the maintenance or dysfunction of the BBB remains to be determined. However, it is conceivable that DIAPH1 perturbation may contribute importantly to endothelial dysfunction and loss of BBB integrity given the roles of this molecule in actin cytoskeleton organization and the observation that ligand stimulation of the RAGE/DIAPH1 axis generates oxidative stress, through NADPH oxidases, and promotes inflammation (Touré et al., 2012). Recent work showed that DIAPH1 is expressed in human aged AD brain to a greater extent than that in age-matched controls and in multiple cell types (Derk et al., 2018a). In the sections to follow, this review will consider settings of CNS dysfunction in which roles for the RAGE axis have been postulated and probed.

5. CNS vascular disorders and the RAGE axis

In human subjects, investigators have studied whether genetic variations in *AGER* might contribute to risk of various forms of vascular disorders in the CNS. In the Sahlgrenska Academy Study on Ischaemic Stroke, 732 Caucasian subjects with first-ever and 112 Caucasian subjects with recurrent ischemic stroke were compared with 668 Caucasian controls. Of three tested *AGER* single nucleotide polymorphisms (SNP), one SNP, rs1035798 (maps to the third *AGER* intron), showed a significant association with small vessel disease subtype of stroke, which was independent of hypertension, diabetes and smoking. However, none of these SNPs demonstrated significant associations with overall ischemic stroke (Olsson and Jood, 2013). In a Chinese population, 384 subjects with ischemic stroke and 425 healthy control subjects were enrolled and three different *AGER* SNPs were examined (82G/S, −429T/C and −374T/A). Only the 82G/S *AGER* SNP (rs2070600) was associated with the risk for ischemic stroke. Of the homozygote carriers (82S/S), there were generally higher levels of inflammation, as evidenced by lower serum sRAGE levels, and higher levels of serum IL6, hsCRP and PAI1 (Cui et al., 2013). In contrast, the SNPs at −374 and −429 loci demonstrated no association with stroke risk or the levels of inflammatory markers. In a distinct study examining risk for hemorrhagic stroke in a Chinese population, it was found that in subjects less than or equal to 50 years of age, the rs1035798 AGER SNP (homozygote) was associated with increased risk of hemorrhagic stroke (Liu et al., 2015). Further, in a Chinese population, *AGER* rs2070600 and *HMGB1* 2249825 were found to bear relationships to stroke (Li et al., 2017b).

Finally, Montaner and colleagues probed whether measurement of RAGE ligand S100B and sRAGE levels (as well as other markers) might aid in differentiating ischemic vs. hemorrhagic stroke. Admission blood samples obtained from 915 patients (776 with ischemic stroke and 139 with hemorrhagic stroke) within 24 h of the event onset revealed that in samples obtained within the first 6 h (or even in the first 3 h after symptoms) of stroke, increased S100B levels and decreased sRAGE levels were found in hemorrhagic vs. ischemic stroke. The authors speculated that measurement of these S100B and sRAGE markers might aid in differentiation of the two forms of stroke (Montaner et al., 2012). Experiments in animal models tested if the RAGE pathway exerted mediating roles in these disorders.

5.1. Ischemic stroke

In a murine model of focal cerebral ischemia, the effects of neuronal RAGE expression on ischemic stroke were tested in transgenic mice expressing either a full-length form of RAGE or a cytoplasmic domain-deleted form of RAGE in neurons. Compared to normal control animals, neuronal RAGE overexpressing mice displayed significantly increased stroke volume while a trend towards decreased stroke volume was observed in the animals with cytoplasmic domain-deleted RAGE, in which RAGE signaling was reduced (Hassid et al., 2009). In a model of global cerebral ischemia induced by bilateral common carotid artery occlusion, wild-type mice, global *Ager* null mice and transgenic mice expressing esRAGE (as decoy receptor) were tested. A time course study in that model was first performed in wild-type mice, which revealed that increased expression of RAGE was first noted in vascular cells within 12 h of injury and later, between 24 h and 7 days after injury, RAGE expression was increased in glial cells in the hippocampus. Compared to the wild-type mice, mice globally devoid of *Ager* or mice expressing esRAGE displayed higher numbers of surviving neurons in the CA1 region of the hippocampus, in parallel with lower degrees of oxidative stress. After 12 h, the expression of inflammatory markers, such as TNFα and iNOS was lower in the *Ager* null and the esRAGE mice vs. the wild-type, consistent with reduced glial inflammation (Kamide et al., 2012).

Others probed the effects of RAGE and its ligand HMGB1 in ischemic stroke in a mouse model. After the authors demonstrated that HMGB1 was elevated in human stroke patients, they reported that HMGB1 was released from ischemic brain tissue in a murine model of cerebral ischemia. Mediating roles for HMGB1 in stroke were demonstrated by reduction of brain damage in mice treated with either antibodies to HMGB1 or an antagonist to this RAGE ligand. As *in vitro* studies suggested that microglia RAGE contributed to the toxic effects of HMGB1, wild-type mice were subjected to lethal irradiation and transplantation with either *Ager* null or wild-type bone marrow. Those studies revealed that recipients of *Ager* null bone marrow demonstrated reduced infarct size compared with those mice receiving wild-type bone marrow and subjected to ischemic stroke (Muhammad et al., 2008). In distinct studies, it was shown that in murine ischemic stroke, RAGE drives a pro-inflammatory and blunting of anti-inflammatory polarization in diabetic mice (Khan et al., 2016). Interestingly, type 1 diabetic rats treated with Niaspan, a cholesterol-lowering agent, during transient middle cerebral artery occlusion, displayed diminished HMGB1-RAGE-dependent inflammatory profiles (Ye et al., 2011). Given that RAGE has previously been implicated in regulating the cholesterol efflux protein, ABCG1 (Daffu et al., 2015), those data suggest that RAGE may drive inflammatory dysregulation of CNS cells during stroke, at least in part, through impairment of cholesterol homeostasis. More work, however, is required to elucidate the precise mechanisms and connections. Collectively, these studies in ischemic stroke models suggest roles for RAGE in exacerbating the pathogenesis of stroke damage and implicate RAGE actions in vascular, immune/inflammatory and neuronal cells, perhaps in a time-dependent manner.

5.2. Intracerebral hemorrhage (ICH)

An antagonist of RAGE, FPS-ZM1, which blocks binding of ligands such as HMGB1 and S100B to the V-type Ig extracellular domain of RAGE, was employed in a rat and murine model of ICH. In a rat model of ICH, induced by collagenase, it was shown that release of HMGB1 results in expression of VEGF, thereby increasing pathological angiogenesis. In that model, a time-dependent increase in expression of RAGE and HMGB1 was noted in the ipsilateral striatum after induction and up to 14 days later. Treatment with FPS-ZM1 suppressed expression of VEGF and vessel density after induction of hemorrhage in this model (Yang et al., 2015). In a distinct species (mice) and with the use of autologous arterial blood injection into the basal ganglia, ICH was induced in wild-type mice. By 12 h after the injury, expression of RAGE and HMGB1 was increased, in parallel with increased expression of NF-κB p65 and increased permeability of the BBB, brain edema, motor dysfunction and neve fiber injury. Paralleling these markers of damage, local levels of IL1β, IL6, IL8R, and MMP9 were also elevated. In mice treated with FPS-ZM1, however, all of these pathological markers were reduced compared to vehicle-treated mice undergoing ICH (Lei et al., 2015). Together, these findings highlight the importance of ligand-RAGE signaling in the pathophysiology of ICH.

5.3. Subarachnoid hemorrhage (SAH)

In contrast to ICH, SAH is characterized by bleeding between the brain and the skull. Once blood accumulates in that region within the CSF, it causes inflammation in the surrounding brain tissue and increases pressure onto the brain as a result of edema. In model systems, such as the rat, SAH may be induced by injection of autologous blood into the prechiasmatic cistern. Induction of hemorrhage by this method in rats was shown to be associated with increased inflammation, as evidenced by increased expression of RAGE ligands HMGB1 and S100 proteins. In this rat model, expression of RAGE and nuclear NF-κB p65 was significantly increased, particularly in neurons and in microglia, but not in astrocytes (Li et al., 2014). The effects of the RAGE antagonist FPS-ZM1 were tested in this model. These studies revealed that at one day after SAH, the mice treated with the RAGE antagonist

displayed reduced brain edema and better neurological score vs. vehicle. However, by 3 days after hemorrhage, the RAGE antagonist-treated mice displayed increased neuronal cell death with higher levels of apoptosis and diminished autophagy (Li et al., 2017a). These data suggested that, at least in mice and in this model system, RAGE may play both damaging and protective roles, perhaps based on its actions in distinct cell types and on the timing of the post-SAH response. Although the work in that study did not provide insight into potentially contrary cell type-specific roles for RAGE, it is nevertheless important to note that neurons and microglia prominently expressed RAGE after the induction of the SAH.

Finally, in distinct work in the rat model of SAH, the specific effects of RAGE ligand HMGB1 were addressed. In that study, the authors found that the highest expression of HMGB1 occurred on day 14 after the hemorrhage. The rats undergoing SAH were treated with two different inhibitors of HMGB1 secretion (ethyl pyruvate or glycyrrhizin) or the RAGE antagonist, FPS-ZM1. These treatments resulted in reduced expression of growth factors and reduced proliferation of cortical neurons. The authors hypothesized that the redox status form of the HMGB1 might regulate its damaging vs. protective effects. Indeed, compared to administration of recombinant HMGB1, administration of oxidized HMGB1 failed to stimulate pro-inflammatory cytokine production and exhibited protection in the brain, as neurotrophin expression was increased, in parallel with brain recovery (Tian et al., 2017). The authors speculated that in late stages after SAH, HMGB1 may be protective, particularly in the oxidized form.

In summary, RAGE and its ligands appear to contribute to the response to ischemic stroke and to stroke induced by various forms of hemorrhage (intracerebral vs. subarachnoid). The finding that the administration of inhibitors to RAGE ligands or to RAGE itself is not uniformly beneficial or deleterious underscores the possibility that RAGE plays differential roles depending on whether the cells are vascular cells (EC and SMC), immune/inflammatory cells such as microglia, astrocytes and infiltrating immune cells, or neurons. Further, the effects of RAGE actions may be protective and/or deleterious, perhaps depending on the timing in the post-stroke or post-hemorrhage period. In order to provide support for RAGE as a potential target for therapeutic intervention in these disorders, it will be necessary to test these concepts using cell type- and time-dependent deletion of *Ager*, which can be achieved, for example, by using the cre-lox recombinase technique. Further, more extensive time course studies with RAGE or ligand inhibitors are essential, that is, varying the time post-stroke event at which the inhibitors are begun/terminated. Also, further elucidation of the concentrations of these compounds that may be detrimental vs. beneficial in stroke subjects will be important to delineate. Only by such meticulous approaches may the full roles for RAGE and its ligands in these disorders be uncovered and the potential for targeting this axis in stroke and hemorrhage of the CNS be potentially realized.

In the sections to follow in this review, the role of the RAGE signaling axis in disorders of neurodegeneration will be discussed.

6. The RAGE axis and neurodegeneration

The RAGE axis has been implicated in a number of neurodegenerative disorders (Derk et al., 2018b). In this review, the influence of this pathway on AD, amyotrophic lateral sclerosis (ALS) and Parkinson's Disease will be considered. Of note, however, although not covered in this review, work has been published suggesting links of RAGE to Huntington's disease and Creutzfeldt-Jakob disease (Anzilotti et al., 2012; Sasaki et al., 2002).

6.1. Alzheimer's disease

RAGE is expressed in multiple cell types germane to the pathogenesis of AD, including neurons, microglia, astrocytes and ECs; in recent work, the expression of the RAGE cytoplasmic domain binding partner, DIAPH1 has been assessed in AD as well. In that work, the medial temporal cortices of AD patients and aged-matched controls were tested for DIAPH1 expression patterns in multiple cell types, including endothelial cells, oligodendrocytes, neurons, astrocytes, pericytes and myeloid cells. In the case of endothelial cells, the expression of the endothelial marker, Claudin-5, was significantly higher in the AD brain compared to the non-demented brain, but there was no change in relative DIAPH1 intensity within endothelial cells. In oligodendrocytes, marked by expression of myelin basic protein (MBP), no changes were observed for DIAPH1 and total MBP expression within non-demented aging and AD brains. In the case of the marker for neurons, microtubule-associated protein 2 (MAP2), a relative decrease of MAP2 expression in the AD brain was noted compared to the non-demented brain. However, there was no associated change in DIAPH1 intensity. In the case of astrocytes, although an increase in GFAP-positive area was observed in the AD brain, as the area of GFAP positivity increased, so did DIAPH1-positive/GFAP-positive overlap area. Thus, there was no specific change in astrocyte DIAPH1 noted in AD versus the non-demented control brain. Testing for pericyte colocalization with DIAPH1 through the use of an α-Smooth Muscle Actin (α-SMA) antibody revealed that there was no colocalization in either the non-demented or AD brain.

In contrast to the above cell types, however, in the case of myeloid cells, using CD68 as a marker, a significant increase in overlap area between DIAPH1 and CD68 and a significant increase in DIAPH1 intensity within $CD68^{+}$ cells in the AD brain relative to the non-demented control brain was observed. Thus, unlike the other cell types noted above, DIAPH1 expression patterns within myeloid cells were found to be significantly increased in AD. Notably, DIAPH1 expression in myeloid cells correlated with increased lipid staining and inflammatory morphology (Derk et al., 2018a).

Genome wide association studies (GWAS) implicated aging (Chauhan et al., 2015) and inflammatory pathways and activation of microglia in the pathogenesis of AD (Guerreiro et al., 2013; Jonsson et al., 2013; Villegas-Llerena et al., 2016; Zhang et al., 2015). Hence, given the roles for RAGE in inflammatory mechanisms, potential genetic links between *AGER* and AD were studied. As *AGER* is one of the genes in the Human Leukocyte Antigen (HLA) Class III region of the Major Histocompatibility Complex (MHC), the potential implications of *AGER* SNPs with AD were studied in 194 Italian patients with AD and 454 healthy controls. The −374 and −429 AGER SNPs were studied, along with those for *TNFA* and the results of haplotype reconstruction studies suggested that the HLA Class III region might be implicated in AD susceptibility (Maggioli et al., 2013), which was affirmed in a follow-up study in which *HSP70* SNPs were also considered (Boiocchi et al., 2015). In another study of the Alzheimer's Disease Neuroimaging Initiative (ADNI), *AGER* rs2070600 (G82S) was found to be associated with the atrophy rate of the right hippocampus CA1 over two years (Wang et al., 2017c). In a Japanese population, 4 AGER SNPs were studied (rs1800624, rs1800625, rs184003 and rs2070600) in 288 subjects with AD, 76 with Lewy body dementia and 105 age-matched controls. In that study, *AGER* rs184003 was associated with an increased risk of AD and haplotype analyses detected genetic associations between AD and the *AGER* gene (Takeshita et al., 2017). In a European cohort, the *AGER* SNP G82S (rs2070600) was associated with an increased risk of AD in 316 AD patients and 579 controls, but there was no interaction between this *AGER* SNP and the *APOE4* or with mini-mental examination scores (Daborg et al., 2010).

On account of the demonstrated association between diabetes and AD and mild cognitive impairment (MCI) (Cukierman et al., 2005; Huang et al., 2014; Ruiz et al., 2016; Xu et al., 2004), the *AGER* G82S SNP (rs2070600) and levels of AGEs and soluble RAGE were examined in 167 hospitalized type 2 diabetic subjects, of whom 82 were diagnosed with MCI and the other 85 were considered non-MCI controls. Patients with MCI demonstrated significantly lower levels of sRAGE and higher levels of serum AGE-peptide compared to control subjects. In

that study, the *AGER* SNP G82S bore no relationship to MCI in the type 2 diabetic subjects (Wang et al., 2016). Collectively, these data suggest that at least in certain populations, RAGE may affect genetic risk for AD or MCI and that in diabetes, the levels of the decoy receptor, sRAGE, are lower in individuals with cognitive dysfunction. Hence, components of the RAGE pathway may hold promise as biomarkers and/or predictors of AD and MCI. Experimental models have probed the cell type specific effects of RAGE using murine models of pathology.

Roles for RAGE in neurons in animal models of AD were directly tested in the commonly used transgenic mouse models of overexpression of mutant amyloid precursor protein (APP) in combination with either full-length or cytoplasmic domain-deleted *Ager* selectively in neurons. Overexpression of neuronal *Ager* accelerated behavioral abnormalities and altered activation of markers of synaptic plasticity and neuropathological abnormalities; these pathologies were observed at time points at which the mutant APP mouse control had yet to exhibit any pathologies. In contrast, in the mutant APP mice expressing the cytoplasmic domain-deleted *Ager*, and thus with suppressed ligand-RAGE signaling, attenuation of behavioral, and neuropathological changes was observed compared to the control mutant APP mice (Arancio et al., 2004). Additional studies suggested that one of the mechanisms by which neuronal RAGE expression activated distinct cells in the AD brain and in AD-like mouse models was through neuronal expression of macrophage colony stimulating factor (MCSF), which consequently triggered activation of microglia (Du Yan et al., 1997).

Other studies focused on expression of RAGE in microglia in neuronal-specific mutant APP mice. In transgenic mutant APP mice expressing either full-length *Ager* or cytoplasmic domain-deleted *Ager* in myeloid cells, whereas overexpression of RAGE increased neuroinflammation (IL1β and TNFα), microgliosis and astrocytosis, accumulation of Aβ and behavioral abnormalities, deletion of the RAGE cytoplasmic domain in microglia in this model exerted protection against these abnormalities compared to those observed in the mutant APP mice (Fang et al., 2010). Of note, the promoter used to drive the expression of RAGE and cytoplasmic domain-deleted RAGE forms in these animals also impacted expression in peripheral myeloid cells and through the development of the organism, which may alter the profile of these cells irrespective of the mutant APP background. Hence, the findings observed in these transgenic mice cannot be solely attributed to the effects of RAGE in adult and aged microglia. In distinct experiments, others tested microglia (myeloid)-cytoplasmic domain-deleted *Ager* in entorhinal cortex dysfunction in mutant APP mice. Early abnormalities in long term potentiation (LTP) in the entorhinal cortex and in associative behavior tasks *in vivo* were also observed in these mice. Evidence of activated stress related kinases (p38 MAPK and JNK pathway) was also attenuated in the transgenic vs. mutant APP alone mice (Criscuolo et al., 2017). These studies specifically examined a highly vulnerable region of the brain early in the course of neuronal deficits in an AD-like mouse model and implicated roles for myeloid/microglia RAGE in the pathogenesis of AD.

In cultured BV2 microglia-like cells, the effects of RAGE ligand AGEs on signal transduction were probed. AGEs activated Rho-associated protein kinase (ROCK) in a manner suppressed by the ROCK inhibitor fasudil or by the RAGE inhibitor FPS-ZM1. AGE-mediated upregulation of ROS, iNOS, COX2, NLRP3 and nuclear NF-κB p65 was attenuated in the BV2 cells by fasudil or FPS-ZM1. AGEs increased expression of pro-inflammatory "M1"-like markers in BV2 cells and decreased expression of anti-inflammatory "M2"-like markers, in a RAGE- and ROCK-dependent manner (Chen et al., 2017). Although "M1" and "M2" markers of the state of inflammation reflect solely *in vitro* designations, these experiments nevertheless suggested that RAGE ligands might affect pro/anti-inflammatory gene programs in BV2 cells. Further, the extent to which BV2 cells truly model *in vivo* microglia must also be considered in interpreting such studies.

In addition to neurons and microglia, RAGE is also prominently expressed in ECs and studies using AD-like mouse models demonstrated the prominent role of RAGE in transporting Aβ across the BBB and via upregulation of inflammatory mediators and endothelin-1 (ET1), RAGE contributed to Aβ-mediated vasoconstriction and suppression of cerebral blood flow (CBF). In mutant APP transgenic mice, administration of sRAGE blocked the adverse effects of the Aβ-RAGE interaction (Deane et al., 2003). In other studies, RAGE was shown to downregulate expression of low density lipoprotein receptor-related protein 1 (LRP1) (Deane et al., 2004). As LRP1 is responsible for Aβ clearance from the brain, such findings strongly suggest that RAGE plays key roles in overall Aβ transport and load in the brain, at least in part through perturbation of the BBB, CBF and expression of LRP1.

In other studies, the effect of hypertension, which is associated with AD, was assessed on the brain vasculature in the context of Aβ. In C57BL/6 mice, hypertension was induced by transverse aortic coarctation (TAC); in that model, by four weeks post-procedure, cerebral amyloid deposition is noted. In parallel, immunohistochemistry studies noted an early (within hours of TAC) and sustained upregulation of RAGE in brain blood vessels in the cortex and hippocampus after TAC. Impaired learning and memory was also observed in the TAC-treated animals. However, in mice globally devoid of *Ager,* evidence of significant protection was noted as follows: 1) reduced cerebral amyloid deposition; 2) improved performance in behavior studies; and 3) reduced oxidative stress; these effects were recapitulated by treatment of wild-type mice undergoing TAC and treated with FPS-ZM1 (Carnevale et al., 2012). Interestingly, in that work it was shown that induction of TAC increases levels of another RAGE ligand, AGEs. Collectively, these studies suggest that in hypertension, multiple RAGE ligands may be generated, which, at least in part via RAGE, aggravate pro-inflammatory and pro-oxidative pathways leading to cellular stress and organ damage.

The effects of RAGE on the BBB have also been addressed in *in vitro* models. For example, in a monolayer BBB model composed of murine ECs (bEnd.3 cells), Aβ(1–42) was shown to increase "BBB leakage" and result in reduction of tight junction scaffold proteins ZO1, claudin-5 and occludin. Incubation of these cells with Aβ(1–42) significantly upregulated their expression of RAGE; when these cells were treated with anti-RAGE IgG or when siRNAs were employed to reduce *Ager* expression, the effects of Aβ(1–42) on expression of scaffold proteins was blocked as well as the upregulation of MMP2 or MMP9. Further, an inhibitor of MMPs (GM6001) also prevented the detrimental effects of Aβ(1–42) on BBB leakage and on expression of tight junction proteins (Wan et al., 2015). In other studies performed in bEnd.3 cells, treatment with Aβ(1–42) increased permeability, disrupted ZO1 expression and increased secretion of intracellular calcium and MMPs, which was prevented by anti-RAGE antibodies (Kook et al., 2012).

6.2. Amyotrophic lateral sclerosis (ALS)

ALS is a complex disorder in which the primary target for dysfunction and death is the motor neuron. Multiple hypotheses have been put forth with respect to the cause of ALS, such as but not limited to increased toxicity from glutamate, increased oxidative stress (increased ROS and reactive nitrogen species (NOS)), protein aggregation and disruptions in proteostasis, defects in RNA processing, endoplasmic reticulum and mitochondrial stress, dysfunction of axonal transport mechanisms, and environmental factors, such as toxins or certain classes of infections (Lyon et al., 2019). Yet, multiple cell types, such as microglia, peripheral monocytes/macrophages, astrocytes and T and B lymphocytes have been postulated to play contributing roles to ALS pathology, especially to its progression and motor neuron death, contributing to the overall presumption that ALS is not a cell-autonomous disease. In this context, RAGE is expressed on many of these cell types and has been studied in both human and animal models of ALS.

In human subject spinal cord, compared to healthy control subjects, ALS spinal cord demonstrated higher levels of RAGE and its ligands,

particularly carboxy methyllysine (CML)-AGE, S100B and HMGB1 (Juranek et al., 2015). Other studies addressed expression patterns of RAGE as well as toll-like receptors 2 and 4 (TLR2 and TLR4) and ligand HMGB1 in 12 sporadic ALS and 6 control subjects. In ALS subjects, TLR2, TLR4 and RAGE were found to be highly expressed in reactive glial cells in the ventral horn and white matter; TLR2 was shown to be predominantly expressed in microglia, whereas RAGE and TLR4 were strongly expressed in astrocytes. By real-time qPCR, levels of HMGB1 mRNA were also shown to be increased in ALS vs. control spinal cord and the protein signal was specifically noted in the cytoplasm of reactive glial cells (Casula et al., 2011). Others examined patterns of sRAGE levels in 20 ALS patients and in 20 control subjects and reported that sRAGE levels were significantly lower in serum of the ALS vs. control individuals and that there was no correlation between the levels of serum sRAGE and disease clinical parameters in the ALS patients; however, it is notable that only 20 ALS patients were examined in the study and whether the work was powered to address such correlations is not clear (Ilzecka, 2009).

Experiments in cultured cellular models for ALS have also assessed a potential role for RAGE in this disease. Prompted by the observation that post-translationally modified forms of nerve growth factor (NGF) were observed in the spinal cord of murine ALS models, these concepts were tested in cellular models. *In vitro* glycation of NGF promoted its oligomerization and resulted in the generation of modified NGF as a RAGE ligand, which induced motor neuron death in culture and astrocyte-mediated motor neuron toxicity and similar findings were observed for nitrated NGF (Kim et al., 2018). In NSC-34 motor neuron like cells, transfection with mutant SOD1 resulted in production of exosomes by those cells, which led to increased expression of microRNA (miRNA) 124 and HMGB1 mRNA and protein. When exosomes from mutant SOD1-transfected NSC-34 cells vs. control were incubated with N9 microglia-like cells, highly significant upregulation of IL10, Arginase 1, TREM2, RAGE and TLR4 was noted. Further, increased expression of HMGB1, miR124, miR146a and miR155 and an increase in inflammatory markers, such as activated NF-κB, was observed as well (Pinto et al., 2017). Strikingly, in N9 cells exposed to the mutant SOD1-transfected NSC-34 cell exosomes, a loss of phagocytic ability and induction of senescence (as noted by senescence-associated β-galactosidase staining) was noted (Pinto et al., 2017). Although direct roles for RAGE in these experiments were not tested, its upregulation in the cells treated with the mutant SOD1-related exosomes suggest that one of the responses of microglia to these apparently toxic species is upregulation of receptors such as RAGE, in parallel with its ligands.

In addition, roles for S100B in ALS were considered, particularly as S100B is released from astrocytes. In a rat model of ALS, *SOD1*^{G93A} modified rats demonstrated a time dependent significant increase in S100B expression in spinal cord astrocytes, which colocalized with increased expression of RAGE. In primary astrocytes from mouse pup cortices, siRNA-knockdown of S100B resulted in a suppression of genes known to be upregulated in ALS, including GFAP, TNFα, CXCL10, and CCL6 (Serrano et al., 2017).

In other studies, potential neuroprotective roles for HMGB1 were tested. Spinal motor neurons from wild-type and *SOD1*^{G93A} mice displayed differential intracellular expression patterns of HMGB1; an increase in HMGB1 shuttling from the nucleus to the cytoplasm of these cells was observed in the mutant vs. wild-type mice, suggesting, perhaps, that HMGB1 in the *SOD1*^{G93A} mice might play protective vs. deleterious roles. Only the astrocytes from wild-type but not the *SOD1*^{G93A} mice were able to increase BDNF and GDNF levels upon stimulation with HMGB1, in a RAGE-dependent manner, suggesting that a beneficial role for astrocyte HMGB1 in neuronal growth factor expression may be dysregulated in ALS (Brambilla et al., 2018).

In vivo studies, to date, testing the role of RAGE in murine models of ALS are limited. In one study, sRAGE was administered to male *SOD1*^{G93A} mutant mice (B6/SJL background) beginning at age 8 weeks and continued until sacrifice. Compared to vehicle-treated animals, life span was extended and progression of ALS symptomatology was delayed by sRAGE treatment. At sacrifice, in the spinal cord tissue, sRAGE-treated animals displayed significantly higher numbers of neurons and lower number of astrocytes vs. the vehicle-treated group (Juranek et al., 2016). In that study, however, the mechanisms by which sRAGE exerted its benefit were not addressed, nor were distinct time courses for initiation of sRAGE administration tested.

Indeed, other studies, in an unrelated model of spinal cord injury (SCI), complex roles for RAGE in repair were uncovered in mice and rats. In a murine model of SCI, it was shown that RAGE expression rose within 12 h after the injury in WT mice; in *Ager* null mice subjected to the same degree of SCI, repair was improved, as evidence by improved functional outcomes, reduced expression of GFAP, and reduced inflammation, as indicated by lower levels of IL1β, TNFα, IL6, and NF-κB activation (Guo et al., 2014). Yet, in a rat model of SCI, animals undergoing the injury received an injection of anti-RAGE antibody directly into the central site of the injury. In contrast to induction of pro-repair mechanisms, the anti-RAGE antibody treatment resulted in reduced neuronal survival, disruption of Wnt/β-catenin signaling, and higher levels of autophagy (Mei et al., 2019; Wang et al., 2017a, 2018). Of course, the species under study are different and the mode of RAGE antagonism was dramatically different, that is, global deletion of *Ager* through development to adulthood in mice or treatment of adult rats with an antibody to RAGE. In any case, however, these studies underscore the pleiotropic roles that RAGE appears to play in neuronal system repair in the spinal cord.

Given the temporal, cell-type and complexity of cell intrinsic vs. cell-cell communications in the pathobiology of ALS and SCI, these studies raise many important questions. For example, it is not clear if sRAGE crosses the BBB. If the principal site of action of this agent was in the periphery, such as on the phenotype of peripheral monocytes and/or on activities at the neuromuscular junction (NMJ), remains an open question that can certainly be addressed experimentally. Also, in light of its close link to RAGE, future studies must examine if there are roles for DIAPH1 in the ALS. In addition, potential roles for breakdown of the blood-spinal cord barrier and roles for vascular cells in ALS, such as in the context of RAGE, require further investigation.

6.3. Parkinson's disease

Increasing evidence links RAGE to Parkinson's disease in human subjects and in animal models (Jiang et al., 2018). For example, pathological analyses were performed in human subject brains of asymptomatic Parkinson's disease with incidental Lewy body disease-related changes versus healthy age-matched controls. Increased expression of RAGE ligand AGEs was identified in the substantia nigra, amygdala, and frontal cortex. In parallel, increased expression of RAGE was noted in the substantia nigra and frontal cortex in human subject cases with early stages of parkinsonian neuropathology (Dalfo et al., 2005). Furthermore, in human subjects, *AGER* gene polymorphisms were studied in 285 Parkinson's Disease patients versus 285 healthy control subjects in the Chinese Han population. The only *AGER* SNP that showed a significant difference between the Parkinson's Disease patients and the controls was the 429T/C polymorphism. The carriers of the −429C allele exhibited a decreased risk of Parkinson's Disease, thereby suggesting that the −429T/C SNP may be a protective factor for Parkinson's Disease, at least in the Chinese Han population (Gao et al., 2014).

Studies in animal models have also begun to probe the role of the RAGE axis in the pathogenesis of Parkinson's Disease-like pathologies. Examples of some of these findings in animals with Parkinson's Disease-like pathologies are as follows: In the classical model for Parkinson's disease induced by 1-methyl-4-phenyl-1,2,3,6-tetrahydropyridine (MPTP), deletion of *Ager* afforded protection in nigral dopaminergic neurons from cell death. Further, as NF-κB has been implicated in the pathogenesis of neuronal injury in this disease, the activation of this

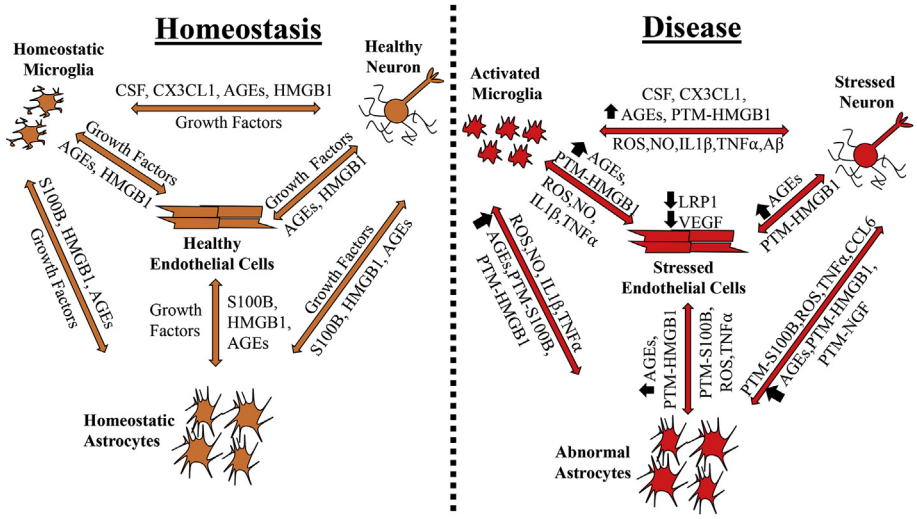

Fig. 3. Working model of RAGE-dependent cross-talk among microglia, neurons, astrocytes and endothelial cells in homeostasis and disease. In homeostasis, these cell types, and others not shown, secrete a number of protective factors, such as growth factors, physiological RAGE ligands, and chemokines. Importantly, blocking physiological RAGE ligands can disrupt homeostasis, as these factors have beneficial functions. In disease, reduced growth factor secretion, such as of BDNF and NGF, may suppress adaptive stress responses and prevent repair. Further, the release of higher concentrations of RAGE ligands (and, perhaps, their oligomerization) and the post-translationally modified (PTM) forms of these ligands from stressed cells may promote pathological RAGE signal transduction. These stressed cells release reactive oxygen species (ROS) and nitric oxide (NO), thereby further promoting wide-spread cellular stress. We posit that targeting pathological RAGE-dependent signaling by proper timing of therapeutic intervention will be key to reducing cellular stress in the CNS, without impacting the homeostatic RAGE-dependent signaling.

factor was tested in *Ager* null and *Ager* expressing mice after MPTP treatment. In the absence of *Ager,* the nuclear translocation of the NF-κB subunit p65 in dopaminergic neurons and glial cells was significantly inhibited, thereby suggesting roles for RAGE in activation of this pro-injury factor. Consistent with this premise, the increased apoptotic cell death induced by MPTP was attenuated in mice devoid of *Ager* (Teismann et al., 2012).

In other work, Gasparotto and colleagues reported that rats treated with 6-hydroxydopamine (6-OHDA) demonstrated increased expression of RAGE in the substantia nigra, in parallel with increased activation of NF-κB, astrocytosis and microgliosis. In rats treated with 6-OHDA and the RAGE inhibitor FPS-ZM1, these adverse effects were reduced and the locomotion and exploratory deficits in the rats induced by 6-OHDA were also attenuated (Gasparotto et al., 2017).

Recently, umbilical cord blood-derived mesenchymal stem cells were CRISPR/Cas9-edited to secrete sRAGE on the premise that local sequestration of RAGE ligands, such as AGEs, might mitigate Parkinson's like pathology. These sRAGE-edited cells were then injected into the corpus striatum of rotenone-treated mice, a Parkinson's Disease-like model. It was reported that neuronal death in the corpus striatum and substantial nigra was significantly reduced in the presence of the sRAGE-expressing injected cells, in parallel with reduced movement abnormalities in the rotenone-treated animals (Lee et al., 2019).

Collectively, these examples of in *vivo* studies targeting the RAGE axis in models of Parkinson's Disease link this receptor and its ligands to this disease. This work therefore suggests that testing RAGE antagonism in subjects with Parkinson's Disease may be logical and timely. In the section to follow, a novel strategy to target the RAGE axis will be considered.

7. Targeting RAGE signal transduction – A novel therapeutic approach

A small molecule antagonist of RAGE, Azeliragon, which targets the binding of RAGE ligands to the extracellular domains of RAGE, failed to show benefit compared to placebo in human subjects with mild AD (VTV Therapeutics, 2018). Multiple experiments have shown that the extracellular domains of RAGE, particularly the V-type Ig domain, are heterogeneous with respect to ligand binding; ligands may bind to distinct pockets on the V-domain such as in hydrophobic or charged sites and certain ligands may preferentially bind at the C-type Ig domains (Koch et al., 2010; Kumano-Kuramochi et al., 2009; Leclerc et al., 2009; Park et al., 2010; Xie et al., 2007, 2008). Such data suggest that targeting the extracellular domains of RAGE might not be an effective strategy to suppress RAGE activity in these disorders, especially given that there is no evidence that individual RAGE-related diseases may be influenced by only one or a very small number of ligands. Rather, multiple cellular stress-related RAGE ligands appear to populate diseased tissues, such as AGEs and S100 molecules in human diabetic atherosclerosis (Burke et al., 2004).

In contrast, strategies that target the intracellular domain of RAGE may be effective, given that the cytoplasmic domain of RAGE is small (less than 45 amino acids) and is essential for RAGE ligand-mediated cellular signaling. As discussed above, the discovery of DIAPH1 as a putative effector of RAGE signaling has unveiled a potentially more strategic therapeutic target. Early work has identified small molecules that block the binding of the RAGE cytoplasmic domain to DIAPH1 and have shown efficacy against the effects of RAGE ligands on signal transduction and changes in gene and functional expression endpoints in *in vitro* and *in vivo* studies (Manigrasso et al., 2016).

If and how such a strategy may be beneficial in RAGE/DIAPH1-related neurovascular and neurodegenerative disorders remains to be tested.

8. Perspectives and future directions

Studies in human subjects and animal models are steadily linking RAGE to the vulnerability to and pathogenesis of neurovascular and neurodegenerative disorders, particularly with respect to driving increased inflammation and barrier dysfunction coincident with aging. No doubt the biology of RAGE is complex and much needs to be learned about the homeostatic/pathobiological roles of this receptor and its downstream effector, DIAPH1. Insights into RAGE's innate functions have emerged from the observations that stress-related inflammation accompanies acute environmental and metabolic cues that shape host defenses. Recent work in primates and rodents has suggested that conserved amino acid residues on the extracellular ligand- and intracellular adaptor-binding regions and receptor oligomerization-related surfaces might convey “adaptive fitness,” that is, such sites on RAGE might confer advantages for host defense and rapid responses to challenge (Wu et al., 2015). Hence, in neurovascular and neurodegenerative disorders, it is plausible that RAGE and its ligands play both beneficial/adaptive and deleterious roles (Fig. 3).

How may such complexities be rectified? Experiments using transgenic mice to imbue tissue-specific and temporally-regulated modulation of RAGE (and DIAPH1) expression, as well as inhibitors of RAGE/

DIAPH1 that may be administered at early onset, mid-progressing phase and at late, end-stage of disease, will be essential to dissect the innate vs. deleterious roles of RAGE and DIAPH1 and to identify the optimal conditions for therapeutic interruption of RAGE signaling. Further, as some studies suggest that post-translational modifications of key RAGE ligands in the CNS, such as HMGB1, may dictate their adaptive vs. deleterious functions, consideration of the physical state of the RAGE ligands will be important. Finally, as a mountain of evidence suggests that RAGE-dependent physiologic vs. pathologic roles in the CNS may be both cell intrinsic and/or dependent on cell-cell networking and communication in vascular and neurodegenerative disorders, experiments testing such concepts *in vitro* and *in vivo* utilizing methods that consider RAGE-dependent cell-cell communication in mixed cultures and, possibly, organoid models (Wang et al., 2017b), will be essential. In this context, complimentary experiments using transcriptomic, proteomic, and metabolomic approaches may aid in uncovering how RAGE and DIAPH1 respond to toxic and detrimental cues in the CNS.

As there is mounting experimental evidence that there are scenarios in which blocking RAGE exerts benefit in the CNS pathology, identifying and harnessing the precise conditions for effectively targeting RAGE will be essential to treat chronic disorders of the CNS, especially those that accompany aging, cerebral ischemia, and diabetes.

Acknowledgements

The authors gratefully acknowledge support from the United States Public Health Service, American Heart Association, JDRF, American Diabetes Association and the Alzheimer's Association. The authors are grateful to Ms. Latoya Woods for her expert assistance in the preparation of this manuscript.

References

Aleshin, A., Ananthakrishnan, R., Li, Q., Rosario, R., Lu, Y., Qu, W., Song, F., Bakr, S., Szabolcs, M., D'Agati, V., Liu, R., Homma, S., Schmidt, A.M., Yan, S.F., Ramasamy, R., 2008. RAGE modulates myocardial injury consequent to LAD infarction via impact on JNK and STAT signaling in a murine model. Am. J. Physiol. Heart Circ. Physiol. 294, H1823–H1832.

Anzilotti, S., Giampa, C., Laurenti, D., Perrone, L., Bernardi, G., Melone, M.A., Fusco, F.R., 2012. Immunohistochemical localization of receptor for advanced glycation end (RAGE) products in the R6/2 mouse model of Huntington's disease. Brain Res. Bull. 87, 350–358.

Arancio, O., Zhang, H.P., Chen, X., Lin, C., Trinchese, F., Puzzo, D., Liu, S., Hegde, A., Yan, S.F., Stern, A., Luddy, J.S., Lue, L.F., Walker, D.G., Roher, A., Buttini, M., Mucke, L., Li, W., Schmidt, A.M., Kindy, M., Hyslop, P.A., Stern, D.M., Du Yan, S.S., 2004. RAGE potentiates Abeta-induced perturbation of neuronal function in transgenic mice. EMBO J. 23, 4096–4105.

Avalos, A.M., Kiefer, K., Tian, J., Christensen, S., Shlomchik, M., Coyle, A.J., Marshak-Rothstein, A., 2010. RAGE-independent autoreactive B cell activation in response to chromatin and HMGB1/DNA immune complexes. Autoimmunity 43, 103–110.

Boiocchi, C., Maggioli, E., Monti, M.C., Zorzetto, M., Sinforiani, E., Cereda, C., Ricevuti, G., Cuccia, M., 2015. The possible involvement of HLA class III haplotype (RAGE, HSP70 and TNF genes) in alzheimer's disease. Curr. Alzheimer Res. 12, 997–1005.

Brambilla, L., Martorana, F., Guidotti, G., Rossi, D., 2018. Dysregulation of astrocytic HMGB1 signaling in amyotrophic lateral sclerosis. Front. Neurosci. 12, 622.

Bucciarelli, L.G., Ananthakrishnan, R., Hwang, Y.C., Kaneko, M., Song, F., Sell, D.R., Strauch, C., Monnier, V.M., Yan, S.F., Schmidt, A.M., Ramasamy, R., 2008. RAGE and modulation of ischemic injury in the diabetic myocardium. Diabetes 57, 1941–1951.

Bucciarelli, L.G., Kaneko, M., Ananthakrishnan, R., Harja, E., Lee, L.K., Hwang, Y.C., Lerner, S., Bakr, S., Li, Q., Lu, Y., Song, F., Qu, W., Gomez, T., Zou, Y.S., Yan, S.F., Schmidt, A.M., Ramasamy, R., 2006. Receptor for advanced-glycation end products: key modulator of myocardial ischemic injury. Circulation 113, 1226–1234.

Burke, A.P., Kolodgie, F.D., Zieske, A., Fowler, D.R., Weber, D.K., Varghese, P.J., Farb, A., Virmani, R., 2004. Morphologic findings of coronary atherosclerotic plaques in diabetics: a postmortem study. Arterioscler. Thromb. Vasc. Biol. 24, 1266–1271.

Carnevale, D., Mascio, G., D'Andrea, I., Fardella, V., Bell, R.D., Branchi, I., Pallante, F., Zlokovic, B., Yan, S.S., Lembo, G., 2012. Hypertension induces brain beta-amyloid accumulation, cognitive impairment, and memory deterioration through activation of receptor for advanced glycation end products in brain vasculature. Hypertension 60, 188–197.

Casula, M., Iyer, A.M., Spliet, W.G., Anink, J.J., Steentjes, K., Sta, M., Troost, D., Aronica, E., 2011. Toll-like receptor signaling in amyotrophic lateral sclerosis spinal cord tissue. Neuroscience 179, 233–243.

Chauhan, G., Adams, H.H.H., Bis, J.C., Weinstein, G., Yu, L., Toglhofer, A.M., Smith, A.V., van der Lee, S.J., Gottesman, R.F., Thomson, R., Wang, J., Yang, Q., Niessen, W.J., Lopez, O.L., Becker, J.T., Phan, T.G., Beare, R.J., Arfanakis, K., Fleischman, D., Vernooij, M.W., Mazoyer, B., Schmidt, H., Srikanth, V., Knopman, D.S., Jack Jr., C.R., Amouyel, P., Hofman, A., DeCarli, C., Tzourio, C., van Duijn, C.M., Bennett, D.A., Schmidt, R., Longstreth Jr., W.T., Mosley, T.H., Fornage, M., Launer, L.J., Seshadri, S., Ikram, M.A., Debette, S., 2015. Association of Alzheimer's disease GWAS loci with MRI markers of brain aging. Neurobiol. Aging 36 1765.e1767-1765.e1716.

Chen, J., Sun, Z., Jin, M., Tu, Y., Wang, S., Yang, X., Chen, Q., Zhang, X., Han, Y., Pi, R., 2017. Inhibition of AGEs/RAGE/Rho/ROCK pathway suppresses non-specific neuroinflammation by regulating BV2 microglial M1/M2 polarization through the NF-kappaB pathway. J. Neuroimmunol. 305, 108–114.

Chesarone, M.A., DuPage, A.G., Goode, B.L., 2010. Unleashing formins to remodel the actin and microtubule cytoskeletons. Nat. Rev. Mol. Cell Biol. 11, 62–74.

Cipollone, F., Iezzi, A., Fazia, M., Zucchelli, M., Pini, B., Cuccurullo, C., De Cesare, D., De Blasis, G., Muraro, R., Bei, R., Chiarelli, F., Schmidt, A.M., Cuccurullo, F., Mezzetti, A., 2003. The receptor RAGE as a progression factor amplifying arachidonate-dependent inflammatory and proteolytic response in human atherosclerotic plaques: role of glycemic control. Circulation 108, 1070–1077.

Criscuolo, C., Fontebasso, V., Middei, S., Stazi, M., Ammassari-Teule, M., Yan, S.S., Origlia, N., 2017. Entorhinal Cortex dysfunction can be rescued by inhibition of microglial RAGE in an Alzheimer's disease mouse model. Sci. Rep. 7, 42370.

Cui, X., Chen, H., Hou, X., Wang, S., Jayaram, S., Zheng, Z., 2013. Polymorphism of the RAGE affects the serum inflammatory levels and risk of ischemic stroke in a Chinese population. Cell. Physiol. Biochem. 32, 986–996.

Cukierman, T., Gerstein, H.C., Williamson, J.D., 2005. Cognitive decline and dementia in diabetes–systematic overview of prospective observational studies. Diabetologia 48, 2460–2469.

Daborg, J., von Otter, M., Sjolander, A., Nilsson, S., Minthon, L., Gustafson, D.R., Skoog, I., Blennow, K., Zetterberg, H., 2010. Association of the RAGE G82S polymorphism with Alzheimer's disease. J. Neural Transm. 117, 861–867.

Daffu, G., Shen, X., Senatus, L., Thiagarajan, D., Abedini, A., Hurtado Del Pozo, C., Rosario, R., Song, F., Friedman, R.A., Ramasamy, R., Schmidt, A.M., 2015. RAGE suppresses ABCG1-mediated macrophage cholesterol efflux in diabetes. Diabetes 64, 4046–4060.

Dalfo, E., Portero-Otin, M., Ayala, V., Martinez, A., Pamplona, R., Ferrer, I., 2005. Evidence of oxidative stress in the neocortex in incidental Lewy body disease. J. Neuropathol. Exp. Neurol. 64, 816–830.

Deane, R., Du Yan, S., Submamaryan, R.K., LaRue, B., Jovanovic, S., Hogg, E., Welch, D., Manness, L., Lin, C., Yu, J., Zhu, H., Ghiso, J., Frangione, B., Stern, A., Schmidt, A.M., Armstrong, D.L., Arnold, B., Liliensiek, B., Nawroth, P., Hofman, F., Kindy, M., Stern, D., Zlokovic, B., 2003. RAGE mediates amyloid-beta peptide transport across the blood-brain barrier and accumulation in brain. Nat. Med. 9, 907–913.

Deane, R., Wu, Z., Zlokovic, B.V., 2004. RAGE (yin) versus LRP (yang) balance regulates alzheimer amyloid beta-peptide clearance through transport across the blood-brain barrier. Stroke 35, 2628–2631.

Derk, J., Bermudez Hernandez, K., Rodriguez, M., He, M., Koh, H., Abedini, A., Li, H., Fenyo, D., Schmidt, A.M., 2018a. Diaphanous 1 (DIAPH1) is highly expressed in the aged human medial temporal cortex and upregulated in myeloid cells during alzheimer's disease. J. Alzheimer's Dis. 64, 995–1007.

Derk, J., MacLean, M., Juranek, J., Schmidt, A.M., 2018b. The receptor for advanced glycation endproducts (RAGE) and mediation of inflammatory neurodegeneration. J Alzheimers Dis Parkinsonism 8.

Du Yan, S., Zhu, H., Fu, J., Yan, S.F., Roher, A., Tourtellotte, W.W., Rajavashisth, T., Chen, X., Godman, G.C., Stern, D., Schmidt, A.M., 1997. Amyloid-beta peptide-receptor for advanced glycation end product interaction elicits neuronal expression of macrophage-colony stimulating factor: a proinflammatory pathway in Alzheimer disease. Proc. Natl. Acad. Sci. U. S. A. 94, 5296–5301.

Dumitriu, I.E., Baruah, P., Bianchi, M.E., Manfredi, A.A., Rovere-Querini, P., 2005. Requirement of HMGB1 and RAGE for the maturation of human plasmacytoid dendritic cells. Eur. J. Immunol. 35, 2184–2190.

Emanuele, E., D'Angelo, A., Tomaino, C., Binetti, G., Ghidoni, R., Politi, P., Bernardi, L., Maletta, R., Bruni, A.C., Geroldi, D., 2005. Circulating levels of soluble receptor for advanced glycation end products in Alzheimer disease and vascular dementia. Arch. Neurol. 62, 1734–1736.

Fang, F., Lue, L.F., Yan, S., Xu, H., Luddy, J.S., Chen, D., Walker, D.G., Stern, D.M., Yan, S., Schmidt, A.M., Chen, J.X., Yan, S.S., 2010. RAGE-dependent signaling in microglia contributes to neuroinflammation, Abeta accumulation, and impaired learning/memory in a mouse model of Alzheimer's disease. FASEB J. 24, 1043–1055.

Farkas, E., Luiten, P.G., 2001. Cerebral microvascular pathology in aging and Alzheimer's disease. Prog. Neurobiol. 64, 575–611.

Gao, J., Teng, J., Liu, H., Han, X., Chen, B., Xie, A., 2014. Association of RAGE gene polymorphisms with sporadic Parkinson's disease in Chinese Han population. Neurosci. Lett. 559, 158–162.

Gao, X., Zhang, H., Schmidt, A.M., Zhang, C., 2008. AGE/RAGE produces endothelial dysfunction in coronary arterioles in type 2 diabetic mice. Am. J. Physiol. Heart Circ. Physiol. 295, H491–H498.

Gasparotto, J., Ribeiro, C.T., Bortolin, R.C., Somensi, N., Rabelo, T.K., Kunzler, A., Souza, N.C., Pasquali, M.A.B., Moreira, J.C.F., Gelain, D.P., 2017. Targeted inhibition of RAGE in substantia nigra of rats blocks 6-OHDA-induced dopaminergic denervation. Sci. Rep. 7, 8795.

Guerreiro, R., Wojtas, A., Bras, J., Carrasquillo, M., Rogaeva, E., Majounie, E., Cruchaga, C., Sassi, C., Kauwe, J.S., Younkin, S., Hazrati, L., Collinge, J., Pocock, J., Lashley, T., Williams, J., Lambert, J.C., Amouyel, P., Goate, A., Rademakers, R., Morgan, K., Powell, J., St George-Hyslop, P., Singleton, A., Hardy, J., 2013. TREM2 variants in Alzheimer's disease. N. Engl. J. Med. 368, 117–127.

Guo, J.D., Li, L., Shi, Y.M., Wang, H.D., Yuan, Y.L., Shi, X.X., Hou, S.X., 2014. Genetic ablation of receptor for advanced glycation end products promotes functional

recovery in mouse model of spinal cord injury. Mol. Cell. Biochem. 390, 215–223.
Hallam, K.M., Li, Q., Ananthakrishnan, R., Kalea, A., Zou, Y.S., Vedantham, S., Schmidt, A.M., Yan, S.F., Ramasamy, R., 2010. Aldose reductase and AGE-RAGE pathways: central roles in the pathogenesis of vascular dysfunction in aging rats. Aging Cell 9, 776–784.
Hassid, B.G., Nair, M.N., Ducruet, A.F., Otten, M.L., Komotar, R.J., Pinsky, D.J., Schmidt, A.M., Yan, S.F., Connolly, E.S., 2009. Neuronal RAGE expression modulates severity of injury following transient focal cerebral ischemia. J. Clin. Neurosci. 16, 302–306.
Huang, C.C., Chung, C.M., Leu, H.B., Lin, L.Y., Chiu, C.C., Hsu, C.Y., Chiang, C.H., Huang, P.H., Chen, T.J., Lin, S.J., Chen, J.W., Chan, W.L., 2014. Diabetes mellitus and the risk of Alzheimer's disease: a nationwide population-based study. PLoS One 9, e87095.
Hudson, B.I., Kalea, A.Z., Del Mar Arriero, M., Harja, E., Boulanger, E., D'Agati, V., Schmidt, A.M., 2008. Interaction of the RAGE cytoplasmic domain with diaphanous-1 is required for ligand-stimulated cellular migration through activation of Rac1 and Cdc42. J. Biol. Chem. 283, 34457–34468.
Iadecola, C., 2017. The neurovascular unit coming of age: a journey through neurovascular coupling in Health and disease. Neuron 96, 17–42.
Ilzecka, J., 2009. Serum-soluble receptor for advanced glycation end product levels in patients with amyotrophic lateral sclerosis. Acta Neurol. Scand. 120, 119–122.
Jiang, X., Wang, X., Tuo, M., Ma, J., Xie, A., 2018. RAGE and its emerging role in the pathogenesis of Parkinson's disease. Neurosci. Lett. 672, 65–69.
Jonsson, T., Stefansson, H., Steinberg, S., Jonsdottir, I., Jonsson, P.V., Snaedal, J., Bjornsson, S., Huttenlocher, J., Levey, A.I., Lah, J.J., Rujescu, D., Hampel, H., Giegling, I., Andreassen, O.A., Engedal, K., Ulstein, I., Djurovic, S., Ibrahim-Verbaas, C., Hofman, A., Ikram, M.A., van Duijn, C.M., Thorsteinsdottir, U., Kong, A., Stefansson, K., 2013. Variant of TREM2 associated with the risk of Alzheimer's disease. N. Engl. J. Med. 368, 107–116.
Juranek, J.K., Daffu, G.K., Geddis, M.S., Li, H., Rosario, R., Kaplan, B.J., Kelly, L., Schmidt, A.M., 2016. Soluble RAGE treatment delays progression of amyotrophic lateral sclerosis in SOD1 mice. Front. Cell. Neurosci. 10, 117.
Juranek, J.K., Daffu, G.K., Wojtkiewicz, J., Lacomis, D., Kofler, J., Schmidt, A.M., 2015. Receptor for advanced glycation end products and its inflammatory ligands are up-regulated in amyotrophic lateral sclerosis. Front. Cell. Neurosci. 9, 485.
Kamide, T., Kitao, Y., Takeichi, T., Okada, A., Mohri, H., Schmidt, A.M., Kawano, T., Munesue, S., Yamamoto, Y., Yamamoto, H., Hamada, J., Hori, O., 2012. RAGE mediates vascular injury and inflammation after global cerebral ischemia. Neurochem. Int. 60, 220–228.
Khan, M.A., Schultz, S., Othman, A., Fleming, T., Lebron-Galan, R., Rades, D., Clemente, D., Nawroth, P.P., Schwaninger, M., 2016. Hyperglycemia in stroke impairs polarization of monocytes/macrophages to a protective noninflammatory cell type. J. Neurosci. 36, 9313–9325.
Kim, M.J., Vargas, M.R., Harlan, B.A., Killoy, K.M., Ball, L.E., Comte-Walters, S., Gooz, M., Yamamoto, Y., Beckman, J.S., Barbeito, L., Pehar, M., 2018. Nitration and glycation turn mature NGF into a toxic factor for motor neurons: a role for $p75^{NTR}$ and RAGE signaling in ALS. Antioxidants Redox Signal. 28, 1587–1602.
Kisler, K., Nelson, A.R., Montagne, A., Zlokovic, B.V., 2017. Cerebral blood flow regulation and neurovascular dysfunction in Alzheimer disease. Nat. Rev. Neurosci. 18, 419–434.
Koch, M., Chitayat, S., Dattilo, B.M., Schiefner, A., Diez, J., Chazin, W.J., Fritz, G., 2010. Structural basis for ligand recognition and activation of RAGE. Structure 18, 1342–1352.
Kook, S.Y., Hong, H.S., Moon, M., Ha, C.M., Chang, S., Mook-Jung, I., 2012. $A\beta_{1-42}$-RAGE interaction disrupts tight junctions of the blood-brain barrier via Ca(2)(+)-calcineurin signaling. J. Neurosci. 32, 8845–8854.
Kühn, S., Geyer, M., 2014. Formins as effector proteins of Rho GTPases. Small GTPases 5, e29513.
Kumano-Kuramochi, M., Ohnishi-Kameyama, M., Xie, Q., Niimi, S., Kubota, F., Komba, S., Machida, S., 2009. Minimum stable structure of the receptor for advanced glycation end product possesses multi ligand binding ability. Biochem. Biophys. Res. Commun. 386, 130–134.
Landis, C.A., Collins, B.J., Cribbs, L.L., Sukhatme, V.P., Bergmann, B.M., Rechtschaffen, A., Smalheiser, N.R., 1993. Expression of Egr-1 in the brain of sleep deprived rats. Brain Res Mol Brain Res 17, 300–306.
Leclerc, E., Fritz, G., Vetter, S.W., Heizmann, C.W., 2009. Binding of S100 proteins to RAGE: an update. Biochim. Biophys. Acta 1793, 993–1007.
Lee, J., Bayarsaikhan, D., Arivazhagan, R., Park, H., Lim, B., Gwak, P., Jeong, G.B., Lee, J., Byun, K., Lee, B., 2019. CRISPR/Cas9 edited sRAGE-MSCs protect neuronal death in Parkinson's disease model. Int J Stem Cells. https://doi.org/10.15283/ijsc18110.
Lei, C., Zhang, S., Cao, T., Tao, W., Liu, M., Wu, B., 2015. HMGB1 may act via RAGE to promote angiogenesis in the later phase after intracerebral hemorrhage. Neuroscience 295, 39–47.
Li, H., Wu, W., Sun, Q., Liu, M., Li, W., Zhang, X.S., Zhou, M.L., Hang, C.H., 2014. Expression and cell distribution of receptor for advanced glycation end-products in the rat cortex following experimental subarachnoid hemorrhage. Brain Res. 1543, 315–323.
Li, H., Yu, J.S., Zhang, D.D., Yang, Y.Q., Huang, L.T., Yu, Z., Chen, R.D., Yang, H.K., Hang, C.H., 2017a. Inhibition of the receptor for advanced glycation end-products (RAGE) attenuates neuroinflammation while sensitizing cortical neurons towards death in experimental subarachnoid hemorrhage. Mol. Neurobiol. 54, 755–767.
Li, Y., Zhu, J., Chen, L., Hu, W., Wang, M., Li, S., Gu, X., Tao, H., Zhao, B., Ma, G., Li, K., 2017b. Genetic predisposition to ischaemic stroke by RAGE and HMGB1 gene variants in Chinese Han population. Oncotarget 8, 100150–100164.
Liu, L.P., Hong, H., Liao, J.M., Wang, T.S., Wu, J., Chen, S.S., Li, Y.Q., Long, Y., Xia, Y.Z., 2009. Upregulation of RAGE at the blood-brain barrier in streptozotocin-induced diabetic mice. Synapse 63, 636–642.
Liu, W., Ge, S., Liu, Y., Wei, C., Ding, Y., Chen, A., Wu, Q., Zhang, Y., 2015. Polymorphisms in three genes are associated with hemorrhagic stroke. Brain Behav 5, e00395.
Loomis, S.J., Chen, Y., Sacks, D.B., Christenson, E.S., Christenson, R.H., Rebholz, C.M., Selvin, E., 2017. Cross-sectional analysis of AGE-CML, sRAGE, and esRAGE with diabetes and cardiometabolic risk factors in a community-based cohort. Clin. Chem. 63, 980–989.
Lopez-Diez, R., Shekhtman, A., Ramasamy, R., Schmidt, A.M., 2016. Cellular mechanisms and consequences of glycation in atherosclerosis and obesity. Biochim. Biophys. Acta 1862, 2244–2252.
Lue, L.F., Walker, D.G., Jacobson, S., Sabbagh, M., 2009. Receptor for advanced glycation end products: its role in Alzheimer's disease and other neurological diseases. Future Neurol. 4, 167–177.
Lyon, M.S., Wosiski-Kuhn, M., Gillespie, R., Caress, J., Milligan, C., 2019. Inflammation, Immunity, and amyotrophic lateral sclerosis: I. Etiology and pathology. Muscle Nerve 59, 10–22.
Maggioli, E., Boiocchi, C., Zorzetto, M., Sinforiani, E., Cereda, C., Ricevuti, G., Cuccia, M., 2013. The human leukocyte antigen class III haplotype approach: new insight in Alzheimer's disease inflammation hypothesis. Curr. Alzheimer Res. 10, 1047–1056.
Manigrasso, M.B., Friedman, R.A., Ramasamy, R., D'Agati, V.D., Schmidt, A.M., 2018. Deletion of the formin, Diaph1, protects from structural and functional abnormalities in the murine diabetic kidney. Am. J. Physiol. Renal. Physiol. 315 (6), 1601–1612.
Manigrasso, M.B., Pan, J., Rai, V., Zhang, J., Reverdatto, S., Quadri, N., DeVita, R.J., Ramasamy, R., Shekhtman, A., Schmidt, A.M., 2016. Small molecule inhibition of ligand-stimulated RAGE-DIAPH1 signal transduction. Sci. Rep. 6, 22450.
Mei, X., Wang, H., Zhang, H., Liu, C., Guo, Z., Wang, Y., Yuan, Y., Zhao, Z., Li, D., Tang, P., 2019. Blockade of receptor for advanced glycation end products promotes oligodendrocyte autophagy in spinal cord injury. Neurosci. Lett. 698, 198–203.
Montagne, A., Barnes, S.R., Sweeney, M.D., Halliday, M.R., Sagare, A.P., Zhao, Z., Toga, A.W., Jacobs, R.E., Liu, C.Y., Amezcua, L., Harrington, M.G., Chui, H.C., Law, M., Zlokovic, B.V., 2015. Blood-brain barrier breakdown in the aging human hippocampus. Neuron 85, 296–302.
Montaner, J., Mendioroz, M., Delgado, P., Garcia-Berrocoso, T., Giralt, D., Merino, C., Ribo, M., Rosell, A., Penalba, A., Fernandez-Cadenas, I., Romero, F., Molina, C., Alvarez-Sabin, J., Hernandez-Guillamon, M., 2012. Differentiating ischemic from hemorrhagic stroke using plasma biomarkers: the S100B/RAGE pathway. J Proteomics 75, 4758–4765.
Moser, B., Szabolcs, M.J., Ankersmit, H.J., Lu, Y., Qu, W., Weinberg, A., Herold, K.C., Schmidt, A.M., 2007. Blockade of RAGE suppresses alloimmune reactions in vitro and delays allograft rejection in murine heart transplantation. Am. J. Transplant. 7, 293–302.
Muhammad, S., Barakat, W., Stoyanov, S., Murikinati, S., Yang, H., Tracey, K.J., Bendszus, M., Rossetti, G., Nawroth, P.P., Bierhaus, A., Schwaninger, M., 2008. The HMGB1 receptor RAGE mediates ischemic brain damage. J. Neurosci. 28, 12023–12031.
Nation, D.A., Sweeney, M.D., Montagne, A., Sagare, A.P., D'Orazio, L.M., Pachicano, M., Sepehrband, F., Nelson, A.R., Buennagel, D.P., Harrington, M.G., Benzinger, T.L.S., Fagan, A.M., Ringman, J.M., Schneider, L.S., Morris, J.C., Chui, H.C., Law, M., Toga, A.W., Zlokovic, B.V., 2019. Blood-brain barrier breakdown is an early biomarker of human cognitive dysfunction. Nat. Med. 25, 270–276.
O'Shea, K.M., Ananthakrishnan, R., Li, Q., Quadri, N., Thiagarajan, D., Sreejit, G., Wang, L., Zirpoli, H., Aranda, J.F., Alberts, A.S., Schmidt, A.M., Ramasamy, R., 2017. The formin, DIAPH1, is a key modulator of myocardial ischemia/reperfusion injury. EBioMedicine 26, 165–174.
Olsson, S., Jood, K., 2013. Genetic variation in the receptor for advanced glycation end-products (RAGE) gene and ischaemic stroke. Eur. J. Neurol. 20, 991–993.
Palanissami, G., Paul, S.F.D., 2018. RAGE and its ligands: molecular interplay between glycation, inflammation, and hallmarks of cancer-a review. Horm Cancer 9, 295–325.
Park, H., Adsit, F.G., Boyington, J.C., 2010. The 1.5 Å crystal structure of human receptor for advanced glycation endproducts (RAGE) ectodomains reveals unique features determining ligand binding. J. Biol. Chem. 285, 40762–40770.
Park, M.H., Lee, J.Y., Park, K.H., Jung, I.K., Kim, K.T., Lee, Y.S., Ryu, H.H., Jeong, Y., Kang, M., Schwaninger, M., Gulbins, E., Reichel, M., Kornhuber, J., Yamaguchi, T., Kim, H.J., Kim, S.H., Schuchman, E.H., Jin, H.K., Bae, J.S., 2018. Vascular and neurogenic rejuvenation in aging mice by modulation of ASM. Neuron 100, 762.
Pinto, S., Cunha, C., Barbosa, M., Vaz, A.R., Brites, D., 2017. Exosomes from NSC-34 cells transfected with hSOD1-G93A are enriched in mir-124 and drive alterations in microglia phenotype. Front. Neurosci. 11, 273.
Presta, I., Vismara, M., Novellino, F., Donato, A., Zaffino, P., Scali, E., Pirrone, K.C., Spadea, M.F., Malara, N., Donato, G., 2018. Innate immunity cells and the neurovascular unit. Int. J. Mol. Sci. 19.
Rai, V., Maldonado, A.Y., Burz, D.S., Reverdatto, S., Yan, S.F., Schmidt, A.M., Shekhtman, A., 2012. Signal transduction in receptor for advanced glycation end products (RAGE): solution structure of C-terminal rage (ctRAGE) and its binding to mDia1. J. Biol. Chem. 287, 5133–5144.
Ramasamy, R., Shekhtman, A., Schmidt, A.M., 2016. The multiple faces of RAGE–opportunities for therapeutic intervention in aging and chronic disease. Expert Opin. Ther. Targets 20, 431–446.
Raucci, A., Cugusi, S., Antonelli, A., Barabino, S.M., Monti, L., Bierhaus, A., Reiss, K., Saftig, P., Bianchi, M.E., 2008. A soluble form of the receptor for advanced glycation endproducts (RAGE) is produced by proteolytic cleavage of the membrane-bound form by the sheddase a disintegrin and metalloprotease 10 (ADAM10). FASEB J. 22, 3716–3727.
Ruiz, H.H., Chi, T., Shin, A.C., Lindtner, C., Hsieh, W., Ehrlich, M., Gandy, S., Buettner, C., 2016. Increased susceptibility to metabolic dysregulation in a mouse model of Alzheimer's disease is associated with impaired hypothalamic insulin signaling and

elevated BCAA levels. Alzheimers Dement 12, 851–861.
Saito, R., Araki, S., Yamamoto, Y., Kusuhara, K., 2017. Elevated endogenous secretory receptor for advanced glycation end products (esRAGE) levels are associated with circulating soluble RAGE levels in diabetic children. J. Pediatr. Endocrinol. Metab. 30, 63–69.
Sasaki, N., Takeuchi, M., Chowei, H., Kikuchi, S., Hayashi, Y., Nakano, N., Ikeda, H., Yamagishi, S., Kitamoto, T., Saito, T., Makita, Z., 2002. Advanced glycation end products (AGE) and their receptor (RAGE) in the brain of patients with Creutzfeldt-Jakob disease with prion plaques. Neurosci. Lett. 326, 117–120.
Schmidt, A.M., 2015. Soluble RAGEs - prospects for treating & tracking metabolic and inflammatory disease. Vasc. Pharmacol. 72, 1–8.
Schmidt, A.M., Hasu, M., Popov, D., Zhang, J.H., Chen, J., Yan, S.D., Brett, J., Cao, R., Kuwabara, K., Costache, G., et al., 1994. Receptor for advanced glycation end products (AGEs) has a central role in vessel wall interactions and gene activation in response to circulating AGE proteins. Proc. Natl. Acad. Sci. U. S. A. 91, 8807–8811.
Serrano, A., Donno, C., Giannetti, S., Peric, M., Andjus, P., D'Ambrosi, N., Michetti, F., 2017. The astrocytic S100B protein with its receptor RAGE is aberrantly expressed in $SOD1^{G93A}$ models, and its inhibition decreases the expression of proinflammatory genes. Mediat. Inflamm. 2017, 1626204.
Shang, L., Ananthakrishnan, R., Li, Q., Quadri, N., Abdillahi, M., Zhu, Z., Qu, W., Rosario, R., Toure, F., Yan, S.F., Schmidt, A.M., Ramasamy, R., 2010. RAGE modulates hypoxia/reoxygenation injury in adult murine cardiomyocytes via JNK and GSK-3beta signaling pathways. PLoS One 5, e10092.
Sokol, B., Wasik, N., Jankowski, R., Holysz, M., Manko, W., Juszkat, R., Malkiewicz, T., Jagodzinski, P.P., 2017. Increase of soluble RAGE in cerebrospinal fluid following subarachnoid haemorrhage. BioMed Res. Int. 2017, 7931534.
Sorci, G., Riuzzi, F., Agneletti, A.L., Marchetti, C., Donato, R., 2003. S100B inhibits myogenic differentiation and myotube formation in a RAGE-independent manner. Mol. Cell Biol. 23, 4870–4881.
Sweeney, M.D., Sagare, A.P., Zlokovic, B.V., 2018. Blood-brain barrier breakdown in Alzheimer disease and other neurodegenerative disorders. Nat. Rev. Neurol. 14, 133–150.
Takeshita, Y., Shibata, N., Kasanuki, K., Nagata, T., Shinagawa, S., Kobayashi, N., Ohnuma, T., Suzuki, A., Kawai, E., Takayama, T., Nishioka, K., Motoi, Y., Hattori, N., Nakayama, K., Yamada, H., Arai, H., 2017. Genetic association between RAGE polymorphisms and Alzheimer's disease and Lewy body dementias in a Japanese cohort: a case-control study. Int. J. Geriatr. Psychiatry 32, 1241–1246.
Tang, S.C., Yang, K.C., Hu, C.J., Chiou, H.Y., Wu, C.C., Jeng, J.S., 2017. Elevated plasma level of soluble form of RAGE in ischemic stroke patients with dementia. NeuroMolecular Med. 19, 579–583.
Tanji, N., Markowitz, G.S., Fu, C., Kislinger, T., Taguchi, A., Pischetsrieder, M., Stern, D., Schmidt, A.M., D'Agati, V.D., 2000. Expression of advanced glycation end products and their cellular receptor RAGE in diabetic nephropathy and nondiabetic renal disease. J. Am. Soc. Nephrol. 11, 1656–1666.
Teismann, P., Sathe, K., Bierhaus, A., Leng, L., Martin, H.L., Bucala, R., Weigle, B., Nawroth, P.P., Schulz, J.B., 2012. Receptor for advanced glycation endproducts (RAGE) deficiency protects against MPTP toxicity. Neurobiol. Aging 33, 2478–2490.
Tian, X., Sun, L., Feng, D., Sun, Q., Dou, Y., Liu, C., Zhou, F., Li, H., Shen, H., Wang, Z., Chen, G., 2017. HMGB1 promotes neurovascular remodeling via Rage in the late phase of subarachnoid hemorrhage. Brain Res. 1670, 135–145.
Touré, F., Fritz, G., Li, Q., Rai, V., Daffu, G., Zou, Y.S., Rosario, R., Ramasamy, R., Alberts, A.S., Yan, S.F., Schmidt, A.M., 2012. Formin mDia1 mediates vascular remodeling via integration of oxidative and signal transduction pathways. Circ. Res. 110, 1279–1293.
Van Dyken, P., Lacoste, B., 2018. Impact of metabolic syndrome on neuroinflammation and the blood-brain barrier. Front. Neurosci. 12, 930.
Villegas-Llerena, C., Phillips, A., Garcia-Reitboeck, P., Hardy, J., Pocock, J.M., 2016. Microglial genes regulating neuroinflammation in the progression of Alzheimer's disease. Curr. Opin. Neurobiol. 36, 74–81.
VTV Therapeutics, 2018. http://ir.vtvtherapeutics.com/phoenix.zhtml?c=254081&p=irol-newsArticle&ID=2341681.
Wan, W., Cao, L., Liu, L., Zhang, C., Kalionis, B., Tai, X., Li, Y., Xia, S., 2015. Aβ(1-42) oligomer-induced leakage in an in vitro blood-brain barrier model is associated with up-regulation of RAGE and metalloproteinases, and down-regulation of tight junction scaffold proteins. J. Neurochem. 134, 382–393.
Wang, H., Mei, X., Cao, Y., Liu, C., Zhao, Z., Guo, Z., Bi, Y., Shen, Z., Yuan, Y., Guo, Y., Song, C., Bai, L., Wang, Y., Yu, D., 2017a. HMGB1/Advanced Glycation End Products (RAGE) does not aggravate inflammation but promote endogenous neural stem cells differentiation in spinal cord injury. Sci. Rep. 7, 10332.
Wang, H., Zhao, Z., Liu, C., Guo, Z., Yuan, Y., Zhao, H., Zhou, Z., Mei, X., 2018. Receptor for advanced glycation end-products (RAGE) blockade do damage to neuronal survival via disrupting Wnt/beta-catenin signaling in spinal cord injury. Neurochem. Res. 43, 1405–1412.
Wang, P., Huang, R., Lu, S., Xia, W., Cai, R., Sun, H., Wang, S., 2016. RAGE and AGEs in mild cognitive impairment of diabetic patients: a cross-sectional study. PLoS One 11 e0145521.
Wang, Z., Wang, S.N., Xu, T.Y., Miao, Z.W., Su, D.F., Miao, C.Y., 2017b. Organoid technology for brain and therapeutics research. CNS Neurosci. Ther. 23, 771–778.
Wang, Z.X., Wan, Y., Tan, L., Liu, J., Wang, H.F., Sun, F.R., Tan, M.S., Tan, C.C., Jiang, T., Tan, L., Yu, J.T., 2017c. Genetic association of HLA gene variants with MRI brain structure in alzheimer's disease. Mol. Neurobiol. 54, 3195–3204.
Wautier, J.L., Zoukourian, C., Chappey, O., Wautier, M.P., Guillausseau, P.J., Cao, R., Hori, O., Stern, D., Schmidt, A.M., 1996. Receptor-mediated endothelial cell dysfunction in diabetic vasculopathy. Soluble receptor for advanced glycation end products blocks hyperpermeability in diabetic rats. J. Clin. Investig. 97, 238–243.
Wu, X., Wu, J., Thompson, C.W., Li, Y., 2015. Adaptive evolution of the MHC class III-encoded receptor RAGE in primates and murine rodents. Int. J. Immunogenet. 42, 461–468.
Xie, J., Burz, D.S., He, W., Bronstein, I.B., Lednev, I., Shekhtman, A., 2007. Hexameric calgranulin C (S100A12) binds to the receptor for advanced glycated end products (RAGE) using symmetric hydrophobic target-binding patches. J. Biol. Chem. 282, 4218–4231.
Xie, J., Reverdatto, S., Frolov, A., Hoffmann, R., Burz, D.S., Shekhtman, A., 2008. Structural basis for pattern recognition by the receptor for advanced glycation end products (RAGE). J. Biol. Chem. 283, 27255–27269.
Xu, W.L., Qiu, C.X., Wahlin, A., Winblad, B., Fratiglioni, L., 2004. Diabetes mellitus and risk of dementia in the Kungsholmen project: a 6-year follow-up study. Neurology 63, 1181–1186.
Xu, Y., Toure, F., Qu, W., Lin, L., Song, F., Shen, X., Rosario, R., Garcia, J., Schmidt, A.M., Yan, S.F., 2010. Advanced glycation end product (AGE)-receptor for AGE (RAGE) signaling and up-regulation of Egr-1 in hypoxic macrophages. J. Biol. Chem. 285, 23233–23240.
Xue, J., Manigrasso, M., Scalabrin, M., Rai, V., Reverdatto, S., Burz, D.S., Fabris, D., Schmidt, A.M., Shekhtman, A., 2016. Change in the molecular dimension of a RAGE-ligand complex triggers RAGE signaling. Structure 24, 1509–1522.
Yan, S.D., Chen, X., Fu, J., Chen, M., Zhu, H., Roher, A., Slattery, T., Zhao, L., Nagashima, M., Morser, J., Migheli, A., Nawroth, P., Stern, D., Schmidt, A.M., 1996. RAGE and amyloid-beta peptide neurotoxicity in Alzheimer's disease. Nature 382, 685–691.
Yang, F., Wang, Z., Zhang, J.H., Tang, J., Liu, X., Tan, L., Huang, Q.Y., Feng, H., 2015. Receptor for advanced glycation end-product antagonist reduces blood-brain barrier damage after intracerebral hemorrhage. Stroke 46, 1328–1336.
Ye, X., Chopp, M., Liu, X., Zacharek, A., Cui, X., Yan, T., Roberts, C., Chen, J., 2011. Niaspan reduces high-mobility group box 1/receptor for advanced glycation end-products after stroke in type-1 diabetic rats. Neuroscience 190, 339–345.
Yonekura, H., Yamamoto, Y., Sakurai, S., Petrova, R.G., Abedin, M.J., Li, H., Yasui, K., Takeuchi, M., Makita, Z., Takasawa, S., Okamoto, H., Watanabe, T., Yamamoto, H., 2003. Novel splice variants of the receptor for advanced glycation end-products expressed in human vascular endothelial cells and pericytes, and their putative roles in diabetes-induced vascular injury. Biochem. J. 370, 1097–1109.
Zhang, Z.G., Li, Y., Ng, C.T., Song, Y.Q., 2015. Inflammation in alzheimer's disease and molecular genetics: recent update. Arch. Immunol. Ther. Exp. 63, 333–344.
Zhou, X., Weng, J., Xu, J., Xu, Q., Wang, W., Zhang, W., Huang, Q., Guo, X., 2018. Mdia1 is crucial for advanced glycation end product-induced endothelial hyperpermeability. Cell. Physiol. Biochem. 45, 1717–1730.

MacLean et al. Journal of Neuroinflammation (2021) 18:139
https://doi.org/10.1186/s12974-021-02191-2

Journal of Neuroinflammation

RESEARCH Open Access

Microglia RAGE exacerbates the progression of neurodegeneration within the *SOD1*^{G93A} murine model of amyotrophic lateral sclerosis in a sex-dependent manner

Michael MacLean[1], Judyta Juranek[1,2], Swetha Cuddapah[1], Raquel López-Díez[1], Henry H. Ruiz[1], Jiyuan Hu[3], Laura Frye[1], Huilin Li[3], Paul F. Gugger[1] and Ann Marie Schmidt[1*]

Abstract

Background: Burgeoning evidence highlights seminal roles for microglia in the pathogenesis of neurodegenerative diseases including amyotrophic lateral sclerosis (ALS). The receptor for advanced glycation end products (RAGE) binds ligands relevant to ALS that accumulate in the diseased spinal cord and RAGE has been previously implicated in the progression of ALS pathology.

Methods: We generated a novel mouse model to temporally delete *Ager* from microglia in the murine *SOD1*^{G93A} model of ALS. Microglia *Ager* deficient *SOD1*^{G93A} mice and controls were examined for changes in survival, motor function, gliosis, motor neuron numbers, and transcriptomic analyses of lumbar spinal cord. Furthermore, we examined bulk-RNA-sequencing transcriptomic analyses of human ALS cervical spinal cord.

Results: Transcriptomic analysis of human cervical spinal cord reveals a range of *AGER* expression in ALS patients, which was negatively correlated with age at disease onset and death or tracheostomy. The degree of *AGER* expression related to differential expression of pathways involved in extracellular matrix, lipid metabolism, and intercellular communication. Microglia display increased RAGE immunoreactivity in the spinal cords of high *AGER* expressing patients and in the *SOD1*^{G93A} murine model of ALS vs. respective controls. We demonstrate that microglia *Ager* deletion at the age of symptomatic onset, day 90, in *SOD1*^{G93A} mice extends survival in male but not female mice. Critically, many of the pathways identified in human ALS patients that accompanied increased *AGER* expression were significantly ameliorated by microglia *Ager* deletion in male *SOD1*^{G93A} mice.

Conclusions: Our results indicate that microglia RAGE disrupts communications with cell types including astrocytes and neurons, intercellular communication pathways that divert microglia from a homeostatic to an inflammatory and tissue-injurious program. In totality, microglia RAGE contributes to the progression of *SOD1*^{G93A} murine pathology in male mice and may be relevant in human disease.

Keywords: ALS, Microglia, Neurodegeneration, Macrophage, Astrocytes, RAGE

* Correspondence: AnnMarie.Schmidt@nyulangone.org
[1]Diabetes Research Program, Department of Medicine, New York University Grossman School of Medicine, New York, NY 10016, USA
Full list of author information is available at the end of the article

© The Author(s). 2021 **Open Access** This article is licensed under a Creative Commons Attribution 4.0 International License, which permits use, sharing, adaptation, distribution and reproduction in any medium or format, as long as you give appropriate credit to the original author(s) and the source, provide a link to the Creative Commons licence, and indicate if changes were made. The images or other third party material in this article are included in the article's Creative Commons licence, unless indicated otherwise in a credit line to the material. If material is not included in the article's Creative Commons licence and your intended use is not permitted by statutory regulation or exceeds the permitted use, you will need to obtain permission directly from the copyright holder. To view a copy of this licence, visit http://creativecommons.org/licenses/by/4.0/. The Creative Commons Public Domain Dedication waiver (http://creativecommons.org/publicdomain/zero/1.0/) applies to the data made available in this article, unless otherwise stated in a credit line to the data.

Background

Amyotrophic lateral sclerosis (ALS), a progressive, fatal, neurodegenerative disease, is characterized by the inexorable death of motor neurons. Affected patients experience progressive muscle atrophy, motor function decline, and eventual paralysis. ALS rapidly progresses in most patients, resulting in an estimated survival of 2–4 years after onset of symptoms [1]. Greater than 90% of ALS patients have no known family history of the disease and hence the non-familial form of the disease is known as sporadic ALS (sALS). A smaller subset of patients (5–10%) is affected by familial ALS (fALS) [1]. Mutations in superoxide dismutase 1 (*SOD1*) account for approximately 20% of fALS patients [1]. Regardless of the underlying disease-related mutation, ALS is characterized by the accumulation of proteinaceous aggregates, which is associated with a pro-damage inflammatory and oxidative stress state involving multiple cell types. Ultimately, these processes collectively augur motor neuron death [2, 3]. Mice carrying multiple copies of a human $SOD1^{G93A}$ transgene display hallmarks of ALS, including accumulation of proteinaceous aggregates, neuroinflammation, and progressive motor function decline with eventual paralysis and death in all $SOD1^{G93A}$ transgenic mice [4, 5]. While ALS results in motor neuron death, several landmark studies have elucidated critical roles for non-neuronal cells during disease progression [6–11]. Altogether, these considerations illustrate that ALS pathology is driven by dysfunction across a myriad of cell types whose intercommunications drive processes that irreparably damage neurons.

Spatial transcriptomic analysis of $SOD1^{G93A}$ mouse spinal cords suggests that microglial dysfunction is evident by post-natal day 30 (P30), with astrocyte dysfunction becoming apparent later, by P70. These findings suggest that microglial dysfunction may precede and contribute to astrocyte dysfunction, which precedes neuronal death [12]. Critically, these key findings implicating glial cells in ALS pathobiology were also observed in spatial transcriptomics analyses of human ALS spinal cord [12]. Studies in $SOD1^{G93A}$ mice affirmed mediating roles for glial cells in impacting survival in $SOD1^{G93A}$ mice; when the myeloid and lymphoid compartment of these mice was replaced with a wild-type (WT) bone marrow transplant within 24 h of birth, the recipient $SOD1^{G93A}$ mice demonstrated improved survival compared to those $SOD1^{G93A}$ mice receiving $SOD1^{G93A}$ bone marrow [9]. Moreover, an expanding number of genes with known ALS-linked mutations mediate myeloid function, including *C9ORF72*, *TARDP*, and *OPTN* [13, 14]. Specifically, *C9ORF72* regulates phagosome and lysosome pathways [15], while *TARDP* regulates phagocytosis [16]. *OPTN* deficiency induces an inflammatory profile in microglia [17]. It has previously been shown that reducing myeloid inflammation increases lifespan of $SOD1^{G93A}$ mice [7, 18]. In a distinct inducible murine model of ALS, microglia were required for the clearance of protein aggregates [19]. Microglia from $SOD1^{G93A}$ mice display unique transcriptomic signatures reminiscent of both protective and inflammatory macrophages [20]. Altogether, these findings suggest that microglia may exert opposing roles in ALS, mediating stage-dependent alterations in protective vs. damage-provoking functions. In fact, accruing evidence suggests that microglia may undergo step-wise activation toward a dysfunctional inflammatory disease-associated microglia (DAM) phenotype, at least in the context of Alzheimer's disease (AD) [21, 22]. Triggering receptor expressed on myeloid cells 2 (TREM2) has been implicated in the step-wise activation of microglia toward this DAM state; however, it is established that additional factors synergize or act independently of TREM2 in this "activation pathway" and that TREM2 plays complex pro- and anti-inflammatory effects in immune cells [23]. The identity of such additional factors is thus essential to discover, as they may unveil new therapeutic targets for neurodegenerative disorders.

The receptor for advanced glycation end products (RAGE) is an immunoglobulin (Ig)-type transmembrane receptor expressed by many cell types and is upregulated in patient and murine ALS tissues [24–26]. RAGE binds a diverse set of ligands, particularly those noted as damage associated molecular patterns (DAMPs), including several upregulated in ALS patient and $SOD1^{G93A}$ mouse spinal cord, such as S100 calcium binding protein B, carboxymethyllysine (CML)-advanced glycation end product (AGE), and high-mobility group box 1 (HMGB1) [25, 27–29]. Spatial transcriptomic analyses recently identified an enrichment of the "AGE-RAGE pathway in diabetic complications" Kyoto Encyclopedia of Genes and Genomes (KEGG) pathway in both murine and human ALS spinal cord within glia-related modules of gene expression [12].

While the discrete role of microglia RAGE in the context of ALS has never been studied, RAGE activation on myeloid cells, including microglia, stimulates NF-κB activity, thereby promoting pro-inflammatory cytokine expression and generation of reactive oxygen species [30–34]. Ligand engagement with RAGE induces a conformational change in its cytoplasmic tail that signals, at least in part, through diaphanous related formin 1 (DIAPH1) [35, 36]. Microglia have been shown to induce motor neuron death and drive pathology in $SOD1^{G93A}$ mice via activation of NF-κB [7]. We hypothesize that microglia RAGE contributes to oxidative stress and exacerbation of pro-inflammatory gene expression, processes which divert microglia from their homeostatic and protective

functions, thereby redirecting them to a phenotype that contributes to neurodegeneration.

In the current study, analysis of human ALS patient RNA-sequencing data uncovered for the first time that a spectrum of expression of *AGER*, the gene encoding RAGE, was evident in ALS cervical spinal cord tissue, and that this was related to alterations in pathways involving lipid metabolism, cellular microenvironment, and intercellular communication. Furthermore, patients with high *AGER* expression displayed increased levels of RAGE in microglia in the cervical spinal cord. In a murine model, we demonstrate a significant survival benefit and improvement in motor function performance in male but not female microglia *Ager*-deficient $SOD1^{G93A}$ $Ager^{fl/fl}$ $Cx3cr1^{Cre/+}$ mice (microglia *Ager* deletion) relative to $SOD1^{G93A}$ $Ager^{+/+}$ $Cx3cr1^{Cre/+}$ mice (Cre-controls; microglia express *Ager*) subjected to deletion of microglia *Ager* at 3 months of age. Remarkably, deletion of microglia *Ager* from $SOD1^{G93A}$ mice modulated the lumbar spinal cord transcriptome in a manner such that a number of pathways related to increased *AGER* expression in human ALS patients were significantly ameliorated. Altogether, these data suggest that RAGE may contribute to the pathological re-programming of innate microglia functions in the ALS spinal cord.

Materials and methods

Animals

All experiments were performed on C57BL/6J mice intercrossed with the following strains: B6.129P2(Cg)-$CX3CR1^{tm2.1(cre/ERT2)Litt/WganJ}$ (JAX Stock No: 021160), $Ager^{Flox/Flox}$ mice (C56BL6J background), and B6.Cg-Tg(SOD1G93A)1Gur/J (JAX Stock No:004435) [4, 37–39]. Note that all mice employed in this study were extensively backcrossed into or generated directly in C57BL/6J background. In all mice, copy number was analyzed and any mice with alterations were not enrolled in the study [40]. Three mice over the course of the study were censored due to non-ALS deaths. All mice were maintained under pathogen-free conditions. Unless otherwise noted, all mice were housed in a temperature (19–23 °C) and humidity (30–70% relative humidity)-regulated environment with 12-h light/dark cycle, lights on/off at 6:30, and received standard chow food pellets (Lab Diets, Cat: 5053) and water ad libitum. Tamoxifen (TAM) was used to delete *Ager* from *Cx3cr1*-expressing cells at 90 days of age. All animals, irrespective of genotype, were administered 0.2 μg of TAM (Sigma, Cat: T5648) dissolved in corn oil (Sigma-Aldrich, Cat: C8267) once daily every day for a total of five intraperitoneal injections except for the female control mice used in validation of *Ager* deletion, which received five intraperitoneal injections administered every other day. Onset of disease was identified by the age at which the animal reached maximum weight. The humane endpoint was determined by 20% weight loss from maximum weight, or the inability of the animal to right itself within 15 s of being placed on its side. When a mouse reached the humane endpoint, by either criterion, it was immediately sacrificed and date of death was recorded for survival analyses. Mice were weighed 2–3 times weekly, same time of day, with calibrated balances.

Motor function

Measurement of motor function was performed using the Hanging Wire test as detailed previously [41]. Briefly, mice were placed on a cage wire lid, inverted 50 cm above padding and observed for up to 1 min. The amount of time until the mouse fell to the padding was recorded. All mice were trained to the procedure for 1 week prior to data acquisition (8 weeks of age). All tests were performed twice-weekly until the mice were no longer able to perform the test. In all cases, the operator was naïve to experimental code. Triplicate measurements were taken and mean value was recorded for each session and weekly means were calculated. Animals were given 30-s breaks between test replicates.

Immunohistochemistry

Murine tissue staining

Mice were anesthetized with Ketamine and Xylazine and then underwent rapid cardiac perfusion with PBS, followed by 4% paraformaldehyde (PFA). The spinal column was rapidly removed, and the lumbar spinal cord was retrieved. Lumbar spinal cords were washed in PBS and then drop-fixed in 4% PFA for an additional 1 h at 4 °C. Gastrocnemius tissue was collected and drop-fixed 16 h in 1% PFA at 4 °C. After fixation, tissue was incubated with 15% sucrose in PBS for 24 h followed by incubation with 30% sucrose in PBS for an additional 24 h. Cyroprotected tissue was frozen in optimal cutting temperature (OCT) compound (FisherScientific, Cat: 23-730-571) and kept at − 80 °C until sectioning. Furthermore, 8-μm-thick serial sections were collected on Superfrost PLUS slides (FisherScientific, Cat: 22-037-246) using a Microm cryostat (ThermoFisher, Model: HM550). Sections were washed 3× with PBS for 5 min and then permeabilized with 0.2% Triton-X 100 in PBS for 10 min and washed 3× with PBS. Blocking was conducted with Serum-Free blocking buffer (Dako, Cat: X090930-2) for 1 h at RT. All primary antibodies were diluted in Antibody Diluent (Dako, Cat: S3022) and applied overnight at 4 °C. Subsequently, slides were washed 3× with PBS, then incubated with secondary antibodies diluted in Antibody Diluent for 1 h at RT. For slides containing DAPI, slides were washed and placed in a 1 μg/mL DAPI (Invitrogen, Cat: D1306) solution for 5 min at RT and washed 3× with PBS before mounting with

fluorescent mounting media (Dako, Cat: S302380-2). Primary antibodies used: 1 μg/mL Mouse anti-RAGE (Millipore, Cat: MAB5328), 0.5 μg/mL Rat anti-CD11B (M1/70) (Invitrogen, Cat:14-0112-82), 0.25 μg/mL Rat anti-GFAP (2.2B10) (Invitrogen, Cat: 13-0300), 5 μg/mL Rat anti-CLEC7A (Invivogen, Cat: mabg-mdect), 1 μg/mL Mouse anti-AMIGO2 (G-7) (SantaCruz, Cat: sc-373699), 5 μg/mL Mouse anti-NeuN (Millipore, Cat: MAB377), 5 μg/mL Rat anti-CD68 (Abcam, Cat: ab53444), 5 μg/mL Rat anti-F4/80 (Abcam, Cat: ab6640), and 3 μg/mL Chicken anti-MAP2 (Abcam, Cat:ab5392). Secondary antibodies utilized: Donkey anti-Rat Alexa Fluor 488 (Invitrogen, Cat: A-21208), Donkey anti-Mouse Alexa Fluor 546 (Invitrogen, Cat: A10036), Donkey anti-Rat Alexa Fluor 594 (Invitrogen, Cat: A-21209), Donkey anti-Mouse Alexa Fluor 488 (Invitrogen, Cat: A21203), and Donkey anti-Chicken Alexa Fluor 647 (Jackson ImmunoResearch, Cat: 703-605-155). All secondary antibodies were used at 1 μg/mL. All experiments included negative controls by omission of primary antibody.

Human tissue staining

De-identified paraffin-embedded tissue sections from sporadic ALS patient and control cervical spinal cord tissue were provided by the Target ALS Multicenter Postmortem Tissue Core (www.targetals.org). Then, 3 × 5 min washes with Clear-Rite 3 (ThermoFisher, Cat: 6901TS) were used to de-paraffinize the sections. Slides were rehydrated in a series of 5 min EtOH washes (2 × 100%, 1 × 90%, 1 × 70%) and then washed 3× with ddH20. Antigen retrieval was performed by steaming in Epitope Retrieval Solution (IHC World, Cat: IW-1100) for 1 h then washed 3× with PBS. Sections were permeabilized for 10 min with 0.4% Triton X100 in PBS then washed 3× with PBS. Autofluorescence was reduced by incubating with 1× TrueBlack in 70% ethanol (Biotium, Cat: 23007) for 30 s, then washed 3× with large volumes of PBS. Blocking was conducted with 5% Donkey Serum (SigmaAldrich, Cat: D9663) in PBS overnight at 4 °C. All primary antibodies were diluted in 2.5% Donkey Serum in PBS and applied for 24 h at 4 °C. Subsequently, slides were washed 3× with PBS, then incubated in secondary antibodies diluted in 2.5% Donkey Serum in PBS for 1 h at RT. Slides were then washed 3× with PBS before mounting with fluorescent mounting media. Primary antibodies utilized: 5 μg/mL Rabbit anti-IBA1 (Wako, Cat: 013-27691), 4 μg/mL Goat anti-RAGE (R&D, Cat: AF1179), 5 μg/mL Mouse anti-GFAP (BD Biosciences, Cat: 556330), and 5 μg/mL Mouse anti-NeuN (Millipore, Cat: MAB377). Secondary antibodies utilized: Donkey anti-rabbit Alexa Fluor 488 (Invitrogen, Cat: A21206), Donkey anti-mouse Alexa Fluor 488 (Invitrogen, Cat: A21203), Donkey anti-Goat Alexa Fluor 594 (Invitrogen, Cat: A32758), and Donkey anti-Goat Alexa Fluor 647 (Invitrogen, Cat: A32849). All secondary antibodies were used at 1 μg/mL. As above, all experiments included negative controls with omission of primary antibodies.

Imaging and quantification

Multicolor wide-field images were taken on a Leica 5500B microscope at × 20 or × 40 magnification, as indicated. All microscope settings were kept identical for each experiment. For mouse tissue imaging: 2–4 images/tissue slice and 3–4 tissue slices/sample were collected for analysis. For human tissue imaging: 2–4 images/tissue slice and 3 tissues slices/patient were collected for analysis, four regions of interest per image,150 × 150 μm in size, were selected as to exclude auto-fluorescent blood vessels for each image before further analysis. All analyses were performed with the Fiji distribution of ImageJ (NIH) [42].

Cell number analyses

Cell numbers that displayed overlap of the designated antibodies with DAPI were manually counted per image and averaged per mouse. All analysis was completed by a naïve experimenter blinded to all experimental codes.

Cell area analysis

To quantify the positive area of each stain in end-stage murine and human tissues, the images underwent background removal with the rolling ball radius set to 50 within ImageJ. Images were then subjected to automated thresholding with the optimal thresholding algorithm of each signal being selected by a naïve experimenter. The following thresholding algorithms were utilized: Li for: CD11B in Wild-Type vs $SOD1^{G93A}$ mice; Moments used for: RAGE, c-Type lectin domain containing 7a protein (or dectin-1) (CLEC7A), glial fibrillary acidic protein (GFAP), microtubule-associated protein 2 (MAP2), and adhesion molecule with Ig like domain 2 (AMIGO2); Triangle used for: CD11B, CLEC7A, on 120 day old tissue, and F4/80, CD68, and neuronal nuclei antigen (NeuN); and Otsu for: human ionized calcium-binding adapter molecule 1 (IBA1), and human GFAP [43–45]. Calculation of positive area was calculated per μm^2 and the average of 4–8 images per sample was used for statistical analysis.

Cell culture

BV2 mouse microglia-like cells were obtained as a generous gift from Dr. Colin K. Combs (University of Nebraska). BV2 cells were grown in growth medium (Dulbecco's modified Eagle's medium (DMEM) (Thermofisher, Cat:11885-084) containing 10% (v/v) heat-inactivated fetal bovine serum (FBS) (Corning, Cat:35-010-CV)) with 100 units/mL penicillin and 100 μg/mL

streptomycin (Thermofisher, Cat:10378016). The cells were incubated at 37 °C under 5% CO_2 and 95% relative humidity.

Lentivirus transfection

BV2 cells were grown to 50% confluency in normal growth medium. Growth medium was replaced with fresh growth medium supplemented with 5 μg/mL polybrene (Sigma, Cat:TR-1003) and 1.5×10^6 lentiviral particles of either sh*Ager* (Sigma, Cat:TRCN0000071745) or non-targeting shRNA control (Sigma, Cat: SHC002H) lentivirus for 8 h. When cells reached 90% confluency, shRNA expressing cells were selected using growth medium with 4 μg/mL puromycin (Thermofisher, Cat: A1113803) and were maintained under puromycin selection for at least three passages before use.

Treatment of BV2 cells

BV2 cells were plated in a 6-well plate at 3×10^5 cells per well and cultured in growth medium containing 1% FBS overnight. Cells were treated with 300 μg/mL RAGE ligand CML-AGE or human serum albumin control for 24 h before lysing in Qiazol reagent (QIAGEN Inc, Cat: 79306) and frozen until RNA was isolated [46]. For RAGE inhibitor studies, cells were first pre-treated with either 10 μM RAGE inhibitor (a C11 analog) or 0.1% v/v dimethyl sulfoxide (DMSO) in 1% FBS containing growth medium for 2 h before treatment [32].

$CD11B^+$ cell isolation via autoMACS

Mice were deeply anesthetized with Ketamine and Xylazine and then cardiac-perfused with 50 mL of ice-cold PBS. Subsequently, mice were decapitated and the brain was removed and collected into ice-cold tubes containing PBS. Brain tissue was dissociated using the Adult Brain Tissue Dissociation Kit (Miltenyi, Cat: 130-107-677) as per manufacturer's guidelines with the gentleMACS dissociator (Miltenyi, Cat:130-093-235) and strained with 70 μm filters (Miltenyi, Cat: 130-098-462). Homogenates underwent debris removal as per the manufacturer's guidelines (Miltenyi, Cat:130-109-398). Samples were then incubated with CD11B-microbeads (Miltenyi, Cat: 130-097-142) as per manufacturer's guidelines, then washed with Running Buffer (Miltenyi, Cat: 130-091-221) and centrifuged at 500×*g* for 5 min. Pellets were resuspended with 2 mL Running Buffer and subjected to the autoMACS Pro Separator (Miltenyi, Cat:130-092-545) "Possel" selection protocol. Positive fractions were collected, centrifuged at 500×*g* for 5 min and then re-suspended in 200 μL Qiazol lysis reagent (Qiagen, Cat: 79306) and flash frozen until RNA was isolated.

Tissue harvest and RNA isolation

Mice were anesthetized with Ketamine and Xylazine. The spinal column was rapidly removed, and the lumbar spinal cord was retrieved. Lumbar spinal cords were flash frozen and stored at − 80 °C until processed. Frozen tissue was kept on dry ice until homogenized in Qiazol reagent (Qiagen Inc, Cat: 79306). Crude homogenate was mixed with chloroform, at a ratio of 70 μL chloroform per 350 μL homogenate, to facilitate removal of lipids, and allowed to equilibrate at room temperature for 2 min. Samples were centrifuged at 13,000×*g* for 15 min at 4 °C. The aqueous phase containing the RNA was transferred to a new tube. Then the following steps were completed as detailed by the manufacturer's instructions using an RNeasy Mini Kit (Qiagen, Cat: 74104) with on-column DNAse digestion (Qiagen, Cat: 79254). RNA concentration was determined via a NanoDrop spectrophotometer (ThermoFisher, Model: ND-1000). RNA integrity (RIN) for RNA-sequencing samples was measured using RNA 6000 Pico Kit in a 2100 Bioanalyzer (Agilent).

Real-time quantitative polymerase chain reaction

One microgram of RNA was used with the iScript cDNA synthesis kit (BioRad, Cat:1708890) as per the manufacturer's instructions to generate cDNA. Taqman gene expression assays were used to evaluate *Ager* (Life Technologies, Cat: Mm01134790_g1), *18s* rRNA (Applied Biosystems, Cat:4310893E), *Hprt* (Life Technologies, Cat:Mm03024075_m1), *Il1a* (Life Technologies, Cat:Mm00439620_m1), and *Malat1* (Life Technologies, Cat: Mm01227912_s1) levels using the Taqman Fast Universal PCR Master Mix (Life Technologies, Cat: 4367846) with the 7500 Fast Real-Time PCR System (Applied Biosystems, Cat: LS4351106). Expression values were calculated using the ΔΔCt method relative to *18s* rRNA or *Hprt*.

Cytokine array

Five hundred nanograms of RNA per biological replicate (1.5 μg total) for each condition was pooled before proceeding with the mouse cytokine cDNA plate array (Signosis, Cat: AP-1141) as per the manufacturer's instructions. Resulting luminescence was quantified using a SpectraMax M5 microplate reader (Molecular Devices, San Jose, CA) and normalized to *18s rRNA*.

Murine RNA sequencing

High-quality lumbar spinal cord RNA samples, as confirmed by Bioanalyzer with RIN values ranging from 7.9 to 8.7, free of DNase and RNase were prepared for sequencing using the TruSeqStranded mRNA library prep kit (Illumina, Cat: 20020594) and the NovaSeq 6000 SP Reagent Kit v1.5 (Illumina, Cat: 20028401). High-

throughput RNA sequencing (RNA-seq) was completed using an Illumina NovaSeq 6000 sequencer performed by the NYU Grossman School of Medicine Genome Technology Core.

Murine RNA-seq data analysis

The resulting 49–61 M read pairs per sample were processed following standard quality control practices to remove low-quality reads and adapter sequence contamination (~ 15% of reads) [47–49]. Remaining high-quality read pairs were aligned to the mouse genome (mm10) using STAR 2.7.3a with a mean of 88% uniquely mapping [50]. Read pair counts per gene were summed with the featureCounts function in subread 1.6.3 using the GENCODE M25 annotation release [50–53]. Read counts were normalized using the trimmed mean of M values (TMM) method in edgeR 3.24.3 within the R environment 3.5.1 [54–56]. Differential expression was analyzed using edgeR via the exactTest function [55, 57]. Significantly differentially expressed genes were determined by a cut-off of adjusted p value < 0.05 and subjected to over representation analysis of KEGG pathways using the R package clusterProfiler v3.16.1 [58–61]. Significantly differentially expressed genes with false-discovery rate (FDR) < 0.05 and corresponding $\log_2$ fold changes were used as input for all ingenuity pathway analysis (IPA) including graphical summary, canonical pathways, upstream regulators, and causal network analyses (QIAGEN Inc.) [62]. Adjustments were made for multiple testing to control the FDR at 0.05 [63].

Human RNA-seq data analysis

Raw RNA-seq data of cervical spinal cord and de-identified metadata were obtained from:The Target ALS Multicentered Postmortem Tissue Core, the New York Genome Center for Genomics of Neurodegenerative Disease, Amyotrophic Lateral Sclerosis Association, and TOW Foundation (www.targetals.org). Illumina paired-end 100-bp read data were downloaded from TargetALS (mean of 43 M reads per sample) and processed following standard quality control practices to remove low-quality reads and adapter sequence contamination (~ 4% of reads) [47–49]. Remaining high-quality read pairs were aligned to the human genome (hg19) using STAR 2.6.1d with a mean of 95% uniquely mapping. Read pair counts per gene were summed with the featureCounts function in subread 1.6.3 using the GENCODE 30 annotation release [50–53]. Only samples with RIN values of ≥ 6 were used for all analyses. Read counts were normalized using the TMM method on $\log_2$ counts per million in edgeR 3.24.3 within the R environment 3.5.1 [54–56]. Differential expression was analyzed using generalized linear models via edgeR, with either (1) diagnosis of ALS spectrum motor neuron disease (n = 76) or non-neurological control (n = 11) as categorical variables; or (2) *AGER* as a continuous variable in ALS patients (n = 76) to control and test for differential expression related to diagnosis or increasing *AGER* expression while controlling for sex and testing for any potential interactions within the model [64]. Significant differentially expressed genes with $\log_2$ fold changes with absolute values of ≥ 0.5 used as the input for evaluation of overrepresentation of KEGG gene sets and for all IPA analyses as per the murine data analysis described above. Competitive gene set testing via CAMERA, and rotational gene set testing via ROAST were both completed using edgeR 3.24.3 to evaluate KEGG and Gene Ontology (GO) gene sets [55, 57–60, 65–68]. Testing for linear correlation was completed by first normalizing *AGER* expression using the TMM method and generating counts per million mapped reads (CPM) with edgeR 3.24.3 as above. A linear model was generated with normalized *AGER* CPM as the predictor of either age at death/tracheostomy or age at onset within the base R environment 3.5.1.

Statistics

Data are shown as mean ±SEM or as indicated. Normality of the data was assessed using the Shapiro-Wilk's normality test. If normality assumption was met, data were subsequently evaluated by independent two-sample t tests, two-way ANOVA with post-hoc Tukey's test, one way ANOVA with post-hoc Holm-Šídák multiple comparisons test, or mixed effects analysis with Geisser-Greenhouse correction with post-hoc Holm-Sidak's multiple comparisons test, as indicated. Non-parametric Mann–Whitney tests were implemented instead to assess differences if normality assumption was violated. Survival data were visualized by Kaplan–Meier curve and the Logrank test (Mantel–Cox) was used to evaluate differences in the survival distributions between groups. All analyses were performed with GraphPad Prism 9 (GraphPad Software, San Diego, CA) and R 3.6.1 using R package "nlme" [56, 69]. p values < 0.05 were used to denote statistical significance.

Results

Evaluation of *AGER* expression in human amyotrophic lateral sclerosis spinal cord

Previous studies have documented increased RAGE expression in human ALS spectrum motor neuron disease (ALS) spinal cord [25, 26]; however, detailed assessments of roles for RAGE in ALS are lacking [41]. To address this key point, we obtained bulk RNA-seq data from ALS and control patient cervical spinal cord tissue from the Target ALS Multicentered Postmortem Tissue Core, the New York Genome Center for Genomics of Neurodegenerative Disease, Amyotrophic Lateral Sclerosis

Association and TOW Foundation. We limited our analysis to RNA-seq samples with RIN ≥ 6. In total, 76 ALS and 11 non-neurological control cervical spinal cord data met these criteria and were eligible for analysis.

Expression of the gene encoding RAGE, *AGER*, was not significantly different (*FDR* = 0.78) between ALS patients and non-neurological controls (Fig. 1A). However, when we examined gene set differences in expression between the ALS patients and non-neurological controls with rotational gene set testing (ROAST) and competitive gene set testing (CAMERA) analyses, we observed significant enrichment of the "AGE-RAGE signaling pathway in diabetic complications" which was visualized by a barcode enrichment plot for the pathway (Fig. 1B, see Additional Files 1 and 2, Supplemental Table 1.1-1.3). Altogether, these analyses suggest upregulation of the AGE-RAGE signaling pathway gene set in ALS patients relative to control patients.

Further analysis revealed that there was a spectrum of *AGER* expression (normalized counts) in the cervical spinal cord across ALS patients (Fig. 1A). Thus, it was logical to determine if the level of *AGER* correlated with available ALS patient phenotypic metadata. The ALS patients had a median onset of 60.5 years of age (range 32–80), median age at death of 65 years (range 32–80), and a median disease duration (onset to death) of 36mo (range 6–156 months), and the majority had no identifiable family history of ALS (see Additional Files 1 and 2, Supplemental Table1.4). We found normalized *AGER* counts per million (CPM) was negatively correlated with the age at disease onset (coefficient = − 2.449, p = 0.07, adjusted r^2 = 0.032) and the age at death or tracheostomy (coefficient = − 2.609, p = 0.037, adjusted r^2 = 0.045) in the ALS patients (Fig. 1C, D). We obtained a randomly-selected and available subset of tissue sections from the patients displaying highest vs. lowest 10% of *AGER* RNA values, that is, the extremes (Fig. 1E). We demonstrated that the difference in *AGER* RNA was also present at the protein level (Fig. 1F, G).

We next sought to examine genes and pathways that may be modulated with increasing *AGER* expression in ALS patients. We tested for differential expression using *AGER* as the predictive variable and found that there were many significantly differentially expressed genes associated with *AGER* expression (see Additional Files 1 and 2, Supplemental Table 1.5). Importantly, there were no differential genes related to *AGER* expression that differed significantly by sex. We narrowed subsequent analyses to differential genes with ≥ 0.5 $|\mathrm{Log}_2|$ fold change; it is important to note that Log_2 fold changes represent the degree to which each gene changes per change in *AGER* expression. KEGG pathway enrichment results indicate upregulation of cell-cell communication and extracellular matrix remodeling pathways with the extent of *AGER* expression (see Additional Files 1 and 2, Supplemental Table 1.6). Ingenuity pathway analysis (IPA) indicated several enriched canonical pathways of genes including hepatic fibrosis/hepatic stellate cell activation (Table 1). Altogether, these data support roles for RAGE in human ALS.

However, as these analyses are from bulk RNA-seq data of cervical spinal cord tissue, it was not possible to discern which cell type(s) may be expressing RAGE and if this too differs across the spectrum of *AGER*-expressing ALS patients. To address this point, we sought to co-localize RAGE expression with several cell type markers within the subset of patients with the extremes of RAGE expression. We performed a series of immunohistochemistry (IHC) experiments to determine which cell types in the ALS cervical spinal cord were expressing RAGE and if that differed between these ALS patients. We found that there were no differences in microglia (ionized calcium-binding adapter molecule 1, IBA1) or astrocyte (glial fibrillary acidic protein, GFAP) staining area in either the ventral horn gray matter or associated white matter between high and low *AGER* patients (Fig. 2A–C). However, there were significantly higher levels of RAGE overlap with IBA1 in both areas, but not with GFAP in either area, in high vs. low *AGER* patients (Fig. 2A, D, E). Furthermore, there was no difference in the overlap of RAGE with a neuronal marker, neuronal nuclei antigen (NeuN), within the ventral horn between high and low *AGER* patients (Fig. 2A, F). However, additional RAGE signal was detected, which was not localized to any of these cell-type markers and the cellular or extracellular nature remains unclear. These data support the recent spatial transcriptomic analyses that indicated enrichment of the AGE-RAGE pathway in a glia module associated with disease progression in the $SOD1^{G93A}$ murine ALS model and in a corresponding module in human ALS patient tissue [12]. Altogether, these data suggest that *AGER* expression may be associated with (1) ALS pathology and (2) glial perturbation.

$SOD1^{G93A}$ mice exhibit increased RAGE-expressing microglia during pathology progression

Based on these analyses in human ALS and the accumulating evidence that microglia are dysfunctional early in the $SOD1^{G93A}$ murine model, which may promote/propagate astrocytic and neuronal dysfunction and that RAGE is known to regulate in vitro microglia-like cell responses to several ligands increased in $SOD1^{G93A}$ mice [25, 33, 34, 70–73], we sought to examine if microglia expressed RAGE in a prototypic murine model of ALS, the $SOD1^{G93A}$ model. There are currently no mouse models of "sporadic" ALS; however, murine models of familial ALS provide a means to model and test fundamental mechanisms of motor degeneration and reduced

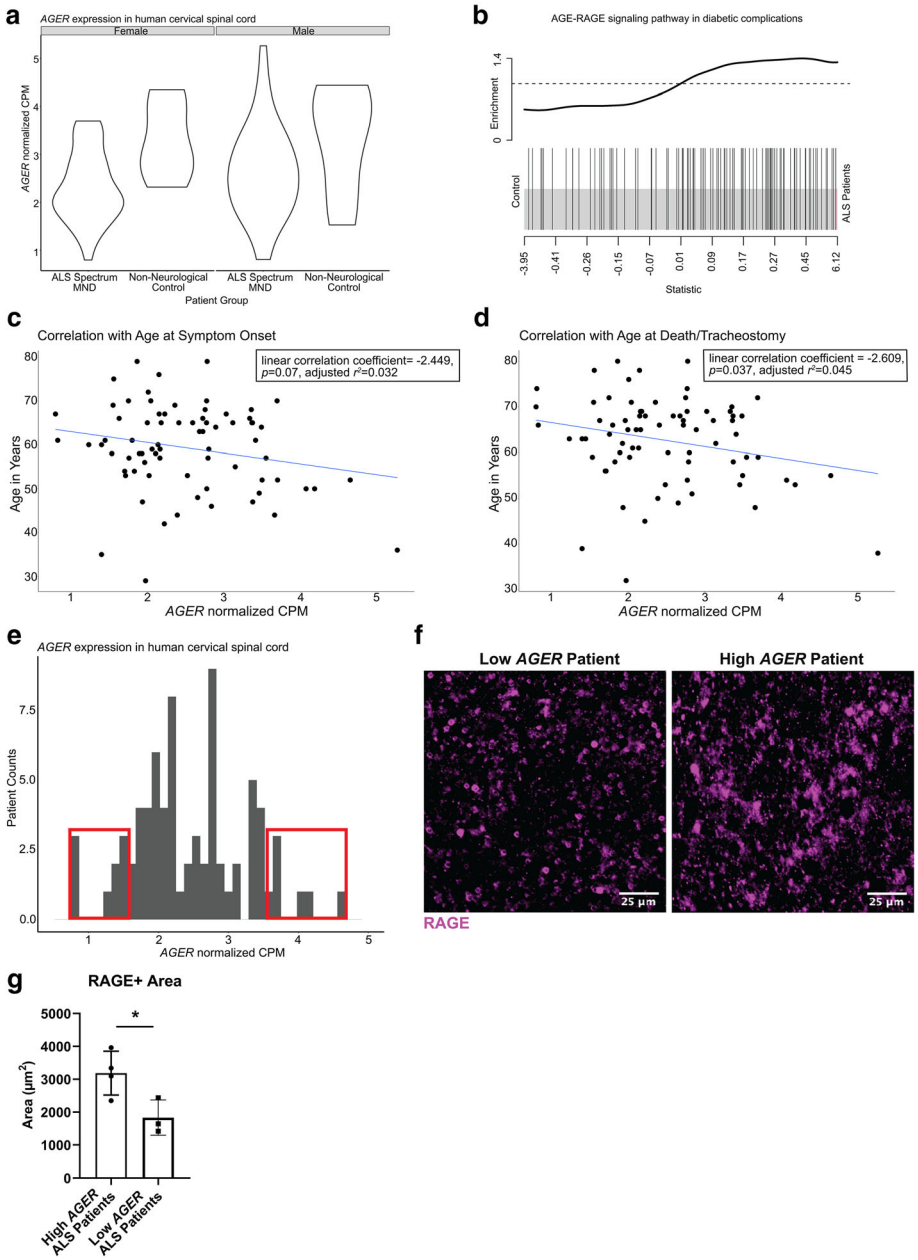

Fig. 1 Analysis of human ALS patient RNA-seq data implicates the RAGE pathway in modulating disease. **a** Normalized *AGER* counts per million mapped reads across patient groups separated by sex (no significant sex-dependent differences). **b** Barcode plot illustrating gene set enrichment of the "AGE-RAGE signaling pathway in diabetic complications" between ALS patients and non-neurological controls. The snake illustrates the enrichment and upregulation of the gene set in ALS patients. **c** Correlation of *AGER* expression (*x*-axis) and age at onset in years (*y*-axis). Regression line shown. Coefficient = − 2.449, $p = 0.07$, adjusted $r^2 = 0.032$. **d** Correlation of *AGER* expression (*x*-axis) and age at death/tracheostomy in years (*y*-axis). Regression line shown. Coefficient = − 2.609, $p = 0.037$, adjusted $r^2 = 0.045$. **e** Histogram of normalized *AGER* expression in ALS patients. Red boxes notate the highest 10% and the lowest 10% of *AGER*-expressing patients. **f** Representative image of regions of interest for RAGE staining in the ventral horn of a high and low *AGER* patient cervical spinal cord. Scale bar: 25 µm. **g** Quantification of RAGE+ area. In **a**: from left to right $N = 38, 5, 38, 6$. In **b**: $N = 76$ ALS patients and $N = 11$ non-neurological control patients. In **c**–**e**: $N = 76$ ALS patients. In **f**, **g**: $N = 4$ high *AGER* and 3 low *AGER* patients. Independent two sample two-sided *t* test. *$p = 0.0349$

survival in these animals vs. their unaffected littermate controls. Hence, we began by performing IHC in $SOD1^{G93A}$ and WT mice (all in the C57BL/6J background) lumbar spinal cord tissue at age 120 days. The overlap area of RAGE with the myeloid marker, integrin subunit alpha m (CD11B), was higher in $SOD1^{G93A}$ mice vs. littermate WT control mice (Fig. 3A, B). While RAGE is expressed in multiple cell-types in spinal cord;

Table 1 Overrepresentation analyses dependent on *AGER* expression within ALS patient cervical spinal cord RNA-seq

Ingenuity canonical pathways	FDR	KEGG pathways	FDR
Hepatic fibrosis/hepatic stellate cell activation	6.46E-08	Protein digestion and absorption	3.71E-07
GP6 signaling pathway	2.69E-07	ECM-receptor interaction	2.79E-05
Agranulocyte adhesion and diapedesis	7.08E-03	Cell adhesion molecules	2.27E-02
Apelin liver signaling pathway	7.08E-03	Calcium signaling pathway	4.21E-02
Sperm motility	9.55E-03	PI3K-Akt signaling pathway	4.21E-02
Atherosclerosis Signaling	1.58E-02		

Genes that were input into these analyses were significantly differentially-expressed genes with FDR < 0.05 with absolute $\log_2$ fold change values of ≥ 0.5. Enriched pathways, FDR < 0.05

the findings that RAGE overlap with microglia is increased in *SOD1*^{G93A} mice and in a subset of human patients with higher *AGER* expression, alongside the spatial transcriptomic analyses, implicating the AGE-RAGE pathway alteration in glia, suggested it was logical to probe potential roles for microglia RAGE in ALS-like pathology in the *SOD1*^{G93A} mouse model.

Microglia *Ager* deletion extends survival in male *SOD1*^{G93A} mice

As accruing evidence has suggested stage-specific roles for microglia in the context of ALS and other neurodegenerative diseases, we sought to assess whether microglia RAGE affects the pathological progression of *SOD1*^{G93A} mice [14]. We employed a tamoxifen (TAM)-inducible model in which microglia expressed *Ager* during development and early life and administered TAM to all mice at the age of 90 days to induce *Ager* deletion in *SOD1*^{G93A} *Ager*$^{fl/fl}$ *Cx3cr1*$^{Cre/+}$, and *SOD1*^{G93A} *Ager*$^{+/+}$ *Cx3cr1*$^{Cre/+}$ mice to evaluate potential roles for RAGE in the progression of pathology (Fig. 4A). We confirmed knock-down of *Ager* expression in primary CD11B cell isolates from central nervous system (CNS) tissues (Fig. 4B). The area of RAGE overlap with IBA1, but not GFAP, was significantly lower in the *SOD1*^{G93A} *Ager*$^{fl/fl}$ *Cx3cr1*$^{Cre/+}$ lumbar spinal cord tissue relative to Cre-expressing controls at the end of the study, suggesting *Ager* knock-down in microglia was maintained (Fig. 4C, D, Supplemental Figure 1A-B). The area of RAGE overlap with the pan neuronal marker microtubule-associated protein 2 (MAP2) at the age of 120 days did not differ between the two genotypes, suggesting that neuronal *Ager* was not modulated by this approach in this study (Supplemental Figure 1C-D).

As *Cx3cr1* Cre-expressing mice, regardless of the administration of TAM, or not, are heterozygous for the *Cx3cr1* locus, we evaluated *SOD1*^{G93A} *Ager*$^{+/+}$ *Cx3cr1*$^{Cre/+}$ (microglia *Ager*-expressing, *Cx3cr1* Cre-expressing) and *SOD1*^{G93A} *Ager*$^{fl/fl}$ *Cx3cr1*$^{Cre/+}$ (microglia *Ager* deficient, *Cx3cr1*-Cre expressing) mice [37]. As expected, there were no differences in the age of disease onset between any groups, as defined as the age at which the mouse reached maximum weight (Supplemental Figure 2A-B, see Additional file 1; $p > 0.05$). We found that male *SOD1*^{G93A} *Ager*$^{fl/fl}$ *Cx3cr1*$^{Cre/+}$ mice displayed significantly longer survival relative to *SOD1*^{G93A} *Ager*$^{+/+}$ *Cx3cr1*$^{Cre/+}$ mice, median lifespan of 159 (range 149–175 days) days vs. 152 days (range 136–171 days), respectively (Fig. 5A; $p < 0.05$). We did not observe differences in lifespan between the female mice groups (Fig. 5B; $p > 0.05$). Altogether, these data suggested that microglia RAGE may contribute to pathology progression in male *SOD1*^{G93A} mice.

Male *SOD1*^{G93A} *Ager*$^{fl/fl}$ *Cx3cr1*$^{Cre/+}$ mice displayed reduced pathology during disease progression

We next investigated if microglia *Ager* contributed to the progressive motor function decline experienced by *SOD1*^{G93A} mice [4, 5, 38]. Mixed effects analysis of motor function data indicated a significant interaction between time and genotype in male but not female mice ($p = 0.038$) suggesting that male but not female *SOD1*^{G93A} *Ager*$^{fl/fl}$ *Cx3cr1*$^{Cre/+}$ mice had time-dependent protection in motor function (Fig. 6A, B). However, there were no significant differences in motor function at any one time point after multiple corrections in either male or female mice (Fig. 6A, B).

As *SOD1*^{G93A} mice experience pronounced weight loss with disease progression, we next examined if microglia *Ager* expression modulated this weight loss [4, 5, 38]. Mixed effects analysis of body weight data normalized to weight at tamoxifen administration indicated significant interactions between time and genotype in male and female mice ($p = 0.0067$, $p = 0.0134$ respectively) suggesting that in *SOD1*^{G93A} *Ager*$^{fl/fl}$ *Cx3cr1*$^{Cre/+}$ mice there are time dependent alterations in body weight (Fig. 6C, D). However, there were no significant differences in normalized body-weight measures at any single time point after multiple corrections in male or female mice (Fig. 6C, D). As female mice did not display any significant differences in survival, or motor function, these mice were not investigated further (Figs. 5B and 6B, D).

While no significant differences in motor function or body weight were noted at any single time point, there

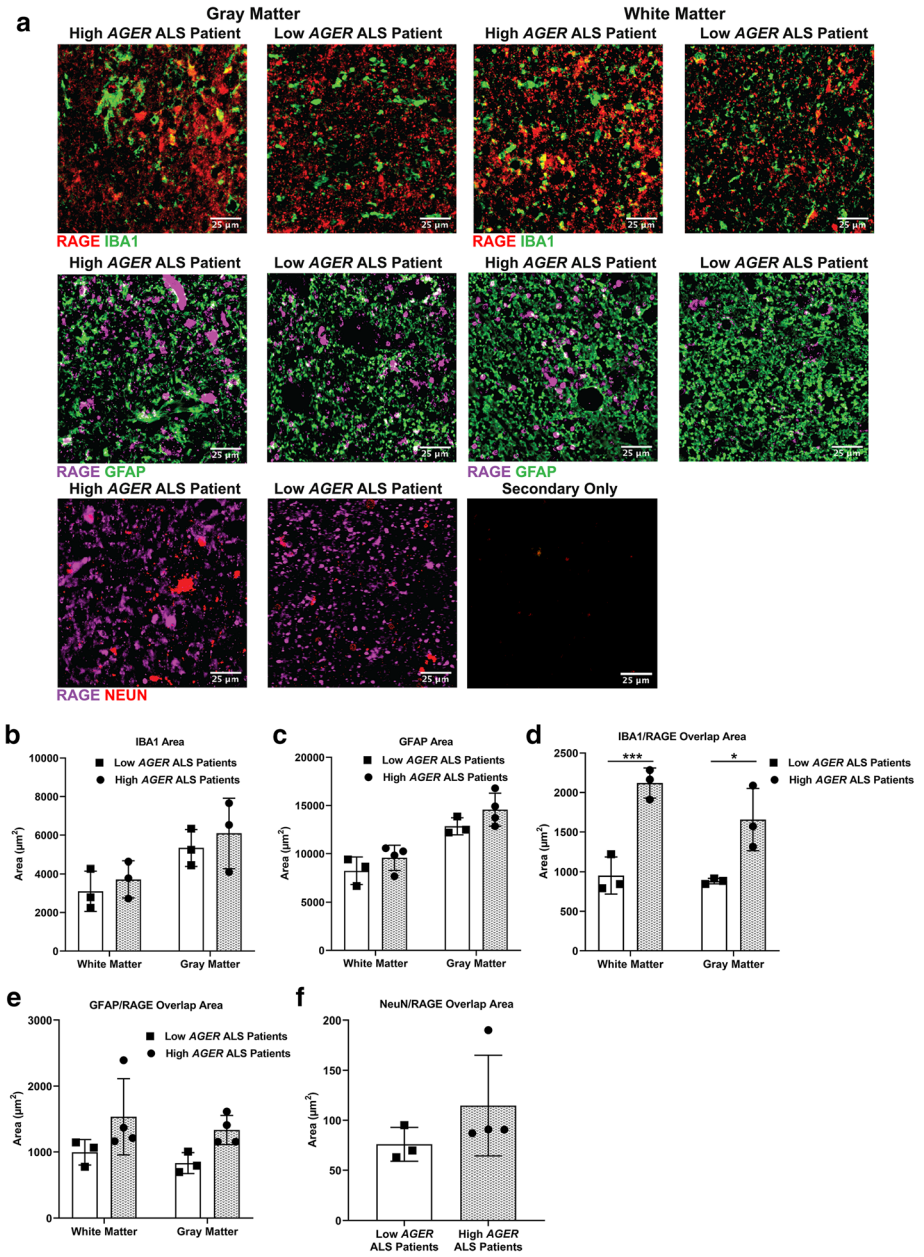

Fig. 2 *AGER* expression changes coincide with alterations in overlap of microglia and RAGE protein. **a** Representative images of regions of interest for RAGE, IBA1, GFAP, and NeuN staining in the ventral horn of high and low *AGER* patient cervical spinal cord and anterior white matter. Scale bar: 25 µm. **b** Quantification of IBA1$^+$ area. **c** Quantification of GFAP$^+$ area. **d** Quantification of overlap of IBA1$^+$ RAGE$^+$ area. **e** Quantification of overlap of GFAP$^+$ RAGE$^+$ area. **f** Quantification of overlap of NeuN$^+$ RAGE$^+$ area. $N = 4$ high *AGER* patients and $N = 3$ low *AGER* patients. Mean ± SD. In **b**–**e**: two-way ANOVA with post-hoc Tukey's test. In **f**: Mann-Whitney *U* test. *$p = 0.0102$, ***$p = 0.0009$

were time-dependent reductions in the rate of motor function decline and weight in male *SOD1*^{G93A} *Ager*$^{fl/fl}$ *Cx3cr1*$^{Cre/+}$ mice suggesting a slower rate of disease progression. This led us to consider the possibility that microglia *Ager* deletion may have affected the numbers of surviving motor neurons within the lumbar ventral horn. We examined the number of surviving motor neurons by IHC at the age of 120 days in male mice and found significantly higher numbers of motor neurons, as labeled by NeuN, DAPI, and choline acetyltransferase (ChAT), in the lumbar ventral horn in the *SOD1*^{G93A} *Ager*$^{fl/fl}$ *Cx3cr1*$^{Cre/+}$ mice relative to the Cre-recombinase expressing controls (Fig. 6E, F). Altogether, these data suggest that deletion of microglia *Ager* may reduce/delay

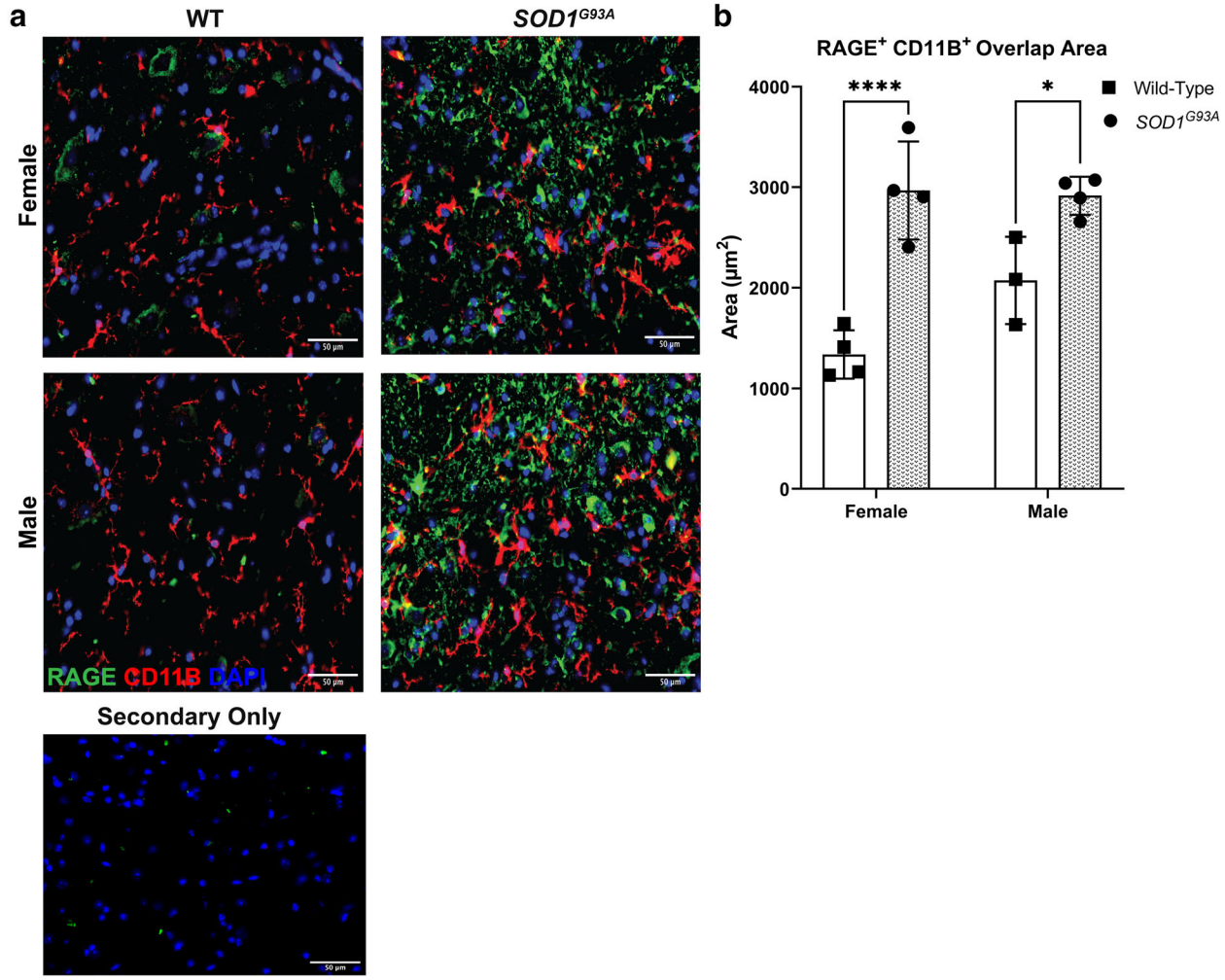

Fig. 3 *SOD1*^{G93A} mice exhibit increased RAGE^{+} microglia at the age of 120 days. **a** Representative images of CD11B and RAGE staining in the ventral horn of *SOD1*^{G93A} mouse lumbar spinal cord. Scale bar: 50 μm. **b** Quantification of overlap of CD11B^{+} RAGE^{+} area. *N* = 3 male WT mice, *N* = 4 male *SOD1*^{G93A} mice, *N* = 4 female WT mice, and *N* = 4 female *SOD1*^{G93A} mice. Mean ± SD. Two-way ANOVA with post-hoc Tukey's test. *p = 0.0192, ****p < 0.0001

neuron death in male *SOD1*^{G93A} mice. These findings led us to perform additional experiments to provide insight into the mechanisms by which this protection may occur.

Microglia *Ager* deletion does not impact skeletal muscle macrophages

Next, we considered that deletion of *Ager* from *Cx3cr1* expressing cells at 90 days of age may have modulated skeletal muscle pathology either by direct or indirect effects on skeletal muscle macrophages and/or peripheral monocyte-derived macrophages. We evaluated end-stage and day 120 gastrocnemius muscle for macrophage content, as labeled by F4/80 and CD68, which revealed no differences between groups at either time point (Supplemental Figure 3A-D, 4A-D). Altogether, these data suggest the beneficial effects of microglia *Ager* reduction were likely restricted to the nervous system.

Male *SOD1*^{G93A} *Ager*$^{fl/fl}$ *Cx3cr1*$^{Cre/+}$ mice lumbar spinal cord exhibits transcriptomic alterations suggestive of improved homeostatic function

Hence, to uncover cell intrinsic and cell-cell communication pathway mechanisms underlying the benefits of microglia *Ager* deletion in male *SOD1*^{G93A} mice, we performed RNA-seq on isolated lumbar spinal cord tissue from male *SOD1*^{G93A} *Ager*$^{fl/fl}$ *Cx3cr1*$^{Cre/+}$ mice and *SOD1*^{G93A} *Ager*$^{+/+}$ *Cx3cr1*$^{Cre/+}$ mice at humane endpoint (end-stage). We identified 78 differentially expressed genes between the two genotypes (Fig. 7, Supplemental Table 1.7, see Additional Files 1 and 2). Overrepresentation analysis of the differential gene list indicated enrichment for several KEGG Pathways (Table 2,

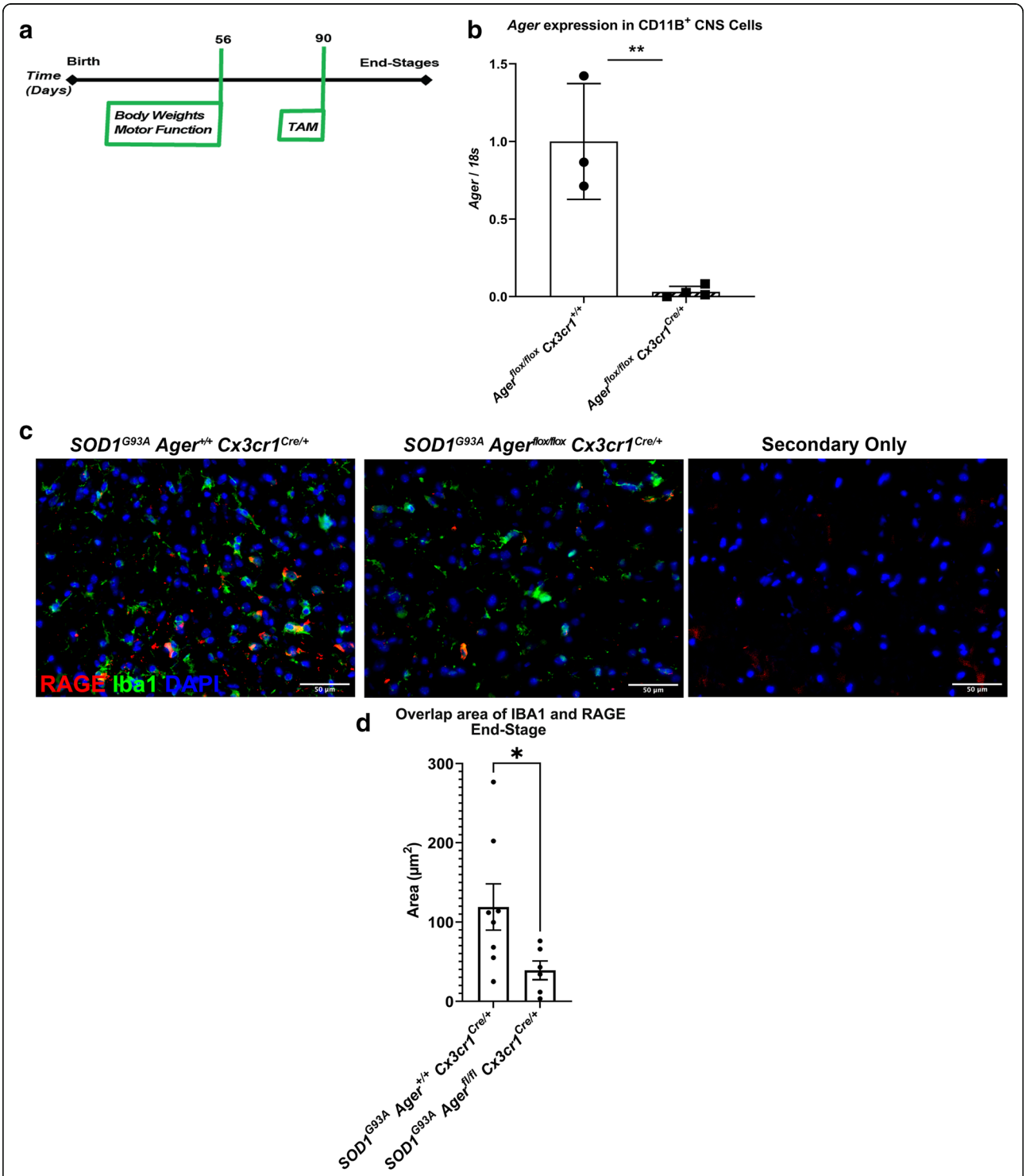

Fig. 4 Study design and validation of microglia *Ager* deletion. **a** Timing of Tamoxifen (TAM) administration and behavioral assessments of animals. **b** Quantification of *Ager* transcripts in primary CD11B$^+$ isolates by RT-qPCR thirty days after TAM administration. **c** Representative images of IBA1 and RAGE staining in the ventral horn of *SOD1*^{G93A} mouse lumbar spinal cord at end-stage. Scale bar: 50 µm. **d** Quantification of IBA1 and RAGE overlap area. Mean ± SD. In **b**, $N = 3$ *Ager*$^{fl/fl}$ *Cx3cr1*$^{+/+}$ mice and $N = 4$ *Ager*$^{fl/fl}$ *Cx3cr1*$^{Cre/+}$ mice. In **c**, **d**, $N = 6$ *SOD1*^{G93A} *Ager*$^{fl/fl}$ *Cx3cr1*$^{Cre/+}$ mice, $N = 8$ *SOD1*^{G93A} *Ager*$^{+/+}$ *Cx3cr1*$^{Cre/+}$ mice. Independent two sample two-sided *t* test. $^{**}p = 0.0031$, $^{*}p = 0.0437$

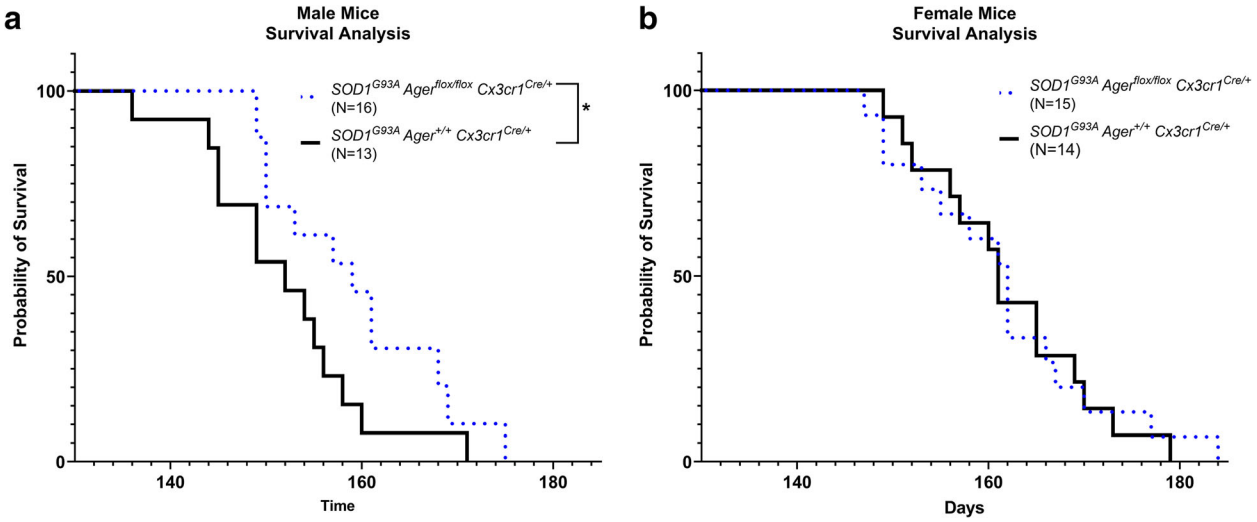

Fig. 5 Microglia *Ager* deletion exerts sex-dependent effects on survival in $SOD1^{G93A}$ mice. **a** Kaplan–Meier estimates of percent of male mice surviving plotted vs. age (days). $N = 16$ $SOD1^{G93A}$ $Ager^{fl/fl}$ $Cx3cr1^{Cre/+}$ mice, and $N = 13$ $SOD1^{G93A}$ $Ager^{+/+}$ $Cx3cr1^{Cre/+}$ mice. **b** Kaplan–Meier estimates of percent of female mice surviving plotted vs. age (days). $N = 15$ $SOD1^{G93A}$ $Ager^{fl/fl}$ $Cx3cr1^{Cre/+}$ mice, and $N = 14$ $SOD1^{G93A}$ $Ager^{+/+}$ $Cx3cr1^{Cre/+}$ mice. The Logrank test was performed to compare the survival distributions between groups. $^{*}p = 0.0496$

Supplemental Table 1.8, see Additional Files 1 and 2). Enriched KEGG pathway gene sets included "Cardiac muscle contraction," "Calcium signaling pathway," "PPAR signaling pathway," "Regulation of actin cytoskeleton," and "Cholesterol metabolism". Furthermore, canonical pathway analysis using IPA indicated enrichment of several pathways within the differential gene list including "Calcium signaling," "Actin cytoskeleton signaling," and "Integrin signaling" among others (Table 2, Supplemental Table 1.9, see Additional Files 1 and 2) [62]. Altogether, these data suggest genotype-dependent effects on cell-cell crosstalk mechanisms, as exemplified by alterations of lipid, metabolic, and integrin signaling gene sets.

To further address this concept, we analyzed potential causal networks that may be modulated in our dataset, which could explain the observed transcriptomic changes [62]. As *Ager* was deleted solely in *Cx3cr1*-expressing cells, we limited our analysis to potential cytokines that could originate from microglia and cause transcriptomic alterations across multiple cell types which would be present in the bulk RNA-sequencing data. We identified several significant putative causal networks belonging to numerous cytokine families, including interleukin-1 (IL1), interleukin-3, interferon-α (IFN-α), and interferon-β (IFN-β) (Table 3, Supplemental Table 1.10, see Additional Files 1 and 2).

To evaluate potential roles of microglia RAGE in mediating cytokine expression changes, we turned to an in vitro system. We first conducted a commercially available cytokine screen to evaluate RAGE-dependent effects of RAGE ligand carboxymethyllysine (CML)-AGE, a ligand increased in $SOD1^{G93A}$ spinal cords and in human patient tissues, on BV2 microglia-like cells (Supplemental 5A) [25, 28, 29, 46]. An interesting candidate discovered by this approach was *Il1a*, as this was also predicted by the RNA-seq causal network analysis (Supplemental Figure 5A, Table 3, Supplemental Table 1.10). In fact, in validation experiments, CML-AGE significantly induced *Il1a* expression, which was significantly reduced by pre-treatment with a RAGE inhibitor in BV2 cells (Supplemental Figure 5B) [32]. Furthermore, lentiviral transduction of BV2 cells with short hairpin RNA to significantly reduce *Ager* expression in BV2 cells prevented the CML-AGE associated increase in *Il1a* expression (Supplemental Figure 5C-D). Interestingly, expression of *Malat1*, a differentially expressed inflammation-associated lncRNA in the microglia *Ager*-deficient spinal cord, exhibited a RAGE-dependent increase in BV2 cells in response to CML-AGE (Supplemental Figure 5E, Supplemental Table 1.7) [74].

Collectively, these results point to significant modulation of intrinsic microglia inflammation. In one or more cell types, prompted by microglia *Ager* deletion, fundamental changes in general cellular health are observed, as exemplified by alterations in actin cytoskeleton and calcium related pathways, both of which would be predicted to fundamentally alter cell intrinsic and intercellular communication properties in the spinal cord. To verify the implications of these transcriptomic alterations, we examined these points specifically in end-stage tissues.

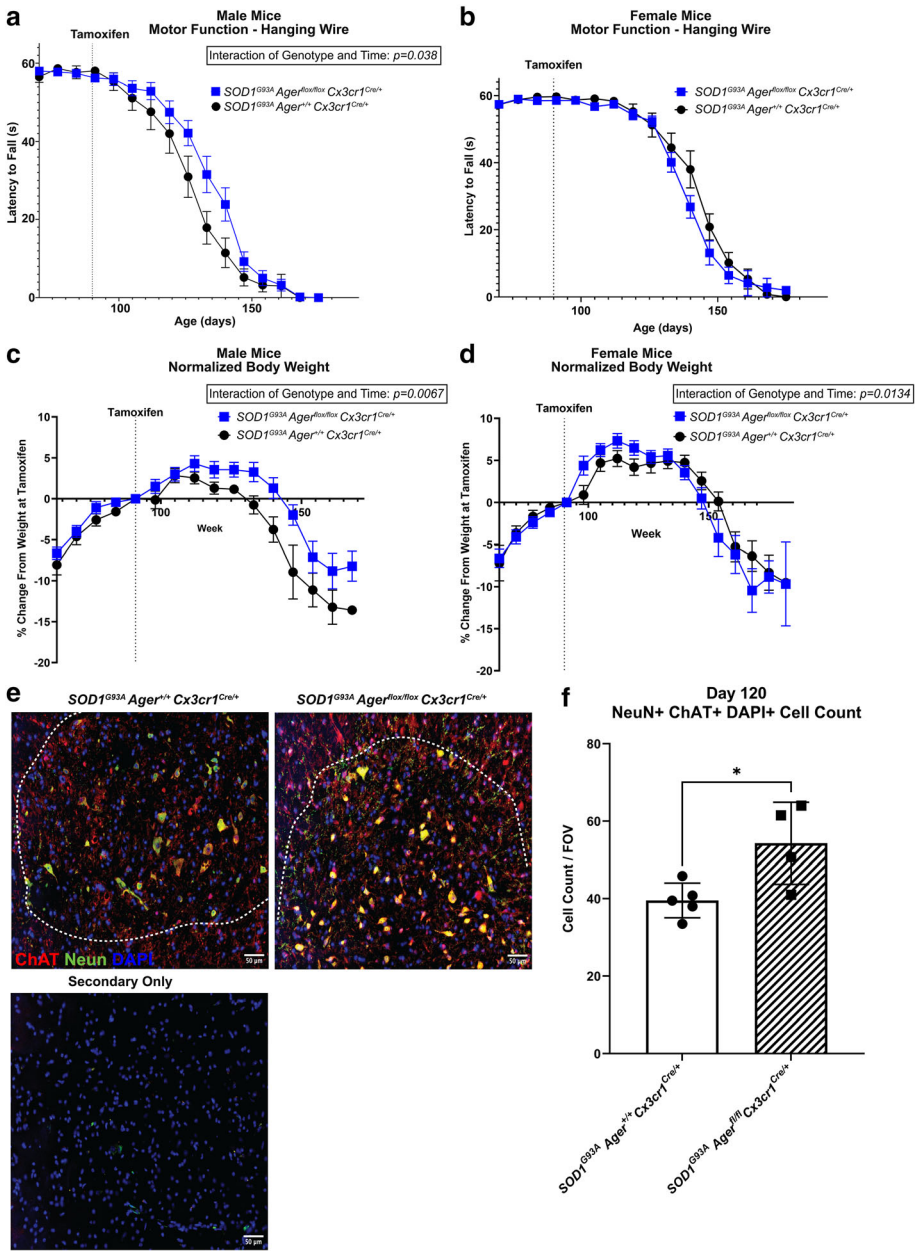

Fig. 6 *SOD1*^{G93A} mice with microglia *Ager* deletion exhibit sex-dependent effects on pathology. **a** Latency to fall as measured by hanging wire test in male mice. **b** Latency to fall as measured by hanging wire test in female mice. **c** Normalized body weight to weight at tamoxifen administration of male mice. **d** Normalized body weight to weight at tamoxifen administration of female mice. Dashed lines indicate age at tamoxifen administration. Mean ± SEM. **e** Representative images of NeuN and DAPI staining in the lumbar spinal cord ventral horn. Scale bar: 50 μm. **f** Quantification of NeuN^{+} DAPI^{+} cell number. Mean ± SD. In **a**, **c** (male mice): $N = 16$ *SOD1*^{G93A} *Ager*$^{fl/fl}$ *Cx3cr1*$^{Cre/+}$ mice, and $N = 13$ *SOD1*^{G93A} *Ager*$^{+/+}$ *Cx3cr1*$^{Cre/+}$ mice. In **b**, **d** (female mice): $N = 15$ *SOD1*^{G93A} *Ager*$^{fl/fl}$ *Cx3cr1*$^{Cre/+}$ mice, and $N = 14$ *SOD1*^{G93A} *Ager*$^{+/+}$ *Cx3cr1*$^{Cre/+}$ mice. In **e**, **f** (male mice): $N = 4$ *SOD1*^{G93A} *Ager*$^{fl/fl}$ *Cx3cr1*$^{Cre/+}$ mice, and $N = 5$ *SOD1*^{G93A} *Ager*$^{+/+}$ *Cx3cr1*$^{Cre/+}$ mice. In **a**–**d**: independent two-sample two-sided *t* test was used to assess the group difference at each time point. Mixed effects analysis was utilized to evaluate effects of genotype, time, and the interaction between genotype and time. In **a**: genotype*time interaction effect: $p = 0.0378$. In **c**: genotype effect: $p = 0.0157$, genotype*time interaction effect: $p = 0.0067$. In **d**: genotype*time interaction effect $p = 0.0134$. In **f**: independent two sample two-sided *t* test. In **f**: $^{*}p = 0.0224$

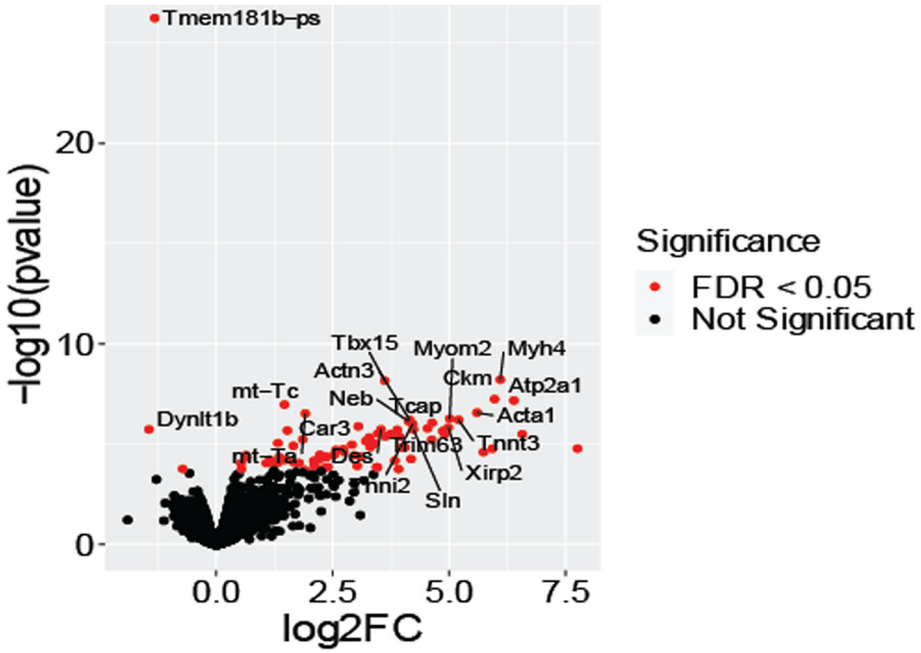

Fig. 7 Differential expression analysis between male *SOD1*^{G93A} mice with microglia devoid of *Ager* and Cre-expressing controls. Volcano plot displaying differentially expressed genes between *SOD1*^{G93A} *Ager*$^{fl/fl}$ *Cx3cr1*$^{Cre/+}$ and *SOD1*^{G93A} *Ager*$^{+/+}$ *Cx3cr1*$^{Cre/+}$ mice. The *y*-axis is $-\log_{10}(p\ value)$ and *x*-axis is the Log_2 fold change of each gene analyzed. Red colored genes are significantly differentially expressed with an FDR < 0.05. The top twenty significant genes are labeled. *N* = 4 independent mice/group

Microglia *Ager* deletion reduces the accumulation of damage-associated microglia in male *SOD1*^{G93A} mice

The RNA-seq data analysis suggested that microglia *Ager* deletion resulted in reduction in IL1 and IFN signaling (Table 3), both of which were previously suggested to be dysfunctional in ALS models and in patients [75–79]. In fact, in vitro experiments supported microglia RAGE affecting *Il1a* and *Malat1* expression (Supplemental Figure 3). Beyond the number and density of microglia, their specific gene expression patterns aid in designation of these cells as pro-damage vs. homeostatic phenotype. Specifically, the c-type lectin domain containing 7a protein (CLEC7A) is an established marker of pro-damage/disease-associated microglia, which has been shown to be highly upregulated in *SOD1*^{G93A} microglia [23]. By IHC, at end-stage, we found that there was a significant reduction in CLEC7A^{+} area, and CLEC7A^{+} cell number in *SOD1*^{G93A} *Ager*$^{fl/fl}$ *Cx3cr1*$^{Cre/+}$ vs. *SOD1*^{G93A} *Ager*$^{+/+}$ *Cx3cr1*$^{Cre/+}$ mice (Fig. 8A–C), suggesting that an attenuated or altered DAM phenotype was induced by deletion of microglia *Ager*. These key findings raise the possibility that RAGE

Table 2 Overrepresentation analyses of differentially expressed genes between *SOD1*^{G93A} *Ager*$^{fl/fl}$ *Cx3cr1*$^{Cre/+}$ and *SOD1*^{G93A} *Ager*$^{+/+}$ *Cx3cr1*$^{Cre/+}$ mice

Ingenuity canonical pathways	FDR	KEGG pathway	FDR
Calcium signaling	1.82E-05	Cardiac muscle contraction	2.02E-05
Actin cytoskeleton signaling	8.91E-05	Hypertrophic cardiomyopathy	2.02E-05
Cellular effects of sildenafil (Viagra)	1.07E-04	Dilated cardiomyopathy	2.02E-05
Epithelial adherens junction signaling	7.24E-04	Calcium signaling pathway	1.2E-3
ILK signaling	7.24E-04	Apelin signaling pathway	1.6E-3
RhoA signaling	1.41E-03	Adrenergic signaling in cardiomyocytes	2.39E-2
Protein kinase A signaling	1.41E-03	Arrhythmogenic right ventricular cardiomyopathy	2.61E-2
Tight junction signaling	2.82E-03	PPAR signaling pathway	3.44E-2
Hepatic fibrosis/hepatic stellate cell activation	2.95E-03	Focal adhesion	4.35E-2
Agranulocyte adhesion and diapedesis	3.47E-03		

Significantly differentially expressed genes, FDR < 0.05 were used as input into each analysis. Top ten enriched pathways, FDR < 0.05

Table 3 Causal network analysis utilizing *SOD1*^{G93A} *Ager*$^{fl/fl}$ *Cx3cr1*$^{Cre/+}$ and *SOD1*^{G93A} *Ager*$^{+/+}$ *Cx3cr1*$^{Cre/+}$ differentially expressed genes

Cytokine	Z-Score (activation score)	FDR
CXCL1	3.464	5.48E-05
CXCL9	3.317	1.24E-04
IL3	3.286	1.98E-08
TSLP	3.266	5.78E-12
IL5	2.985	4.36E-07
IFNA1/IFNA13	2.837	4.26E-08
IL22	2.828	4.09E-06
CD70	2.828	8.82E-05
IL1A	2.4	9.75E-06
IL15	1.569	9.70E-08
WNT1	1.414	6.43E-12
IFNB1	1.183	1.29E-11
TNFSF10	0.365	8.95E-09
IL6	0.333	2.89E-04
TNFSF12	-1	9.70E-04

Results of IPA predicted causal network regulators, which are labeled as "cytokine". Positive values indicate predicted activation in *SOD1*^{G93A} *Ager*$^{+/+}$ *Cx3cr1*$^{Cre/+}$ mice

contributes to a cell-intrinsic transition of microglia from a homeostatic to a dysfunctional phenotype.

Microglia *Ager* deletion reduces accumulation of reactive astrocytes at the end-stage of disease in *SOD1*^{G93A} mice

The RNA-seq results indicated reduction of a putative causal network involving IL1 (Table 3). In this context, accumulating evidence suggests that microglia-secreted molecules complement component 1q (C1q), IL1α, and TNF can induce astrocyte reactivity and promote neurotoxicity [70, 71]. Prompted by this consideration, we thus investigated if the *SOD1*^{G93A} *Ager*$^{fl/fl}$ *Cx3cr1*$^{Cre/+}$ mice displayed alterations in astrocytes. At end-stage, we found that GFAP$^+$ area was significantly lower in *SOD1*^{G93A} *Ager*$^{fl/fl}$ *Cx3cr1*$^{Cre/+}$ mice relative to Cre-expressing controls (Fig. 9A, B). Recent work has suggested distinct reactive astrocyte phenotypes and identified markers of those states [70, 80]. AMIGO2, adhesion molecule with Ig-like domain 2, was proposed as a marker of "A1" reactive inflammatory astrocytes induced specifically by C1q, IL1α and TNF [70]. Although it is acknowledged that this classification likely does not illuminate the breadth of astrocyte properties and contributions to ALS operative in vivo, we nevertheless examined if the GFAP alterations were concomitant alongside alterations in "A1" astrocytes to begin to define if microglia RAGE might impact astrocyte gene expression. Indeed, we found that GFAP$^+$ AMIGO2$^+$ overlap area was significantly reduced in *SOD1*^{G93A} *Ager*$^{fl/fl}$ *Cx3cr1*$^{Cre/+}$ mice vs. the Cre-expressing controls (Fig. 9A, C). Altogether, these data suggest that microglia *Ager* deletion may reduce astrocytic dysfunction likely through altered cytokine expression.

Microglia *Ager* deletion reduces microgliosis at an earlier stage in male *SOD1*^{G93A} mice

We next considered that it was important to also examine microglia and expression of CLEC7A at a time point within the progression phase, but short of end-stage analysis. It is important to note that microglial CLEC7A expression increases over time in this model, and not all microglia may have notable expression of CLEC7A at 120 days of age [20]. Thus, we addressed this point by examining the expression of both CD11B and CLEC7A at day 120. The results indicated significant reductions in the amount of CD11B$^+$ cells and CD11B$^+$ area in *SOD1*^{G93A} mice devoid of microglia *Ager* (Fig. 10A–C). Similar to the end-stage tissue analysis, we observed reduced CLEC7A$^+$ area at day 120 (Fig. 10D, E). Altogether, these data suggested that RAGE expression on microglia may contribute to the promotion of microgliosis (Fig. 10A–D), and may affect CLEC7A expression at a stage within the microglia phenotypic transition but prior to frank end-stage tissue pathologies (Figs. 8A–C and 10D, E). As such, we surmised that the overall RAGE-dependent mechanisms in microglia in *SOD1*^{G93A} mice were likely through alterations in microglia cell intrinsic and cell-cell communication pathways between microglia and other cell-types.

Finally, we considered the possibility that the processes affected by microglia *Ager* deletion in *SOD1*^{G93A} mice might relate to the processes accompanied by increasing human *AGER* expression in ALS patients. Accordingly, we compared the results of both RNA-seq analyses and found that half of the ingenuity canonical pathways identified in the human data analysis overlapped between the two data sets: "Hepatic fibrosis/Hepatic Stellate Cell Activation," "Atherosclerosis Signaling," and "Agranulocyte Adhesion and Diapedesis" (Tables 1 and 2, Supplemental Figure 6-8). Collectively, although it is acknowledged that the human and mouse spinal cord sequencing experiments were not identically designed, these analyses nevertheless suggest that RAGE may modulate extracellular matrix composition, cell-cell communication and lipid metabolism in ALS spinal cord tissues in patients and in *SOD1*^{G93A} mice.

Discussion

Our study sought to uncover potential RAGE-dependent roles in ALS by utilizing human patient cervical spinal cord RNA-seq data and the *SOD1*^{G93A} mouse model of ALS-like pathology. Although RAGE expression was not significantly different between human ALS patients

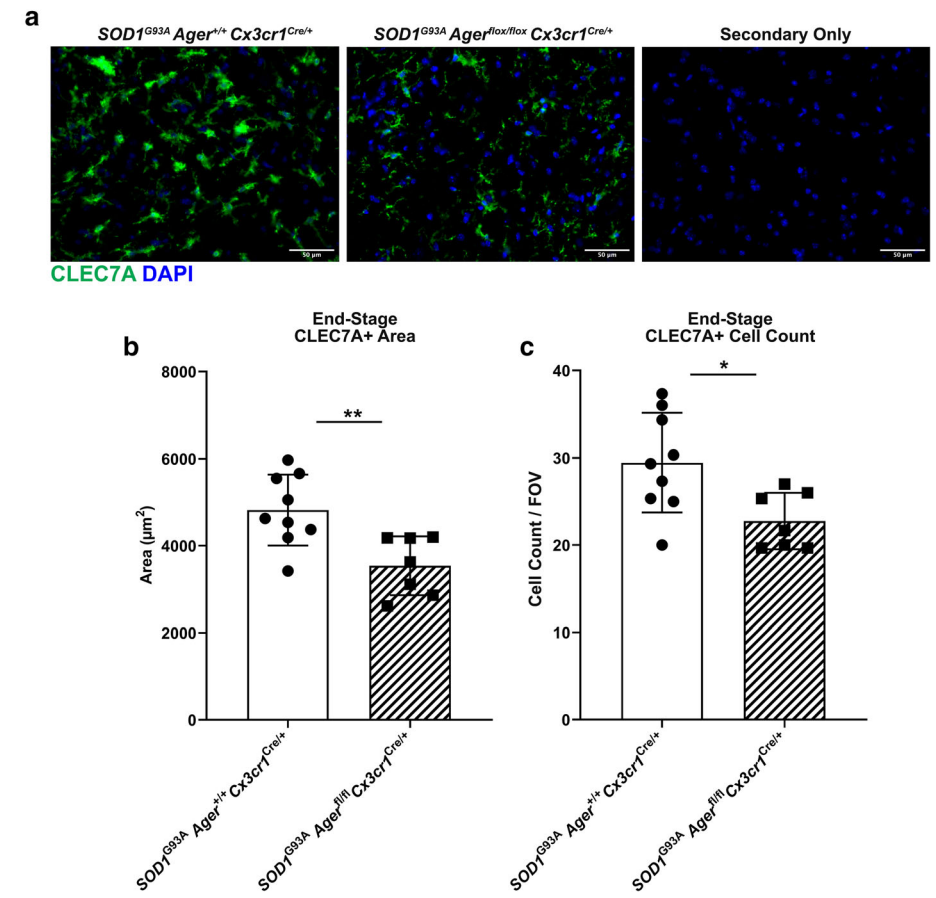

Fig. 8 Microglia *Ager* deletion in male $SOD1^{G93A}$ mice reduces the accumulation of disease-associated microglia at end-stage. **a** Representative images of CLEC7A staining in the lumbar spinal cord ventral horn of the indicated mouse groups. Scale bar: 50 μm. **b** Quantification of $CLEC7A^+$ area. **c** Quantification of $CLEC7A^+$ $DAPI^+$ cell number. Mean ± SD. $N = 7$ $SOD1^{G93A}$ $Ager^{fl/fl}$ $Cx3cr1^{Cre/+}$ mice and $N = 9$ $SOD1^{G93A}$ $Ager^{+/+}$ $Cx3cr1^{Cre/+}$ mice. Independent two sample two-sided *t* test. In **b**, $^{**}p < 0.0048$. In **c**, $^{*}p = 0.0154$

relative to non-neurological controls, this might have been accounted for, in part, by the unexpected observation that ALS patients displayed a range of *AGER* mRNA in the spinal cord. Accordingly, our analysis revealed up-regulation of the "AGE-RAGE pathway in diabetic complications" within cervical spinal cord RNA-seq data of ALS vs. control patients. We found that the amount of *AGER* negatively correlated with age at onset and age at death or tracheostomy in ALS patients' cervical spinal cord. If and to what degree the stratification of ALS patients by spinal cord *AGER* expression may be useful in prediction of prognosis, putative responsiveness to pharmacological interventions and/or the identification of ALS predictive biomarkers, for example, is an important subject for future investigation.

Furthermore, analysis of the consequences of varied degrees of *AGER* expression across patients' transcriptomic analyses, using *AGER* expression as a continuous variable, indicated enrichment in pathways involved in lipid metabolism, extracellular matrix, and cell-cell communication. In fact, microglia displayed increased RAGE protein overlap within both the anterior white matter and the ventral horn in high *AGER* patients relative to low *AGER* patients. Of note, our data in human ALS did not suggest sex-dependent differences in *AGER*-related gene expression patterns. In parallel, the present work in the murine model indicated that there was a significant increase in overlap of RAGE with microglia in $SOD1^{G93A}$ mice at the age of 120 days.

Beyond microglia, other cell-types express RAGE in the spinal cord of both $SOD1^{G93A}$ and human ALS patients. In fact, the roles of RAGE expression in astrocytes are not clear either in homeostasis or in neurodegeneration. RAGE expression in motor neurons has been posited to play a role in the cell-death pathways induced by conditioned media from $SOD1^{G93A}$-expressing astrocytes [81, 82]. A recent report indicated that global constitutive *Ager* deletion caused a decrease in survival of $SOD1^{G93A}$ mice, while administering a CNS-permeable RAGE antagonist, FPS-ZM1, starting at 60 days of age,

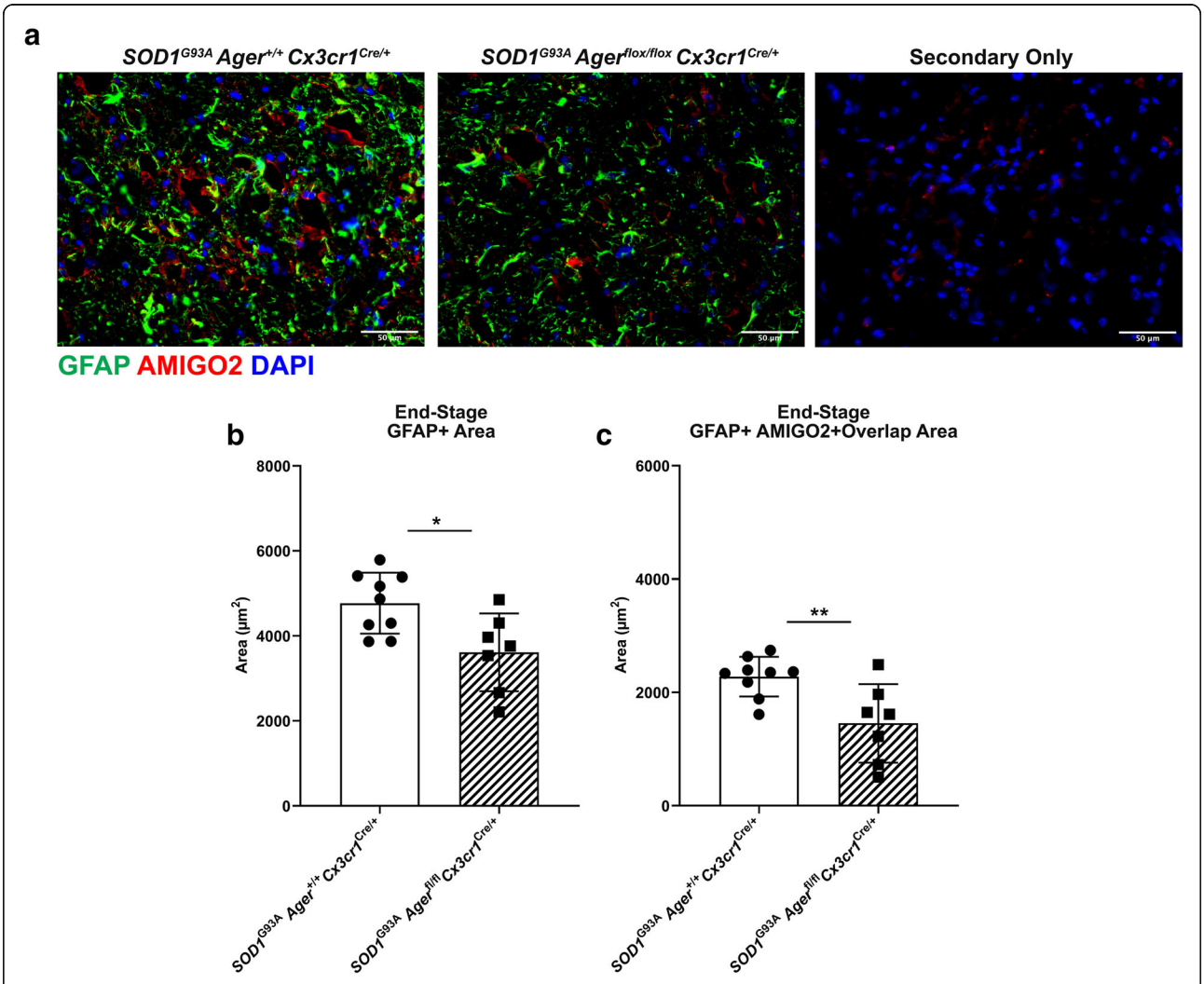

Fig. 9 Reactive A1 astrocytes are reduced in male *SOD1*^{G93A} mice by microglia *Ager* deletion. **a** Representative images of GFAP and AMIGO2 staining in the lumbar spinal cord ventral horn of the indicated mouse groups. **b** Quantification of GFAP^{+} area. **c** Quantification of GFAP^{+} and AMIGO2^{+} overlap area. Mean ± SD. *N* = 7 *SOD1*^{G93A} *Ager*$^{fl/fl}$ *Cx3cr1*$^{Cre/+}$ mice, and *N* = 9 *SOD1*^{G93A} *Ager*$^{+/+}$ *Cx3cr1*$^{Cre/+}$ mice. Independent two sample two-sided *t* test. In **b**, *p = 0.0132. In **c**, **p = 0.0076

reduced gliosis, and increased motor neuron number at 130 days; but did not alter survival in either sex [82]. However, the authors reported a potential sex-dependent impact on the progression of weight loss and time to death following 10% weight loss [82]. In a separate report, another global constitutive *Ager* deleted *SOD1*^{G93A} mouse line exhibited increased survival; however, this *Ager* deleted mouse line has been reported to harbor a large genomic duplication, which may have confounded the results and explained the discrepancy between the two studies [83, 84]. However, both studies suggested RAGE inhibition reduced gliosis and improved motor function. Treatment of *SOD1*^{G93A} mice with soluble RAGE (sRAGE), which sequesters RAGE ligands, reduced motor pathology, and extended lifespan in *SOD1*^{G93A} mice [41]. As there was no significant blood-brain permeability of sRAGE when administered peripherally [85], the mechanism by which sRAGE exerted protective effects remains elusive. It is possible that circulating soluble factors, modulated by sRAGE treatment, entered the CNS and exerted beneficial effects. Altogether, these studies suggest RAGE could exert complex protective and deleterious effects in a time- and location-dependent manner but cell-types responsible for any of these effects are unclear and warrant further study.

Our findings revealed that deletion of microglia *Ager* improved survival and motor function in male but not female *SOD1*^{G93A} mice. In this context, in the mouse model employed in our study, the "knock-in" of the Cre recombinase into the *Cx3cr1* locus results in an obligate heterozygous deletion of this gene in all mice, that is

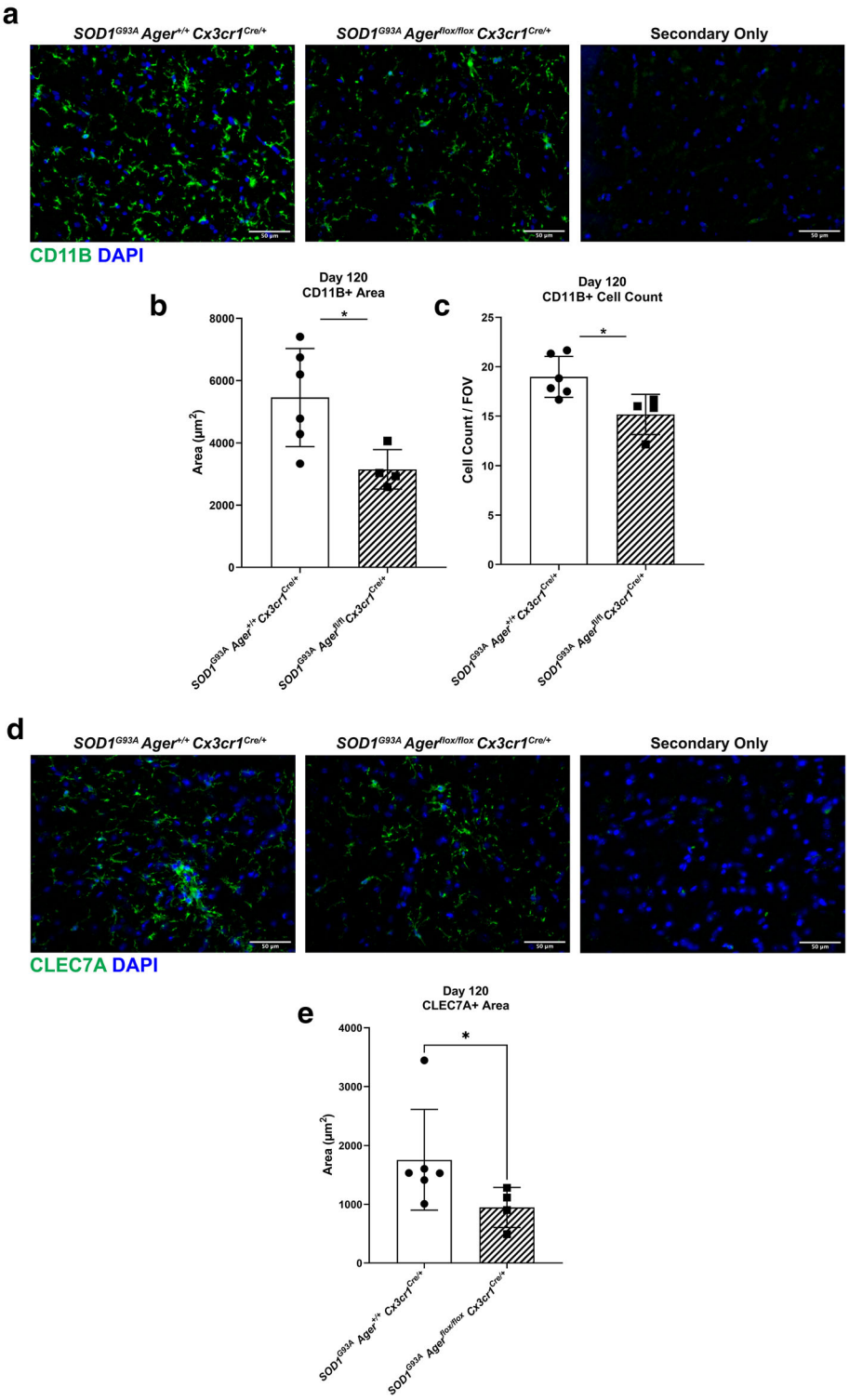

Fig. 10 Microglia *Ager* deletion in male $SOD1^{G93A}$ mice reduces microgliosis at 120 days of age. **a** Representative images of CD11B staining in the lumbar spinal cord ventral horn of the indicated mouse groups. **b** Quantification of $CD11B^+$ area. **c**. Quantification of $CD11B^+$ $DAPI^+$ cell number. **d** Representative images of CLEC7A staining in the lumbar spinal cord ventral horn of the indicated mouse groups. **e** Quantification of $CLEC7A^+$ area. Mean ± SD. $N = 4$ $SOD1^{G93A}$ $Ager^{fl/fl}$ $Cx3cr1^{Cre/+}$ mice, $N = 6$ $SOD1^{G93A}$ $Ager^{+/+}$ $Cx3cr1^{Cre/+}$ mice. In **b**, **c**, independent two sample two-sided *t* test. In **e**, Mann-Whitney *U* test. In **b**, * $p = 0.0253$. In **c**, *$p = 0.0212$. In **e**, *$p = 0.0381$

fully independent of tamoxifen administration. Thus, all Cre-expressing mice in our study are susceptible to the effects of hemizygous deletion of *Cx3cr1*. After the initiation of the present work, recent studies have independently implicated *Cx3cr1* in the pathogenesis of several neurodegenerative diseases, including ALS. For example, heterozygous deletion of *Cx3cr1* induces changes within microglia reminiscent of aged cells [86–88]. In fact, in a model of Alzheimer disease (AD), heterozygosity of *Cx3cr1* in male mice resulted in reductions of pathology [87]. In contrast, homozygous global deletion of *Cx3cr1* in male but not female $SOD1^{G93A}$ mice reduced survival [86]. Altogether, these considerations led us to conclude that it was critical to directly compare our findings in microglia *Ager*-deleted mice to the *Cx3cr1*-Cre-control mice to account for the obligate allelic loss of *Cx3cr1*. As we only observed differences in the male mice, we focused further investigation into these groups to determine what may drive the observed phenotypic differences.

Skeletal muscle macrophage content was not significantly different between the genotypes suggesting the beneficial effects of microglia *Ager* deletion were likely restricted to the nervous system. Accordingly, transcriptomic analysis of male $SOD1^{G93A}$ $Ager^{fl/fl}$ $Cx3cr1^{Cre/+}$ and Cre-control lumbar spinal cord tissues indicated microglia *Ager* deletion reduced gene expression in pathways related to lipid metabolism, actin cytoskeleton, extracellular matrix, and cell-cell communication. Predicted cytokine regulators of these effects included cytokines, such IL1α, C-X-C motif chemokine ligand 1 (CXCL1), C-X-C motif chemokine ligand 9 (CXCL9), TNF superfamily member 10 (TNFSF10), and IFNs. Several of these cytokines are known to be dysregulated in the context of ALS in murine models and in patients [75–77]. IFN was recently linked to the acquisition of the damage/disease-associated (DAM) microglia phenotype [89]. DAM are known to accumulate in the $SOD1^{G93A}$ mouse model and are thought to both provoke and ameliorate disease-related pathways [20, 21, 23]. The transition of microglia to this dysfunctional state is theorized to occur in at least several stages with later stages being TREM2-dependent [21]. Critically, CLEC7A, a marker of DAM highly upregulated over time by $SOD1^{G93A}$ microglia [23], was significantly downregulated via microglia *Ager* deletion at day 120 and in end-stage tissues. Furthermore, the number of $CLEC7A^{+}$ microglia reduced by microglia *Ager* deletion suggested that microglia *Ager* deletion reduces the activation/acquisition of the DAM phenotype or, alternatively, shifts microglia to a novel phenotype. In fact, BV2 microglia-like cells treated with CML-AGE, a canonical RAGE ligand present in the ALS spinal cord, demonstrated a RAGE-dependent increase in *Il1a* and the DEG identified by RNA-seq *Malat1*. *Malat1* has been linked to the regulation of pro-inflammatory responses of peripheral macrophages. *Malat1*-deficient macrophages display reduced LPS responsiveness and altered fibrotic phenotypes [74]. Altogether, these considerations suggest that microglia RAGE may amplify this dysfunctional state, at least in male mice.

Recent work has implicated microglia-sourced IL1α, TNF, and C1q in inducing astrocyte dysfunction and promoting their neurotoxicity in neurodegeneration [70, 90]. In this context, and the considerations that we observe less DAM and that IL1α activity was predicted to be downregulated by microglia *Ager* deletion, we examined the impact of microglia *Ager* deletion on the accumulation of GFAP+ "pan" reactive astrocytes as well as the overlap of GFAP with an "A1" reactive astrocyte marker, AMIGO2 [70, 80]. Consistent with the predicted downregulation of IL1α activity in the transcriptomic data and reductions in DAM, we observed lower $GFAP^{+}$ area and lower overlap area of $GFAP^{+}$ and $AMIGO2^{+}$. These data indicate that microglia RAGE signaling may contribute to transformation of astrocytes to a more neurotoxic phenotype.

As we had performed bulk RNA-seq on the murine lumbar spinal cords at sacrifice, we compared the results between the analysis of the ALS patients and the murine dataset. This exercise revealed that *half* of the ingenuity canonical pathways overlapped between the two analyses and suggests that microglia RAGE may modulate extracellular matrix composition, cell-cell communication, and fatty acid metabolism in ALS and that this may influence disease pathology.

It is important to note that we are unable to distinguish if microglia *Ager* deletion interacted with potential *Cx3cr1*-mediated sex-dependent impacts on pathology, or if microglia RAGE has sex-dependent roles in microglia. In support of the latter, male microglia exhibited an enrichment of the RAGE receptor binding Gene Ontology term relative to female microglia isolated from cortical tissues [91]. Furthermore, recent work indicated sex-dependent actions of HMGB1, a known RAGE ligand, on spinal cord microglia in a model of hypersensitivity [92]. Additionally, recent work indicated unexplained sex-dependent effects of FPS-ZM1 treatment on several measures of progression in $SOD1^{G93A}$ mice [82]. Yet, the transcriptomic signature we observed in human ALS patients related to *AGER* expression was independent of sex. However, the human patient data analyzed were obtained almost entirely from sporadic ALS patients with no known family history of illness; thus, the generalizability of our sex-dependent findings in this model of familial ALS is unclear. Finally, it is also possible that the observed sex-dependent effect in mice is a result of a complex interaction between roles of

RAGE within microglia that were altered due to the developmental loss of one allele of *Cx3cr1*. Further study in distinct models of ALS will be required to discern if microglia RAGE has sex-dependent effects in the pathogenesis of ALS.

Hence, although we may not be able to fully disentangle the effects of the *Cx3cr1* heterozygosity on survival from potential roles for RAGE in pathology the $SOD1^{G93A}$ mouse model, the direct comparison to the Cre-control reflects the most rigorous design for this work. Importantly, it is known that monocytes also express *Cx3cr1*; however, these cells replenish from *Cx3cr1* deficient pre-cursors within a few days, and monocyte recruitment into the $SOD1^{G93A}$ spinal cord has been a point of contention within the field. Recent tracing studies have suggested that recruitment is limited until late states of pathology [93]. While we cannot entirely rule out early incipient roles for monocytic RAGE in the context of $SOD1^{G93A}$ pathology, we predict that the largest benefits were from microglia *Ager* reduction within the CNS. Hence, future studies require testing the RAGE hypothesis in distinct models of ALS, and in a model employing Cre-recombinase mice in which expression of native microglia genes is not affected, and is more specific to microglia, such as the recently developed *Tmem119*-2A-CreERT2 mouse model [94].

Altogether, these data demonstrate that microglia RAGE expression may contribute to microglia dysfunction and ultimately to the disruption of communication with multiple cell types including astrocytes and neurons in the diseased ALS spinal cord. Our findings that motor neuron numbers were higher in lumbar spinal cords of male mice devoid of microglia *Ager* vs. controls at day 120 indicate that such communications emitted from microglia cues were, ultimately, aligned with neuronal survival in the pre-morbid/end-stage state. Collectively, our findings implicate microglia and RAGE in human ALS and provide mechanistic evidence that microglia RAGE contributes to pathology in male $SOD1^{G93A}$ mice.

Conclusions

In summary, our findings suggest microglia RAGE may impact human ALS and contribute to ALS-like pathology in male $SOD1^{G93A}$ mice. Male $SOD1^{G93A}$ mice bearing microglia *Ager* deficiency from the age of 3 months exhibited reduced gliosis, neuronal and motor function loss, and reduced dysfunctional transcriptomic signatures in lumbar spinal cord tissue. Critically, the observation of a spectrum of *AGER* and RAGE expression in human ALS spinal cord unveils a myriad of areas for research with respect to implications for ALS vulnerability, severity of disease, and, perhaps, responsiveness to RAGE-directed therapeutics. In this very context, the observed overlap between the human and murine dataset analyses indicate that the pathways altered in mice may be relevant in human patient pathologies. In conclusion, these data provide novel evidence that microglia-specific RAGE expression is a disease-modifying factor in ALS, potentially through modulation of the molecular switch from homeostatic microglia to dysfunctional microglia.

Abbreviations

AGE: Advanced glycation end product; ALS: Amyotrophic lateral sclerosis; AMIGO2: Adhesion molecule with Ig like domain 2; C1q: Complement component 1q; CD11B: Integrin subunit alpha m; ChAT: Choline acetyltransferase; CLEC7A: c-Type lectin domain containing 7a protein (or dectin-1); CML: Carboxymethyllysine; CNS: Central nervous system; CXCL1: C-X-C motif chemokine ligand 1; CXCL9: C-X-C motif chemokine ligand 9; DAM: Damage/disease-associated microglia; DIAPH1: Diaphanous related formin 1; fALS: Familial amyotrophic lateral sclerosis; GFAP: Glial fibrillary acidic protein; HMGB1: High-mobility group box 1; hSOD1: Human SOD1; IBA1: Ionized calcium-binding adapter molecule 1; IFN: Interferon; IHC: Immunohistochemistry; IL1: Interleukin 1; IPA: Ingenuity pathway analysis; MAP 2: Microtubule-associated protein 2; NeuN: Neuronal nuclei antigen; RAGE: Receptor for advanced glycation end products; sALS: Sporadic amyotrophic lateral sclerosis; SOD1: Superoxide dismutase 1; sRAGE: Soluble RAGE; TAM: Tamoxifen; TREM2: Triggering receptor expressed on myeloid cells 2; WT: Wild-type

Supplementary Information

The online version contains supplementary material available at https://doi.org/10.1186/s12974-021-02191-2.

Additional file 1. Figures and figure legend for Supplemental Figure 1–8. Also, table legends for Supplemental Tables 1.1–1.10.

Additional file 2. Excel workbook containing Supplemental Tables 1.1–1.10.

Acknowledgements

The authors gratefully acknowledge the expert assistance of Ms. Latoya Woods of the Diabetes Research Program, Department of Medicine, NYU Grossman School of Medicine, in the preparation of this manuscript. We thank the NYU Grossman School of Medicine's Genome Technology Center; which is partially funded by the Cancer Center Support grant P30CA016087 at NYU Langone Health's Cancer Center. We acknowledge the Target ALS postmortem tissue core for providing us with human cervical spinal cord sections. We acknowledge the Target ALS Multicentered Postmortem Tissue Core, the New York Genome Center for Genomics of Neurodegenerative Disease, Amyotrophic Lateral Sclerosis Association and TOW Foundation for access to the human RNA-seq data and corresponding metadata.

Authors' contributions

M.M. designed the research, performed experiments, analyzed data, wrote the first draft of the manuscript, and edited the manuscript. J.J., S.C., R.L.D., H.H.R., and L.F. performed experiments and edited the manuscript. J.H., H.L., and P.F.G. contributed analytically and intellectually to the interpretation of the data and edited the manuscript. A.M.S. conceived the studies, designed the research, supervised the design and completion of the experiments, analyzed data, and wrote and edited the final manuscript. All authors read and approved the final manuscript.

Funding

Funding for this project included: Department of Defense award: W81XWH-17-1-0346 to A.M.S; F31NS120424 from the National Institutes of Health National Institute of Neurological Disorders and Stroke to M.M; and support from the Diabetes Research Program, NYU Grossman School of Medicine.

Availability of data and materials

Murine raw FastQ sequencing data and corresponding normalized count data are uploaded for public access on the NCBI GEO database under

accession number: GSE160402. All raw Human RNA-seq data from Target ALS samples are publicly available via The Target ALS Multicentered Postmortem Tissue Core, the New York Genome Center for Genomics of Neurodegenerative Disease, Amyotrophic Lateral Sclerosis Association and TOW Foundation (www.targetals.org). Access can be requested by emailing ALSData@nyugenome.org.

Declarations

Ethics approval and consent to participate

All mouse experiments were performed under protocols approved by the New York University Grossman School of Medicine Institutional Animal Care and Use Committee (IACUC) in accordance with international and NIH guidelines. All human data, and tissue used in this study was provided by TargetALS in a de-identified manner.

Consent for publication

Not applicable.

Competing interests

A.M.S is an inventor on awarded (US 9,353,3078, US 9364472) and pending (US 16/094270, Europe 177864360.0) patent applications assigned to NYU Grossman Medical Center.

Author details

[1]Diabetes Research Program, Department of Medicine, New York University Grossman School of Medicine, New York, NY 10016, USA. [2]Department of Human Physiology and Pathophysiology, School of Medicine, University of Warmia and Mazury, Olsztyn, Poland. [3]Division of Biostatistics, Department of Population Health and the Department of Environmental Medicine, New York University Grossman School of Medicine, New York, NY 10016, USA.

Received: 10 February 2021 Accepted: 1 June 2021
Published online: 15 June 2021

References

1. NINDS. Amyotrophic Lateral Sclerosis (ALS) Fact Sheet. Bethesda: NIH Neurological Institute; 2013. No. 16-916
2. Chen H, Kankel MW, Su SC, Han SWS, Ofengeim D. Exploring the genetics and non-cell autonomous mechanisms underlying ALS/FTLD. Cell Death Differ. 2018;25(4):646–60.
3. Nguyen DKH, Thombre R, Wang J. Autophagy as a common pathway in amyotrophic lateral sclerosis. Neurosci Lett. 2019;697:34–48. https://doi.org/10.1016/j.neulet.2018.04.006. Epub 2018 Apr 4.
4. Gurney ME, Pu H, Chiu AY, Dal Canto MC, Polchow CY, Alexander DD, et al. Motor neuron degeneration in mice that express a human Cu,Zn superoxide dismutase mutation. Science. 1994;264(5166):1772–5. https://doi.org/10.1126/science.8209258.
5. Dal Canto MC, Gurney ME. Neuropathological changes in two lines of mice carrying a transgene for mutant human Cu,Zn SOD, and in mice overexpressing wild type human SOD: a model of familial amyotrophic lateral sclerosis (FALS). Brain Res. 1995;676(1):25–40. https://doi.org/10.1016/0006-8993(95)00063-V.
6. Haidet-Phillips AM, Hester ME, Miranda CJ, Meyer K, Braun L, Frakes A, et al. Astrocytes from familial and sporadic ALS patients are toxic to motor neurons. Nat Biotechnol. 2011;29(9):824–8. https://doi.org/10.1038/nbt.1957.
7. Frakes AE, Ferraiuolo L, Haidet-Phillips AM, Schmelzer L, Braun L, Miranda CJ, et al. Microglia induce motor neuron death via the classical NF-kappaB pathway in amyotrophic lateral sclerosis. Neuron. 2014;81(5):1009–23. https://doi.org/10.1016/j.neuron.2014.01.013.
8. Boillee S, Yamanaka K, Lobsiger CS, Copeland NG, Jenkins NA, Kassiotis G, et al. Onset and progression in inherited ALS determined by motor neurons and microglia. Science. 2006;312(5778):1389–92. https://doi.org/10.1126/science.1123511.
9. Beers DR, Henkel JS, Xiao Q, Zhao W, Wang J, Yen AA, et al. Wild-type microglia extend survival in PU.1 knockout mice with familial amyotrophic lateral sclerosis. Proc Natl Acad Sci U S A. 2006;103(43):16021–6. https://doi.org/10.1073/pnas.0607423103.
10. Miller SJ, Glatzer JC, Hsieh YC, Rothstein JD. Cortical astroglia undergo transcriptomic dysregulation in the G93A SOD1 ALS mouse model. J Neurogenet. 2018;32(4):322–35. https://doi.org/10.1080/01677063.2018.1513508.
11. Philips T, Rothstein JD. Glial cells in amyotrophic lateral sclerosis. Exp Neurol. 2014;262 Pt B:111–20.
12. Maniatis S, Aijo T, Vickovic S, Braine C, Kang K, Mollbrink A, et al. Spatiotemporal dynamics of molecular pathology in amyotrophic lateral sclerosis. Science. 2019;364(6435):89–93. https://doi.org/10.1126/science.aav9776.
13. Hardiman O, Al-Chalabi A, Chio A, Corr EM, Logroscino G, Robberecht W, et al. Amyotrophic lateral sclerosis. Nat Rev Dis Prim. 2017;3(1):17085. https://doi.org/10.1038/nrdp.2017.85.
14. Li Q, Barres BA. Microglia and macrophages in brain homeostasis and disease. Nat Rev Immunol. 2018;18(4):225–42. https://doi.org/10.1038/nri.2017.125.
15. O'Rourke JG, Bogdanik L, Yanez A, Lall D, Wolf AJ, Muhammad AK, et al. C9orf72 is required for proper macrophage and microglial function in mice. Science. 2016;351(6279):1324–9. https://doi.org/10.1126/science.aaf1064.
16. Paolicelli RC, Jawaid A, Henstridge CM, Valeri A, Merlini M, Robinson JL, et al. TDP-43 Depletion in microglia promotes amyloid clearance but also induces synapse loss. Neuron. 2017;95(2):297–308 e6. https://doi.org/10.1016/j.neuron.2017.05.037.
17. Ito Y, Ofengeim D, Najafov A, Das S, Saberi S, Li Y, et al. RIPK1 mediates axonal degeneration by promoting inflammation and necroptosis in ALS. Science. 2016;353(6299):603–8. https://doi.org/10.1126/science.aaf6803.
18. Bartlett R, Sluyter V, Watson D, Sluyter R, Yerbury JJ. P2X7 antagonism using Brilliant Blue G reduces body weight loss and prolongs survival in female SOD1(G93A) amyotrophic lateral sclerosis mice. PeerJ. 2017;5:e3064. https://doi.org/10.7717/peerj.3064.
19. Spiller KJ, Restrepo CR, Khan T, Dominique MA, Fang TC, Canter RG, et al. Microglia-mediated recovery from ALS-relevant motor neuron degeneration in a mouse model of TDP-43 proteinopathy. Nat Neurosci. 2018;21(3):329–40. https://doi.org/10.1038/s41593-018-0083-7.
20. Chiu IM, Morimoto ET, Goodarzi H, Liao JT, O'Keeffe S, Phatnani HP, et al. A neurodegeneration-specific gene-expression signature of acutely isolated microglia from an amyotrophic lateral sclerosis mouse model. Cell Rep. 2013;4(2):385–401. https://doi.org/10.1016/j.celrep.2013.06.018.
21. Keren-Shaul H, Spinrad A, Weiner A, Matcovitch-Natan O, Dvir-Szternfeld R, Ulland TK, et al. A unique microglia type associated with restricting development of Alzheimer's disease. Cell. 2017;169(7):1276–90 e17. https://doi.org/10.1016/j.cell.2017.05.018.
22. Deczkowska A, Keren-Shaul H, Weiner A, Colonna M, Schwartz M, Amit I. Disease-associated microglia: a universal immune sensor of neurodegeneration. Cell. 2018;173(5):1073–81. https://doi.org/10.1016/j.cell.2018.05.003.
23. Krasemann S, Madore C, Cialic R, Baufeld C, Calcagno N, El Fatimy R, et al. The TREM2-APOE pathway drives the transcriptional phenotype of dysfunctional microglia in neurodegenerative diseases. Immunity. 2017;47(3):566–81 e9. https://doi.org/10.1016/j.immuni.2017.08.008.
24. MacLean M, Derk J, Ruiz HH, Juranek JK, Ramasamy R, Schmidt AM. The receptor for advanced glycation end products (RAGE) and DIAPH1: implications for vascular and neuroinflammatory dysfunction in disorders of the central nervous system. Neurochem Int. 2019;126:154–64. https://doi.org/10.1016/j.neuint.2019.03.012.
25. Juranek JK, Daffu GK, Wojtkiewicz J, Lacomis D, Kofler J, Schmidt AM. Receptor for advanced glycation end products and its inflammatory ligands are upregulated in amyotrophic lateral sclerosis. Front Cell Neurosci. 2015;9:485.
26. Casula M, Iyer AM, Spliet WG, Anink JJ, Steentjes K, Sta M, et al. Toll-like receptor signaling in amyotrophic lateral sclerosis spinal cord tissue. Neuroscience. 2011;179:233–43. https://doi.org/10.1016/j.neuroscience.2011.02.001.
27. Lo Coco D, Veglianese P, Allievi E, Bendotti C. Distribution and cellular localization of high mobility group box protein 1 (HMGB1) in the spinal cord of a transgenic mouse model of ALS. Neurosci Lett. 2007;412(1):73–7. https://doi.org/10.1016/j.neulet.2006.10.063.
28. Kikuchi S, Shinpo K, Ogata A, Tsuji S, Takeuchi M, Makita Z, et al. Detection of N epsilon-(carboxymethyl)lysine (CML) and non-CML advanced glycation end-products in the anterior horn of amyotrophic lateral sclerosis spinal cord. Amyotroph Lateral Scler Other Motor Neuron Disord. 2002;3(2):63–8. https://doi.org/10.1080/146608202760196020.
29. Kaufmann E, Boehm BO, Sussmuth SD, Kientsch-Engel R, Sperfeld A, Ludolph AC, et al. The advanced glycation end-product N epsilon-(carboxymethyl)lysine level is elevated in cerebrospinal fluid of patients with

amyotrophic lateral sclerosis. Neurosci Lett. 2004;371(2-3):226–9. https://doi.org/10.1016/j.neulet.2004.08.071.
30. Yeh CH, Sturgis L, Haidacher J, Zhang XN, Sherwood SJ, Bjercke RJ, et al. Requirement for p38 and p44/p42 mitogen-activated protein kinases in RAGE-mediated nuclear factor-kappaB transcriptional activation and cytokine secretion. Diabetes. 2001;50(6):1495–504. https://doi.org/10.2337/diabetes.50.6.1495.
31. Shen C, Ma Y, Zeng Z, Yin Q, Hong Y, Hou X, et al. RAGE-specific inhibitor FPS-ZM1 attenuates AGEs-induced neuroinflammation and oxidative stress in rat primary microglia. Neurochem Res. 2017;42(10):2902–11. https://doi.org/10.1007/s11064-017-2321-x.
32. Manigrasso MB, Pan J, Rai V, Zhang J, Reverdatto S, Quadri N, et al. Small molecule inhibition of ligand-stimulated RAGE-DIAPH1 signal transduction. Sci Rep. 2016;6(1):22450. https://doi.org/10.1038/srep22450.
33. Bianchi R, Kastrisianaki E, Giambanco I, Donato R. S100B protein stimulates microglia migration via RAGE-dependent up-regulation of chemokine expression and release. J Biol Chem. 2011;286(9):7214–26. https://doi.org/10.1074/jbc.M110.169342.
34. Bianchi R, Giambanco I, Donato R. S100B/RAGE-dependent activation of microglia via NF-kappaB and AP-1 Co-regulation of COX-2 expression by S100B, IL-1beta and TNF-alpha. Neurobiol Aging. 2010;31(4):665–77. https://doi.org/10.1016/j.neurobiolaging.2008.05.017.
35. Hudson BI, Kalea AZ, Del Mar AM, Harja E, Boulanger E, D'Agati V, et al. Interaction of the RAGE cytoplasmic domain with diaphanous-1 is required for ligand-stimulated cellular migration through activation of Rac1 and Cdc42. J Biol Chem. 2008;283(49):34457–68. https://doi.org/10.1074/jbc.M801465200.
36. Rai V, Maldonado AY, Burz DS, Reverdatto S, Yan SF, Schmidt AM, et al. Signal transduction in receptor for advanced glycation end products (RAGE): solution structure of C-terminal rage (ctRAGE) and its binding to mDia1. J Biol Chem. 2012;287(7):5133–44. https://doi.org/10.1074/jbc.M111.277731.
37. Parkhurst CN, Yang G, Ninan I, Savas JN, Yates JR 3rd, Lafaille JJ, et al. Microglia promote learning-dependent synapse formation through brain-derived neurotrophic factor. Cell. 2013;155(7):1596–609. https://doi.org/10.1016/j.cell.2013.11.030.
38. Wooley CM, Sher RB, Kale A, Frankel WN, Cox GA, Seburn KL. Gait analysis detects early changes in transgenic SOD1(G93A) mice. Muscle Nerve. 2005;32(1):43–50. https://doi.org/10.1002/mus.20228.
39. Hurtado del Pozo C, Ruiz HH, Arivazhagan L, Aranda JF, Shim C, Daya P, et al. A Receptor of the immunoglobulin superfamily regulates adaptive thermogenesis. Cell Rep. 2019;28(3):773–91.e7.
40. Scott S, Kranz JE, Cole J, Lincecum JM, Thompson K, Kelly N, et al. Design, power, and interpretation of studies in the standard murine model of ALS. Amyotroph Lateral Scler. 2008;9(1):4–15. https://doi.org/10.1080/17482960701856300.
41. Juranek JK, Daffu GK, Geddis MS, Li H, Rosario R, Kaplan BJ, et al. Soluble RAGE treatment delays progression of amyotrophic lateral sclerosis in SOD1 mice. Front Cell Neurosci. 2016;10:117.
42. Schindelin J, Arganda-Carreras I, Frise E, Kaynig V, Longair M, Pietzsch T, et al. Fiji: an open-source platform for biological-image analysis. Nat Methods. 2012;9(7):676–82. https://doi.org/10.1038/nmeth.2019.
43. Otsu N. A threshold selection method from Gray-level histograms. IEEE Trans Syst Man Cybern. 1979;9(1):62–6. https://doi.org/10.1109/TSMC.1979.4310076.
44. Tsai WH. Moment-preserving thresholding—a new approach. Comput Vision Graph. 1985;29(3):377–93. https://doi.org/10.1016/0734-189X(85)90133-1.
45. Zack GW, Rogers WE, Latt SA. Automatic measurement of sister chromatid exchange frequency. J Histochem Cytochem. 1977;25(7):741–53. https://doi.org/10.1177/25.7.70454.
46. Senatus L, López-Díez R, Egaña-Gorroño L, Liu J, Hu J, Daffu G, Li Q, Rahman K, Vengrenyuk Y, Barrett TJ, Dewan MZ, Guo L, Fuller D, Finn AV, Virmani R, Li H, Friedman RA, Fisher EA, Ramasamy R, Schmidt AM. RAGE impairs murine diabetic atherosclerosis regression and implicates IRF7 in macrophage inflammation and cholesterol metabolism. JCI Insight. 2020;5(13):e137289. https://doi.org/10.1172/jci.insight.137289.
47. Wingett S, Andrews S. FastQ Screen: a tool for multi-genome mapping and quality control [version 2; peer review: 4 approved]. F1000Research. 2018;7:1338.
48. Andrews S. FastQC: a quality control tool for high throughput sequence data; 2010.
49. Bolger AM, Lohse M, Usadel B. Trimmomatic: a flexible trimmer for Illumina sequence data. Bioinformatics. 2014;30(15):2114–20. https://doi.org/10.1093/bioinformatics/btu170.
50. Dobin A, Davis CA, Schlesinger F, Drenkow J, Zaleski C, Jha S, et al. STAR: ultrafast universal RNA-seq aligner. Bioinformatics. 2013;29(1):15–21. https://doi.org/10.1093/bioinformatics/bts635.
51. Liao Y, Smyth GK, Shi W. featureCounts: an efficient general purpose program for assigning sequence reads to genomic features. Bioinformatics. 2014;30(7):923–30. https://doi.org/10.1093/bioinformatics/btt656.
52. Liao Y, Smyth GK, Shi W. The Subread aligner: fast, accurate and scalable read mapping by seed-and-vote. Nucleic Acids Res. 2013;41(10):e108. https://doi.org/10.1093/nar/gkt214.
53. Frankish A, Diekhans M, Ferreira AM, Johnson R, Jungreis I, Loveland J, et al. GENCODE reference annotation for the human and mouse genomes. Nucleic Acids Res. 2019;47(D1):D766–D73. https://doi.org/10.1093/nar/gky955.
54. Robinson MD, Oshlack A. A scaling normalization method for differential expression analysis of RNA-seq data. Genome Biol. 2010;11(3):R25. https://doi.org/10.1186/gb-2010-11-3-r25.
55. Robinson MD, McCarthy DJ, Smyth GK. edgeR: a Bioconductor package for differential expression analysis of digital gene expression data. Bioinformatics. 2010;26(1):139–40. https://doi.org/10.1093/bioinformatics/btp616.
56. Team RC. R: A language and environment for statistical computing. Vienna: R Foundation for Statistical Computing; 2018.
57. Nikolayeva O, Robinson MD. edgeR for differential RNA-seq and ChIP-seq analysis: an application to stem cell biology. Methods Mol Biol. 2014;1150:45–79. https://doi.org/10.1007/978-1-4939-0512-6_3.
58. Kanehisa M, Sato Y, Furumichi M, Morishima K, Tanabe M. New approach for understanding genome variations in KEGG. Nucleic Acids Res. 2019;47(D1):D590–D5. https://doi.org/10.1093/nar/gky962.
59. Kanehisa M, Goto S, Kawashima S, Okuno Y, Hattori M. The KEGG resource for deciphering the genome. Nucleic Acids Res. 2004;32(Database issue):D277–80. https://doi.org/10.1093/nar/gkh063.
60. Kanehisa M, Goto S. KEGG: kyoto encyclopedia of genes and genomes. Nucleic Acids Res. 2000;28(1):27–30. https://doi.org/10.1093/nar/28.1.27.
61. Yu G, Wang LG, Han Y, He QY. clusterProfiler: an R package for comparing biological themes among gene clusters. OMICS. 2012;16(5):284–7. https://doi.org/10.1089/omi.2011.0118.
62. Kramer A, Green J, Pollard J Jr, Tugendreich S. Causal analysis approaches in ingenuity pathway analysis. Bioinformatics. 2014;30(4):523–30. https://doi.org/10.1093/bioinformatics/btt703.
63. Benjamini Y, Hochberg Y. Controlling the false discovery rate: a practical and powerful approach to multiple testing. J R Stat Soc Ser B Methodol. 1995;57(1):289–300. https://doi.org/10.1111/j.2517-6161.1995.tb02031.x.
64. Lun AT, Chen Y, Smyth GK. It's DE-licious: a recipe for differential expression analyses of RNA-seq experiments using quasi-likelihood methods in edgeR. Methods Mol Biol. 2016;1418:391–416. https://doi.org/10.1007/978-1-4939-3578-9_19.
65. Wu D, Smyth GK. Camera: a competitive gene set test accounting for inter-gene correlation. Nucleic Acids Res. 2012;40(17):e133. https://doi.org/10.1093/nar/gks461.
66. Wu D, Lim E, Vaillant F, Asselin-Labat ML, Visvader JE, Smyth GK. ROAST: rotation gene set tests for complex microarray experiments. Bioinformatics. 2010;26(17):2176–82. https://doi.org/10.1093/bioinformatics/btq401.
67. The Gene Ontology C. The gene ontology resource: 20 years and still GOing strong. Nucleic Acids Res. 2019;47(D1):D330–D8.
68. Ashburner M, Ball CA, Blake JA, Botstein D, Butler H, Cherry JM, et al. Gene ontology: tool for the unification of biology. The gene ontology consortium. Nat Genet. 2000;25(1):25–9. https://doi.org/10.1038/75556.
69. Pinheiro J BD, DebRoy S, Sarkar D, R Core Team. nlme: linear and nonlinear mixed effects models. 2020.
70. Liddelow SA, Guttenplan KA, Clarke LE, Bennett FC, Bohlen CJ, Schirmer L, et al. Neurotoxic reactive astrocytes are induced by activated microglia. Nature. 2017;541(7638):481–7. https://doi.org/10.1038/nature21029.
71. Joshi AU, Minhas PS, Liddelow SA, Haileselassie B, Andreasson KI, Dorn GW 2nd, et al. Fragmented mitochondria released from microglia trigger A1 astrocytic response and propagate inflammatory neurodegeneration. Nat Neurosci. 2019;22(10):1635–48. https://doi.org/10.1038/s41593-019-0486-0.
72. Chen J, Sun Z, Jin M, Tu Y, Wang S, Yang X, et al. Inhibition of AGEs/RAGE/Rho/ROCK pathway suppresses non-specific neuroinflammation by

regulating BV2 microglial M1/M2 polarization through the NF-kappaB pathway. J Neuroimmunol. 2017;305:108–14. https://doi.org/10.1016/j.jneuroim.2017.02.010.
73. Serrano A, Donno C, Giannetti S, Peric M, Andjus P, D'Ambrosi N, et al. The astrocytic S100B protein with its receptor RAGE is aberrantly expressed in SOD1(G93A) models, and its inhibition decreases the expression of proinflammatory genes. Mediat Inflamm. 2017;2017:1626204.
74. Cui H, Banerjee S, Guo S, Xie N, Ge J, Jiang D, Zörnig M, Thannickal VJ, Liu G. Long noncoding RNA Malat1 regulates differential activation of macrophages and response to lung injury. JCI Insight. 2019;4(4):e124522. https://doi.org/10.1172/jci.insight.124522.
75. Hensley K, Floyd RA, Gordon B, Mou S, Pye QN, Stewart C, et al. Temporal patterns of cytokine and apoptosis-related gene expression in spinal cords of the G93A-SOD1 mouse model of amyotrophic lateral sclerosis. J Neurochem. 2002;82(2):365–74. https://doi.org/10.1046/j.1471-4159.2002.00968.x.
76. Meissner F, Molawi K, Zychlinsky A. Mutant superoxide dismutase 1-induced IL-1beta accelerates ALS pathogenesis. Proc Natl Acad Sci U S A. 2010;107(29):13046–50. https://doi.org/10.1073/pnas.1002396107.
77. Hu Y, Cao C, Qin XY, Yu Y, Yuan J, Zhao Y, et al. Increased peripheral blood inflammatory cytokine levels in amyotrophic lateral sclerosis: a meta-analysis study. Sci Rep. 2017;7(1):9094. https://doi.org/10.1038/s41598-017-09097-1.
78. Ye J, Cheung J, Gerbino V, Ahlsen G, Zimanyi C, Hirsh D, et al. Effects of ALS-associated TANK binding kinase 1 mutations on protein-protein interactions and kinase activity. Proc Natl Acad Sci U S A. 2019;116(49):24517–26. https://doi.org/10.1073/pnas.1915732116.
79. Liu J, Gao L, Zang D. Elevated Levels of IFN-gamma in CSF and serum of patients with amyotrophic lateral sclerosis. PLoS One. 2015;10(9):e0136937. https://doi.org/10.1371/journal.pone.0136937.
80. Zamanian JL, Xu L, Foo LC, Nouri N, Zhou L, Giffard RG, et al. Genomic analysis of reactive astrogliosis. J Neurosci. 2012;32(18):6391–410. https://doi.org/10.1523/JNEUROSCI.6221-11.2012.
81. Kim MJ, Vargas MR, Harlan BA, Killoy KM, Ball LE, Comte-Walters S, Gooz M, Yamamoto Y, Beckman JS, Barbeito L, Pehar M. Nitration and Glycation Turn Mature NGF into a Toxic Factor for Motor Neurons: A Role for p75NTR and RAGE Signaling in ALS. Antioxid Redox Signal. 2018;28(18):1587–602. https://doi.org/10.1089/ars.2016.6966. Epub 2017 Jun 26.
82. Liu L, Killoy KM, Vargas MR, Yamamoto Y, Pehar M. Effects of RAGE inhibition on the progression of the disease in hSOD1(G93A) ALS mice. Pharmacol Res Perspect. 2020;8(4):e00636. https://doi.org/10.1002/prp2.636.
83. Lee JD, McDonald TS, Fung JNT, Woodruff TM. Absence of receptor for advanced glycation end product (RAGE) reduces inflammation and extends survival in the hSOD1(G93A) mouse model of amyotrophic lateral sclerosis. Mol Neurobiol. 2020;57(10):4143–55. https://doi.org/10.1007/s12035-020-02019-9.
84. Bartling B, Zunkel K, Al-Robaiy S, Dehghani F, Simm A. Gene doubling increases glyoxalase 1 expression in RAGE knockout mice. Biochim Biophys Acta Gen Subj. 1864;2020(1):129438.
85. Deane R, Du Yan S, Submamaryan RK, LaRue B, Jovanovic S, Hogg E, et al. RAGE mediates amyloid-beta peptide transport across the blood-brain barrier and accumulation in brain. Nat Med. 2003;9(7):907–13. https://doi.org/10.1038/nm890.
86. Liu C, Hong K, Chen H, Niu Y, Duan W, Liu Y, et al. Evidence for a protective role of the CX3CL1/CX3CR1 axis in a model of amyotrophic lateral sclerosis. Biol Chem. 2019;400(5):651–61. https://doi.org/10.1515/hsz-2018-0204.
87. Hickman SE, Allison EK, Coleman U, Kingery-Gallagher ND, El Khoury J. Heterozygous CX3CR1 deficiency in microglia restores neuronal beta-amyloid clearance pathways and slows progression of Alzheimer's like-disease in PS1-APP mice. Front Immunol. 2019;10:2780. https://doi.org/10.3389/fimmu.2019.02780.
88. Gyoneva S, Hosur R, Gosselin D, Zhang B, Ouyang Z, Cotleur AC, Peterson M, Allaire N, Challa R, Cullen P, Roberts C, Miao K, Reynolds TL, Glass CK, Burkly L, Ransohoff RM. Cx3cr1-deficient microglia exhibit a premature aging transcriptome. Life Sci Alliance. 2019;2(6):e201900453. https://doi.org/10.26508/lsa.201900453.
89. Roy ER, Wang B, Wan YW, Chiu G, Cole A, Yin Z, et al. Type I interferon response drives neuroinflammation and synapse loss in Alzheimer disease. J Clin Invest. 2020;130(4):1912–30. https://doi.org/10.1172/JCI133737.
90. Guttenplan KA, Weigel MK, Adler DI, Couthouis J, Liddelow SA, Gitler AD, et al. Knockout of reactive astrocyte activating factors slows disease progression in an ALS mouse model. Nat Commun. 2020;11(1):3753. https://doi.org/10.1038/s41467-020-17514-9.
91. Guneykaya D, Ivanov A, Hernandez DP, Haage V, Wojtas B, Meyer N, et al. Transcriptional and translational differences of microglia from male and female brains. Cell Rep. 2018;24(10):2773–83 e6. https://doi.org/10.1016/j.celrep.2018.08.001.
92. Agalave NM, Rudjito R, Farinotti AB, Khoonsari PE, Sandor K, Nomura Y, et al. Sex-dependent role of microglia in disulfide high mobility group box 1 protein-mediated mechanical hypersensitivity. Pain. 2021;162(2):446–58. https://doi.org/10.1097/j.pain.0000000000002033.
93. Chiot A, Zaidi S, Iltis C, Ribon M, Berriat F, Schiaffino L, et al. Modifying macrophages at the periphery has the capacity to change microglial reactivity and to extend ALS survival. Nat Neurosci. 2020;23(11):1339–51. https://doi.org/10.1038/s41593-020-00718-z.
94. Kaiser T, Feng G. Tmem119-EGFP and Tmem119-CreERT2 Transgenic Mice for Labeling and Manipulating Microglia. eNeuro. 2019;6(4):ENEURO.0448-18.2019. https://doi.org/10.1523/ENEURO.0448-18.2019.

Publisher's Note

Springer Nature remains neutral with regard to jurisdictional claims in published maps and institutional affiliations.

Ready to submit your research? Choose BMC and benefit from:

- fast, convenient online submission
- thorough peer review by experienced researchers in your field
- rapid publication on acceptance
- support for research data, including large and complex data types
- gold Open Access which fosters wider collaboration and increased citations
- maximum visibility for your research: over 100M website views per year

At BMC, research is always in progress.

Learn more biomedcentral.com/submissions

BMC